CHARACTERISTICS OF WIND FIELDS AND AIR-SEA INTERACTIONS OVER THE UPWELLING REGION OF THE SOMALI COAST

Ali J. Mafimbo

Supervisor:
Prof. Chris Reason

Department of Oceanography, University of Cape Town
Rondebosch, South Africa

Dissertation submitted to the faculty of Science, University of Cape Town in fulfilment of the academic requirements for the degree of Master of Science.

February 2008

Table of Contents

Abstract iii

Acknowledgements v

List of Figures, Tables vi

Chapter 1 1

Introduction 1

Chapter 2 10

Literature Review 10

2.1 The Indian Monsoons 12
2.2 East African Low Level (Somali) Jet 15
2.2.1 Characteristics of local summer winds over the Somali region. 19
2.2.2 The influence of Topography and Orography of the Somali Coast on the Jet. 21
2.3 Indian Ocean Surface Currents. 22
2.4 The Somali current and Upwelling at the Somali coast 25
Chapter 3 34

Data and Methodology 34

3.1 Significant southern upwelling event 35
3.2 Temporal variability of alongshore winds 38
3.2.1 Continuous Wavelet Analysis (CWA) 39
3.3 Temporal variability in Sea level pressure index during the year 2005 43
Chapter 4 46

Results and Discussion 46

4.1 Significant southern upwelling event 47
4.3 Temporal variability of Winds over the upwelling region. 59
4.4 Summary 62
4.5 Spatial variability of winds and SSTs: 26-30 July 2005 68
4.6 Summary 72
4.7 Mesoscale SST-Wind co-variability over the upwelling region 76
4.8 Summary 78
4.9 Alongshore wind stress, Wind Stress Curl and the significant upwelling. 80
4.9.1 Variability of the alongshore and across-shore winds. 80
4.9.2 Wind stress curl and upwelling. 82
4.10 Summary 84
Chapter 5 89

Summary and Conclusions 89

References 94

Abstract

During the southwest monsoon two upwelling cells are established along the Somali coast, one to the south around 4-5^{0}N and the other further north near the tip of the Great Horn of Africa around 10^{0}N. The SSTs over these regions can fall to about 22^{0}C on the average during this time. The southern upwelling region is of great importance to the East African fishing community since it represents a major fish landing zone.

The mesoscale structure of the low-level wind field associated with a strong upwelling event was investigated. During July 2005 when a strong upwelling event occurred, the Somali jet was found to have oscillated at lower frequency of 3-7 weeks than the normal bi-weekly mode observed in several studies and the mesoscale winds exhibited high co-variability with the prevailing SSTs. Strong values of alongshore winds were deduced from late June to mid-July. These winds weakened significantly in the third and fourth week of July. A large off-shore pressure gradient due to differential thermal properties of land and sea was also observed.

The results as discussed in this thesis show that the prolonged active and break periods of the Somali Jet results in the acceleration (deceleration) of the alongshore winds. The strong alongshore wind stress during a prolonged active period of the jet, which could be intensified further by the thermal forcing due to the land-ocean temperature constraints as observed by Chao (1985), accelerates the Somali current. The acceleration of this current enhances the Ekman pumping resulting into strong upwelling. In the prolonged break period the current decelerates turns east and then southwards.

The high co-variability of the mesoscale winds and SSTs results in the deceleration (acceleration) of the winds upstream (downstream) of the upwelling zone leading to atmospheric convergence (divergence) respectively. This convergence upstream of the cold filament results in oceanic divergence and further enhances the upwelling.

The quasi-biweekly oscillations of the jet have been found to be related to similar oscillations in rainfall over India associated with break and active Indian monsoon phases, with cross-equatorial winds being stronger during a strong monsoon than a weak one.

A correlation has been found between rainfall over the western coast of India and the intensity of low-level equatorial winds over Kenya. Further studies have shown that a break of the monsoon rain over India occurs when the wind intensity is weak along the East African coast. These observations suggest a need to examine the relationship between a strong southern Somalian upwelling event, the Indian monsoon and rainfall over the coastal region of Kenya.

Acknowledgements

I would like to express my deepest gratitude to Dr. Joseph R. Mukabana, the Director of Kenya Meteorological Department for his tireless efforts to secure government funding that enabled me to attend this course and his constant encouragement throughout the training; to my supervisor Professor Chris Reason who greatly assisted me in putting this thesis together through his positive advice, continuous discussion sessions and guidance; to Professor Frank Shillington who was always there for his guidance and encouragement; to Professor George Philander who in a special way enhanced my belief that everything is possible in the way he handled very complicated scientific issues to make them look simple and easy to tackle.

Sincere thanks is extended to Dr. Jean Melice of the Oceanography Department of University of Cape Town who greatly assisted me in understanding the CWA technique and to all staff of the department for their availability and willingness to assist anytime all the time. They make quite a great team to belong to.

I thank and acknowledge the following organizations for the data used in this thesis; Cersat Ifremer for the QuikSCAT Mean Wind Fields; the National Centre for Environmental Prediction (NCEP) in collaboration with National Centre for Atmospheric Research (NCAR) for the Sea Level Pressure data; and the National Aeronautics and Space Administration (NASA) together with National Space Development Agency of Japan for the TMI SSTs

And the last salute goes to my wife Josephine and children Nana and Tina. My two year absence from them brought to me the knowledge that I have a strong family that is able to rally together in every presenting situation. While Josephine ably played the roles of a father, mother and loving wife of an absentee husband, Nana and Tina played their roles as good daughters and competing students challenging their student father. It was quite an inspiration from them.

"We are nothing but pencils in the hands of the creator" God bless you all.

List of Figures and Tables

Figure		Page
1.1	Seasonal wind flow patterns over the study region adapted from Gatebe et al (1999)	7
1.2	Topography of the East African coast showing the Somali region with terrain height of above 1 km.....	8
1.3	Schematic diagram on the development of the two upwelling regions on the Somali coast adapted from Schott et al (2001)	9
2.1	Movement of the ITCZ (red line) and the zero absolute vorticity contour (yellow line). Surface pressure (black solid contours) and 925mbar horizontal wind (vectors) adapted from P. J. Webster et al (1988)	28
2.2	Mean OLR (wm^{-2}) for January and July from Gadgil (2003)	29
2.3	Schematic diagram of the nine elements of the monsoon system following Krishnamurti et al. 1976.....	30
2.4	Mean flow pattern at 1 Km level for July, following Findlater (1971)....	30
2.5	Mean sea level pressure for July (after van de Boogaard, 1977). Contour interval 1 mb.	31
2.6	Topography of Somali basin with the smoothed 4000 m depth contour..	31
2.7	A schematic representation of currents during January–February (Northern winter) and July-August (Northern summer) respectively from Schott et al' 2001.....	32
2.8	Strong eastwards flowing jets during Northern spring.....	33
2.9	Mean velocity sections across Somali Current on the equator during the summer monsoon (left), during the winter monsoon (middle) and annual mean (right) from Schott et al., 1990.....	33

3.1 Time series of SSTs showing high correlation of data from Central Pacific buoys TAO buoy (51023, red) and NDBC buoy (51028, blue) with TMI SST data..... **44**

3.2 Time-frequency windows used in (a) Fourier Transform (FT), (b) a Windowed Fourier Transform (WFT), and (c) Wavelet Transform(WT), taken from Lau and Weng, 1995..... **45**

3.3 Example of morlet Wavelet with different value of scale a, from Lau and Weng (1995) **45**

4.1 Meridional Hovmuller plot along 50.125E between latitudes 10S and 10N. **50**

4.2 SST surface plots for June, July, August and September from 1999 – 2007..... **50**

4.3 Time series correlation of SST (^{0}C) and Wind stress (Pascals) at 4.75^{0}N and 50.25^{0}E..... **63**

4.4 Time series SSTs at 4.75^{0}N and 50.25^{0}E over the region of the significant upwelling event. **64**

4.5 Time series of weeky QuikSCAT winds at 4.75^{0}N and 50.25^{0}E over the region of the significant upwelling event. **65**

4.6 Standardized frequency plot of the annual variation of the Somali Jet showing a more uniform pattern..... **66**

4.7 Standardized frequency plot of the semiannual variations of the Somali Jet. **66**

4.8 Standardized series of the 2-7 weeks oscillation of the Somali Jet with the instantaneous amplitude (thick blue) and instantaneous frequency (red) showing periods of significant power..... **67**

4.9 **panel a,b,c,d,e** showing the evolution of SSTs (left) and wind vector (right) during the 5 weeks from 26 June-30 July 2005..... **73**

4.10 Time series of alongshore wind (blue) and SSTs (red) extracted from the box bounded by 3.25 – 4.25^{0}N and 49.25 – 52.25^{0}E over the upwelling region for the period 6 June – 29 August..... **79**

4.11 Weekly alongshore (left) and across-shore wind stress for the period 26 June- 30 July 2005..... **85**

4.12 July 2005 surface temperature anomalies constructed from NOAA/NCEP Reanalysis showing zonal thermal gradient with the upwelling region in the box to the right and indicated by the black arrow..... **87**

4.13 Box average SLPI between the boxes 2.5^0 - 5.0^0N, 50.0^0 – $52.5.^0$E over the ocean and 2.5^0 - 5.0^0N, 42.5^0 – 45.0^0E over land for the year 2005... **87**

4.14 Wind stress Curl plots for the period 26 June – 30 July 2005 ..... **88**

Table 1 Correlation coefficients between variables as found by Vecchi et al. in the Western Arabian Sea showing strong positive correlation between At-SST and heat flux Q **77**

Chapter 1

Introduction

The coastal waters of East Africa contain a wide range of oceanographic environments and some of the most dynamically varying large marine ecosystems in the world. The fisheries sector is one of the important contributors to the socio-economic development of the East African coastal region. The total marine fishery catches in the western Indian Ocean increased from a catch of ~0.5 million tonnes in the 1950's to nearly 3.8 million tonnes in 1992, since when they have declined slightly (FAO Fisheries Circular No. 920 of 1997). Fishing takes place mainly over the nutrient rich upwelling regions at about 3-4^{0}N and 10-12^{0}N along the Somali coast. The former region is of interest to Kenya because it constitutes one of the country's major fishing zones.

Upwelling is a phenomenon that involves upward motion of dense, cooler, and usually nutrient-rich water towards the ocean surface, replacing wind-driven warmer, usually nutrient-depleted surface water which drifts at an angle to the wind stress just above it (Smith, 1968). Ekman (1905) developed theories to explain why the ocean's surface layer drifts at an angle to the wind stress just above it. He attributed the apparent deflection to the combined effects of the Earth's rotation (Coriolis force) and frictional force due to the wind stress (Ekman, 1905). Key to the study of the Ekman transport and in particular upwelling in coastal regions, therefore, are accurate descriptions of near surface wind fields over the region of study.

In the Indian Ocean region, upwelling is a process critical to its climate. By all estimates, the heat flux into the surface layer of the northern Indian Ocean is positive (Godfrey *et al.*, 1995). Godfrey *et al.* (1995) observed that on the annual average, there is positive heat flux into the Indian Ocean nearly everywhere north of 15° S.

The integral of the net heat influx into the Indian Ocean over the area north of 15° S ranges between 0.5–1.0 x 10^{15} W. Thus, on the annual mean, there must be a net inflow of cold water (into the North Indian Ocean), and a corresponding removal of warmed water, to carry this heat influx southward, out of the tropical Indian Ocean since Asia bounds the North Indian Ocean at low latitude. The Indian Ocean consequently has a unique system of three-dimensional currents and interactions with the atmosphere that redistribute heat to keep the ocean approximately in a long-term thermal equilibrium. Areas of upwelling together with southward Ekman heat transport and inflow of cold water at depth are required to balance the surface heat budget.

The upwelling of cold, nutrient-rich waters over the Somali coast region is essentially wind driven. Winds and ocean current off the Somali coast up to the Horn of Africa combine to produce upwelling of subsurface water during northern summer. This coastal circulation known as the Somali Current forms the northward extension of Southern Equatorial Current (SEC) and the East African Coastal Current (EACC) systems. It develops during the southwest monsoon to become one of the fastest open-ocean currents in the world. During the summer monsoon of 1995, two hydrographic and direct velocity sections were occupied over the continental shelf and slope off the coast of Somalia in order to capture the flux of this western boundary current. The first section was in early June, just after the onset of the monsoon winds, during which time an anticyclonic eddy at the boundary with a small net northward transport of 3.5+/-1.5Sv was observed. The second section was occupied in mid-September when a strong Somali Current was evident. The strength of the current observed was 37+/-5Sv. (Beal *et al.*, 2003).

In September, the Somali Current as observed by Beal *et al.* (2003), extended far into shallow coastal waters of less than 200m depth, with speeds over 150cms^{-1}, resulting in a considerable transport of 14Sv over the shelf. It has been shown that the volume transport of the current can exceed values of 70Sv (Fischer *et al.*, 1996; Schott *et al.*, 1997) and it has been observed to have a speed that increases in a linear fashion with latitude from 170 cms^{-1} at 2^{0}S to about 350cms^{-1} at 8^{0}N (Stommel and Wooster, 1965).

The alongshore winds that drive the current are predominantly southwesterly during the northern summer, and northeasterly in the austral summer. These winds form part of the Somali jet during the southwest monsoon. A relationship exists between the intensity of the cross-equatorial wind flow along the East African coast and eastward propagation of mid-latitude depressions in the southern hemisphere (Cadet and Desbois., 1981).

There is some evidence that the jet is forced by low-level divergence in the subtropical high pressure belt over the southern Indian Ocean which includes the Mascarene High and convergence in the monsoon trough over India (Anderson, 1976; Hart, 1977). These synoptic cross equatorial winds over the Somali region are modulated by the movement of the Intertropical Convergence Zone (ITCZ), **Fig. 1.1**, and the East African topography (Gatebe *et al.,* 1999). Cadet and Desbois (1981) found that the weakening of the jet was related to a wind discontinuity to the east of Madagascar, due to fluctuations of midlatitude weather systems to the south which pulse the trade winds, drastically reducing the flow into the area of the jet. The orography of the Somali region which rises to an elevation of over 1 km (**Fig.1.2)** is a crucial element in the intensification of the Somali jet (Bannon, 1982).

In sympathy with the strong northern summer monsoon winds (South-Westerlies), an offshore drift of surface water is initiated east of the Somali coast. Compensating this Ekman transport, an upwelling cell develops. Concurrently the SSTs in the region drop as the thermocline is lifted by localized Ekman suction driven by the southwesterly wind fields. The upwelling develops off the Somali coast at about 4-10^{0}N (southern upwelling). As the winds intensify in June/July, a second upwelling appears in the region of 10-12^{0}N (northern upwelling) (Schott *et al.*, 2001). (**Fig.1.3**)

This upwelling in the northern summer is one of the most intense large-scale seasonal coastal upwelling systems in the world. In their observations of the Somali current, (Stommel and Wooster, 1965) observed sea surface temperatures of about 13^0C in the upwelling region. It is estimated that upwelling off the Somali coast is about 12 Sv., which corresponds to a subduction of water in the southeastern subtropical Indian Ocean at a density less than 25.7 kg $m^{-3,}$ (Karstensen and Quadfasel, 2002).

A large off-shore temperature gradient at the Somali coast exists in the lower atmosphere during the strong southwesterly monsoon when conditions favour active upwelling (see Figs.4.12). In addition, the Somali upwelling region is characterized by pronounced orographic, topographic, and bathymetric features.

The synoptic wind patterns of the southwesterly monsoon which are responsible for the upwelling in the Somali region are fairly well understood. What is less understood is the characteristics of mesoscale wind fields during strong upwelling events over the southern upwelling region. A literature review of air-sea interaction research conducted in the East African coastal region has revealed gaps in our knowledge. This thesis attempts to address some of these gaps.

This research on the investigation of characteristics of wind fields over the upwelling Somali region being undertaken in this thesis has benefited extensively from similar investigations done on the Cape Peninsula and other regions of the world as documented in Chapter Two. The investigation focuses on the mesoscale characteristics of the near surface winds for an identified significant upwelling event over the Somali coast that occurred in the last nine years (1999-2007) during the Southwesterly monsoon which will be used as a case study.

The role of mesoscale spatial and temporal variability in wind stress forcing in controlling the southern upwelling along the Somali coast in the region 4-10^{0}N will be investigated. Since understanding of the spatial variability of the local wind fields which results from the adjustment of the large scale flow to regional topography and thermal gradients is limited by lack of observations, an attempt is made in this study to utilize reanalysed data from various data centres. The sea level pressure came from NCEP/NCAR, weekly SSTs from TMI and weekly wind stress and wind stress curl from QuikSCAT.

The high resolution weekly mean Sea Surface Temperatures (SSTs) data from the Tropical Rainfall Measuring Mission (TRMM) satellite is utilized to identify the significant upwelling event by extracting SSTs for the region from the global data and creating Hovmuller and surface plots. Wind vector plots from QuikSCAT Scatterometer data are used to investigate prevailing wind strengths during the event.

To investigate temporal variability in wind stress at the upwelling region, an inter-annual time series of local alongshore wind stress was created by extracting weekly wind stress values during the 26 July 1999 - 4 June 2007 period. These data are the CERSAT 0.5^0 x 0.5^0 gridded product (Wentz, 1992). A second time series was created to assess variability in a Sea Level pressure Index (SLPI) based on daily reanalysis sea level pressure data with a grid of 2.5^0 x 2.5^0 from NCEP/NCAR for the year during which the significant upwelling event occurred. The SLPI is a measure of the local synoptic across-shore pressure gradient.

Continuous Wavelet Analysis was then applied to investigate dominant modes of variability and how these modes vary in time. This method is discussed further in Chapter 3. Weekly wind vector plots for the year corresponding to the significant upwelling event were constructed from quikSCAT data and used to investigate the spatial variability of the winds during the upwelling.

This introductory chapter is followed by Chapter Two (Literature Review) which outlines similar work already done in other upwelling regions and studies done on the Somali jet, coastal currents and the Somali Current. The third chapter outlines the data and methodology used. This includes a description of the data and analytical techniques used in this thesis. In the fourth chapter, the results are presented whereas chapter five contains the summary and conclusions.

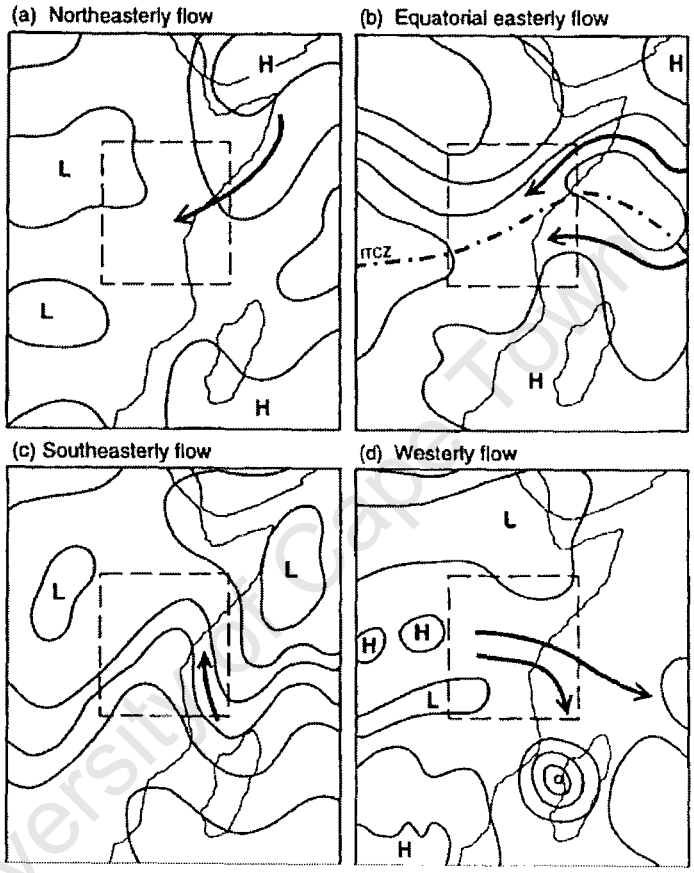

Fig. 1.1: *Seasonal wind flow patterns over the study region adapted from Gatebe et al (1999)*

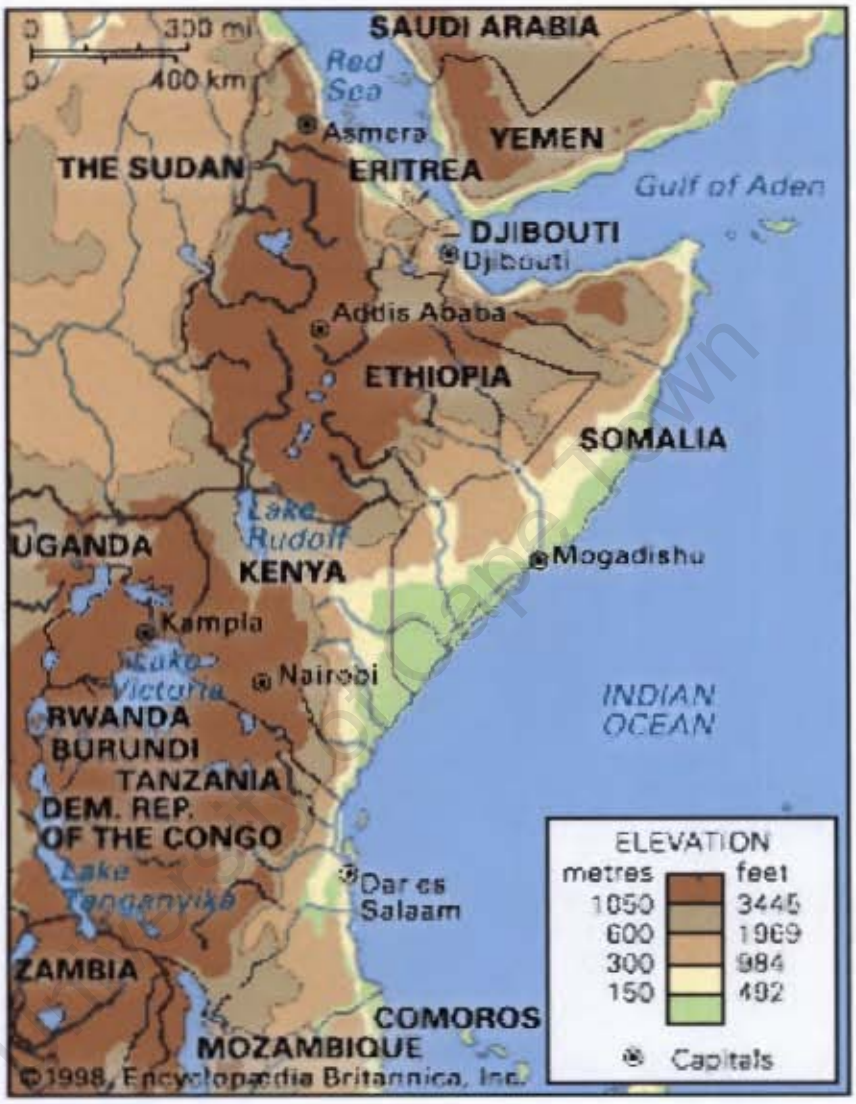

Fig 1.2: Topography of the East African coast showing the Somali region with terrain height of above 1km. Picture from http://www.britannica.com/eb/art-61110

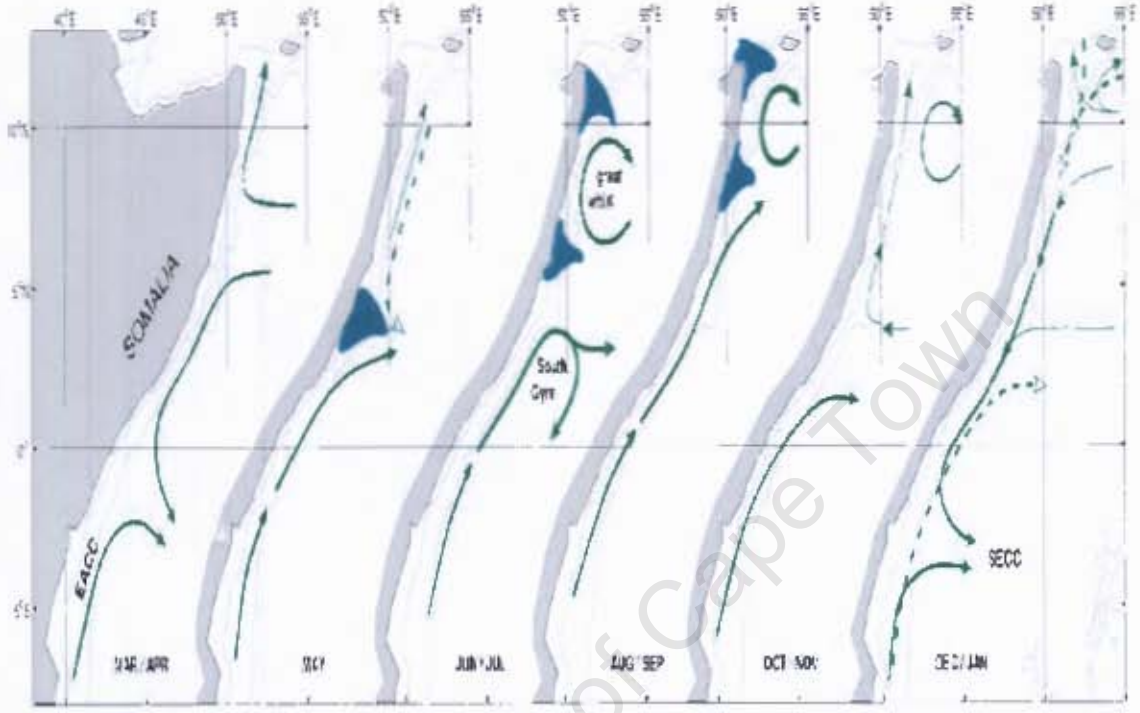

Fig. 1.3 *Schematic diagram showing the development of the two upwelling regions on the Somali coast up to the horn of Africa in June/July, adapted from Schott et al (2001)*

Chapter 2

Literature Review

Studies of variations in the marine wind field together with sea surface temperatures were accomplished in the 1970's over many wind driven ocean circulation systems [Gill and Clark (1974), Halpern (1976), Clancy *et al.* (1979)]. This development led to significant awareness of the dominant role played by wind forcing of surface currents, particularly in upwelling regimes (Jury, 1983).

Studies conducted in areas like Oregon, N. West Africa, and Peru by the Coastal Upwelling Ecosystems Analysis (CUE) group showed interesting results concerning air-sea interactions over upwelling regions. These have included positive correlations between the location and intensity of steady alongshore wind maxima and seasonal upwelling plumes along the Peruvian coast (Watson, 1978; Moody, 1979).

Using a centered differencing technique, Nelson (1977) ; Bakun (1973, 1978); and Parrish *et al.* (1981) have studied the relationships between cyclonic wind stress curl and enhanced seasonal upwelling along certain portions of the California coast. Areas of cyclonic wind stress curl were found to coincide with persistent upwelling plumes of cool water, particularly next to large capes or headlands. Along the coasts of Peru and North West Africa, Uhart (1976), Watson (1978), Godwin (1979), Moody (1979) and Stuart *et al.* (1981) found that coastal headlands accelerate winds and lead to localized upwelling. Wind acceleration by coastal headlands was also suggested by Bang (1973) in his description of the current dynamics of the Cape Peninsula upwelling plume. He suggested that oceanic momentum, favourable bathymetry and winds accelerated by the Cape Peninsula coastal headlands created an intense equatorward flowing current 'jet' at the outside of the plume. Similar suggestions were made by Atkins (1970) and Van Ieperen (1971) in their correlation of the surface currents at False Bay with data at nearby weather stations.

To effectively study the variations of wind fields together with sea surface temperatures and upwelling over the Somali coast, a good understanding of the Indian Monsoons, the East African Low Level Jet, the Indian Ocean surface currents including the Somali Current is essential.

2.1 The Indian Monsoons

Of the three major oceans, Pacific, Atlantic, and Indian, the latter is the only one that is not open to the northern high latitude regions. This is a consequence of the presence of the Asian landmass restricting the Indian Ocean to the south of about 25°N. The Indian Ocean is also the only ocean with a low-latitude opening in its eastern boundary. This unique geography has important implications for the oceanic circulation physics and climate of the Indian Ocean region.

The monsoon is the characteristic feature of Indian Ocean climate. The topography of the Asian landmass is dominated by the Tibetan Plateau which has an area of about a million square kilometres and an average height of about 5 km. The plateau acts as an elevated heat source for the atmosphere during the northern summer through uplifting of warm air. The warming of the Indian subcontinent during boreal summer, June-August (JJA), creates a powerful land-based convection and large scale cross-equatorial flow, characterized with winds blowing from the southwest over the Somali region and Arabian Sea, to replace the ascending air masses. During this time, the Inter-Tropical Convergence Zone (ITCZ) virtually covers the entire Bay of Bengal, the surrounding lands, and the eastern Arabian Sea (Figure 2.1). Significant rainfall occurs over a broad zone around 20^0N, stretching northwestward from the Bay of Bengal during the northern summer. Variations of all-India summer monsoon rainfall are highly correlated with variation of rainfall over this zone which has been called the monsoon zone (Sikka and Gadgil, 1980).

In the transition period to austral summer, September-November (SON), the continent cools faster than the sea. By boreal winter, December-February (DJF), the Asian landmass is cooler than the ocean to the south and the winds reverse to form the northeast monsoon, consequently rainfall over the Indian monsoon zone drastically reduces (Parthasarathy *et al.* 1992, 1995). During this time the ITCZ is located primarily in the southern hemisphere. These seasonal reversals of winds and rainfall intensity over the monsoon zone are two of the characteristic elements of the well known Indian or southwest monsoon (Krishnamurti *et al.* 1976).

Over 300 years ago, Halley (1686) suggested that the primary cause of the monsoon was the differential heating between ocean and land, thus the monsoon was considered to be a gigantic land-sea breeze. This is still considered to be the basic mechanism for the monsoon by several scientists (e.g.; Webster 1987). The second hypothesis is that in which the monsoon is considered as a manifestation of the seasonal migration of the ITCZ (e.g.; Charney 1969) or the equatorial trough (e.g.; Riehl 1954, 1979). The discussion of these two hypotheses is beyond the scope of this thesis but suffice to note that Simpson (1921) pointed out that India is much hotter in May before the monsoon sets in than in July when it is at its height, thus showing that observations are not consistent with the first hypothesis. The alternative hypothesis in which the monsoon is considered to be a manifestation of the seasonal migration of the ITCZ is also not acceptable to some scientists. For example Murakami (1987) pointed out that the latitudinal extent of the region characterised by low values of out going long wave radiation (OLR) is much larger over the Indian longitudes in the Northern Hemispheric summer than that characterizing the ITCZ over the Atlantic and Pacific (Fig. 2.2) and suggested that "the ITCZ over the Indian Ocean changes its existence drastically from winter to summer." However both hypotheses have been used to investigate the behaviour of the monsoon.

The elements of the monsoon system were well described by Krishnamurti *el al.* (1976) to consist of the monsoon trough over northern India that is part of the global equatorial trough of the northern summer season; the Mascarene high, a high pressure area near the Mascarene Islands east of Madagascar; a low-level cross-equatorial jet or the Somali Jet (Findlater, 1969); the Tibetian high that is known to have its largest amplitude near 200mb during the northern summer (also see Krishnamurti and Rogers, 1970; Krishnamurti, 1971; Krishnamurti *et al.*, 1973); a Tropical Easterly Jet near 150mb with winds of roughly 80-100knots; monsoon cloudiness, cloud cover over the monsoon zone; monsoon rainfall over central India; and dry and moist static stability in the monsoon belt over northern India (Fig. 2.3).

The monsoon has been seen to undergo both interannual and intraseasonal variations. There has been considerable work on documenting the nature of these variations of the monsoon and their interrelationships [e.g.; Ramamurthy 1969, Krishnamurti and Bhalme 1976, Sikka and Gadgil 1980, Ferranti *et al.* 1997, Goswami *et al.* 1998, Lawrence and Webster 2001, Sperber *et al.* 2000]. However, the processes that lead to the fluctuation between active and weak spell or breaks are yet to be understood.

In their study of the oscillations of the monsoon, Krishnamurti *et al.* (1976) observed bi-weekly oscillations in all the nine elements of the monsoon. In his observational studies of the monsoon, Murakami (1976) noted both 5-day and 15-day oscillations in the pressure and motion fields.

In their study of daily satellite imagery over the Indian longitudes, Sikka and Gadgil (1980) showed that the cloud band over the Indian subcontinent on an active monsoon day is strikingly similar to that characterizing the ITCZ over other parts of the tropics. Sikka and Gadgil (1980) also pointed out two important features of the variation of the cloudbands over the Indian longitudes during the summer, the presence of two favourable locations for the cloudbands/ITCZ with one over the heated subcontinent and the other over the warm waters of the equatorial Indian Ocean.

They noted that a prominent feature of the intraseasonal variation is northward propagation of the cloudbands from the equatorial Indian Ocean into the Indian monsoon zone at intervals of 2-6 weeks. These cloudbands occur farther and farther northward in the onset phase and more and more southward in the retreat phase.

The East African Low-Level jet or the Somali Jet is an important monsoonal element as discussed in the next section.

2.2 East African Low Level (Somali) Jet

The low-level cross-equatorial jet is a crucial element of the Indian monsoon and has been the focus of several modelling studies, including Krishnamurti *et al.* (1976); Krishnamurti *et al.* (1982); Anderson (1976); Hart (1977) and Bannon (1979, 1982). The jet represents by far the largest time-mean low-level cross-equatorial flow at any longitude and time of the year and may be expected to transport not only moisture but also negative potential vorticity from southern hemisphere to northern hemisphere (Rodwell and Hoskins, 1995).

The structure of the low-level monsoon winds over the Indian Ocean during July consists of three elements: the Southeast trades of the Southern Hemisphere; a strong narrow cross-equatorial flow over East Africa and the western edges of the Indian Ocean; and the southwest monsoon over the Arabian Sea. Together these components are often collectively called the East African Jet or Findlater Jet or Somali jet (Bannon, 1982). This jet forms on the western boundary of a broad cross-equatorial current of moisture-laden air which feeds directly into the Indian peninsula during the southwest monsoon and has been found to exhibit variability over a broad range of timescales (Findlater (1969), Ardanuy (1979), Bannon (1979b), Cadet *et al.* (1981) and Rao *et al.* (1982)). The jet has a strong annual cycle while the Asian monsoon, to which it is connected, evolves. The jet axis progresses steadily to the northwest as the summer monsoon circulation develops. By June, the low-level jet axis is located directly over the horn of northeast Africa (Findlater, 1971). From observational aspects of the Somali Jet (Findlater, 1977), its major features can be summarised as follows. The origin of the jet lies over the South Indian Ocean in the South East Trades with typical speeds of 5-10ms^{-1}. Following the flow westwards, a relative wind speed maximum occurs just north of the tip of Madagascar with a zone of calm winds to the west of the island. The jet crosses the equator as a strong southerly flow. There, the jet core is at an altitude of 1.5-2.0 Km. and reaches its maximum speed of about 15ms^{-1} near 5^{0}N. The flow is laterally bounded in the west by the East African Highlands. Further downstream the jet leaves the coast at ~10^{0}N. (Fig. 2.4)

The mean sea-level pressure field associated with the flow is shown in (Fig.2.5). In the Southern Hemisphere, the subtropical high-pressure cell, the Mascarene High, dominates while the Monsoon Trough extends across South Asia in the Northern Hemisphere. The isobars in the figure depict a strong ridge over East Africa and a trough is present over northern Somalia. Analysis of wind data reveals a minimum in wind speed near the equator yet there is no equatorial trough present in the pressure field.

Bannon (1979a) showed that the jet is a result of the interplay between the inertial and coriolis force, surface friction and weak subsidence. He further noted that the inner shear of the jet is produced locally by bottom friction acting in conjunction with the sloping coastal orography and that in order for the easterly flow south of the equator to change into westerly, north of the equator, convergence of the flow must occur at the transition latitude and the meridional mass flux must vanish. The differential surface drag between land and sea is important in the eastward displacement of the jet core (Bannon, 1979a).

Using monthly mean winds, Findlater (1971) showed that the jet splits into two branches over the Arabian Sea (Fig. 2.4), one branch passing southeastwards towards Sri Lanka and the other eastwards through peninsular India. This split was attributed to barotropic instability (Krishnamurti *et al.,* 1976; Murakami *et al.,* 1970). This was however disproved by Joseph and Sijikumar (2004) who suggest that such analysis as used by Findlater (1971) is likely to show the two branches of the jet as occurring simultaneously suggesting a split. Their study of 12-year composites of the monsoon onset and active and break spells and individual days showed that there is no splitting of the jet over the Arabian Sea. They found that the jet passes through India only if there is active monsoon convection in the latitudes 10^0-20^0N over the Southern Asia, and that in the absence of strong convection over the region, the jet curves clockwise over the Arabian Sea under conservation of potential vorticity and passes east close to the equator. The two branch structure is also not supported by studies undertaken by Halpern *et al.* (1998) and Halpern and Woiceshyn (1999).

Evidence exists that the jet is forced by low-level divergence in the subtropical high-pressure belt over the South Indian Ocean and convergence in the monsoon trough over India (Anderson, 1976; Hart, 1977; Cadet and Desbois, 1981) and has a quasi-biweekly oscillation [Krishnamurti *et al.*, 1976; Joseph and Sijikumar, 2004]. Krishnamurti *et al.* (1976) observed that the meridional pressure gradient between these two regions has a strong component with a 14-day period during the Northern Summer monsoon. Their analysis also revealed a similar oscillation in wind speed of the jet. In their investigation of a fluctuation of the Somali Jet during the Indian summer monsoon of 1978, Cadet and Desbois (1981) used low-level air circulation analysis to study cross-equatorial winds over the Arabian Sea. They found that the weakening of the jet was related to a wind discontinuity to the east of Madagascar drastically reducing the flow into the area of the jet and that the wind intensity within the jet reaches its lowest value two or three days after the first appearance of the wind discontinuity. Observations of wind speeds at Garissa, Kenya, show that increases in the wind speed lagged pressure drops over central India by a few days during July 1973 (Raghavan *et al.*, 1978). These results suggest that the 14 –day pressure oscillation over the Indian Ocean causes surges in the Somali jet.

The quasi-biweekly oscillation of the jet has been found to be related to a similar oscillation in rainfall over India associated with break and active monsoon phases, with cross-equatorial winds being stronger during a strong monsoon than a weak one (Krishnamurti and Bhalme, 1976). A correlation has been found between rainfall over the western coast of India and the intensity of low-level equatorial winds over Kenya (Findlater, 1977). Cadet and Desbois (1981) observed that a break of the monsoon rain over India occurred when the wind intensity was weak along the East African coast.

As stated earlier, if the jet transports significant negative potential vorticity into the Northern Hemisphere, this may lead to instabilities (see Hoskins, 1974) and, importantly to strong southward (anticyclonic) turning of the low-level flow so that the jet tends to avoid India potentially leading to a monsoon break there.

Knox (1976) and McPhaden (1982) showed that westerly winds in the equatorial Indian Ocean have strong intraseasonal oscillations which are associated in summer with fluctuations in the Indian summer monsoon [Sikka and Gadgil, 1980; Webster *et al.,* 1998; Goswami and Ajaya Mohan, 2001].

2.2.1 Characteristics of local summer winds over the Somali region.

The synoptic winds which drive the upwelling along the East African coast are predominantly southwesterly during the northern summer. These winds form part of the Somali jet during the southwest monsoon. The jet is forced by low-level divergence in the subtropical high pressure belt over the Southern Indian Ocean which includes the Mascarene High and convergence in the monsoon trough over India (Anderson, 1976; Hart, 1977). The jet is modulated by the Intertropical Convergence Zone (ITCZ) and the East African topography (Gatebe *et al.,* 1999).

The mesoscale winds over the region, on the other hand, are driven by topographic and thermal contrasts. It has been found that the surface temperatures over land for the region increase by 18^0C during the morning (Hart *et al.,* 1977), indicating that the effect of the localized land-sea heating contrast is present in the pressure field and, consequently, the wind field. Ardanuy (1979) found a change of direction of the low-level winds at Obbia on the coastal plain of Somalia which back to a slightly inland component during the morning and early afternoon, and then veer slightly offshore during the evening and night. Findlater (1972) observed a pronounced sea-breeze front over the Kenya coast where the axis of the jet crosses it. Thus some interaction between the jet and a sea-breeze circulation normal to the jet axis is expected. In explaining wind speed variations of the jet, Ardanuy (1979), Findlater (1971) and Bannon (1979) suggested that the land and sea breeze circulation could cause displacements in the jet near the coast.

The land-sea breeze circulation is driven directly by land sea surface temperature contrasts. When the synoptic pressure gradients are weak, sea/land breeze dominate in the coastal zone. During periods of strong synoptic pressure gradients, sea breeze effects are superimposed upon the cross-equatorial flow, resulting in alongshore acceleration of wind during the day time. A thermal front is established during the day as the land heats up and the across-shore horizontal thermal gradient increases.

Over upwelling regions, cool SSTs established through the upwelling response to the jet winds act to sharpen the air mass boundary between the cool moist air over the ocean and warm dry air over the land. Onshore flow associated with seabreezes is rotated towards the along-shore direction by the coriolis effect as the day progresses.

Mesoscale wind variability over ocean regions of upwelling is highly coupled to the variability of the underlying SSTs. The mechanism responsible for the coupling between SST and surface wind is the change of boundary layer stability that occurs as air crosses the cold SSTs and blows over the warmer water. The advection of relatively warm boundary layer air over the cold SSTs stabilizes the atmospheric boundary layer and inhibits downward turbulent mixing of momentum from aloft. This decoupling of the surface winds from the stronger winds aloft decelerates the near-surface wind and results in lower surface wind over the cold water (Bond, 1992). As the surface winds cross the SST front towards warmer water, the boundary layer is destabilized and surface sensible heat flux and evaporation increase greatly (Zhang and McPhaden, 1995). Convection driven by the enhanced surface heat fluxes increases the downward flux of momentum from aloft and accelerates the surface winds. The downwind acceleration results in a divergence of the surface wind field over the SST front (Wallace *et al.*, 1989; Chelton *et al.*, 2001a).

The wind stress response to geographical variations of the underlying SST field can be better characterized in terms of the wind stress divergence. The largest wind stress divergences are located directly over the strongest SST gradients and the divergence is locally larger where the wind stress is aligned perpendicular to isotherms (i.e., parallel to the SST gradient vector). Wallace *et al.* (1989) hypothesized an SST modification of the wind stress field such that the wind stress curl is positive where the winds blow parallel to isotherms (i.e., perpendicular to the SST gradient vector). This pattern in the wind stress curl field develops because the winds are stronger over the warmer water to the right of the wind direction in the Northern Hemisphere, resulting in a lateral gradient of the wind stress that corresponds to a positive wind stress curl. This hypothesis by Wallace *et al.* (1989) was confirmed by Chelton *et al.* (2001a).

2.2.2 The influence of Topography and Orography of the Somali Coast on the Jet.

The East African coastal region is bounded to the west by mountains which rise to over 1 km within a few km of the coastline. The coastline of the Somali region up to the Horn of Africa has an eastward inclination of about 40^0 away from the north and the ocean topography of the region includes a narrow continental shelf with a steep coast line to the Somali basin that falls to 4000m, with the Carlsberg ridge to the northeast (Fig. 2.6).

Numerical experiments have indicated the important role of orography in the intensification of local winds. In his model, Bannon (1982) found that the mountains of East Africa are crucial to western intensification of the cross-equatorial flow of the Somali jet. He found in this model that approximately 40-55% of the Southern Hemisphere easterlies are deflected meridionally.

2.3 Indian Ocean Surface Currents.

The winds over the Indian Ocean north of 10°S reverse direction twice a year. Over the North Indian Ocean, they generally blow from the southwest during June–August (summer monsoon) and from the northeast during December–February (winter monsoon), March–April and September-October being the months of monsoon transition with weak winds. The winds are much stronger during the summer monsoon than during the winter monsoon. These seasonally reversing monsoon winds over the North Indian Ocean force a seasonally reversing circulation in the upper ocean (Shankar *et al.*, 2002).

There are four upper ocean currents affecting the East African coast. These are the South Equatorial Current (SEC), the East African Coastal Current (EACC), the Equatorial Counter Current (ECC) and the Somali Current (SC) (Figure 2.7*)*. The westward moving South Equatorial Current, driven by the Southeast Trades, divides into two branches once it approaches the northeastern tip of Madagascar. These are the South East Madagascar Current (SEMC) which flows southwards, and the North East Madagascar Current (NEMC) which flows past the northern tip of Madagascar at Cape Amber and feeds into the East African Coastal Current. The East African Coastal Current flows northwards all year round at least as far as 3^0S. During the Southwest Monsoon, it continues north of this latitude, joins with the Somali Current and continues right to the Horn of Africa. During the Northeast Monsoon (November to March), the northward extent of the East African Coastal Current is more restricted.

At this time, it meets and joins the southward flowing Somali Current (which changes direction under the influence of the monsoon) with this convergence taking place anywhere between 3^0S and 1^0S, depending on the strength of the monsoon in any particular year. The two streams then turn eastward and flow offshore as the South Equatorial Counter Current (SECC). (Tychsen, 2006; Schott *et al.*, 2001).

The circulation in the Indian Ocean north of 10^0S is strongly seasonal, and the currents experience a complete reversal from January-February to July-August in sympathy with monsoon wind reversals (Schott *et al.*, 2001).

A climatology of ship-drift data shows that the surface currents in the equatorial Indian Ocean reverse direction four times a year. They flow westward during the boreal winter, weakly westward in the central and western ocean during the corresponding summer, and strongly eastward during the spring and autumn (Schott *et al.*, 2001).

The eastward jets during spring and autumn are called Wyrtki Jets and they are strongest between 60^0E – 90^0E (Fig.2.8) (Wyrtki, 1973). Other seasonally reversing currents include the Somali Current along the coast of Somalia; the winter Northern Monsoon Current (NMC) and the summer Southern Monsoon Current (SMC) in the mid-basin (Shankar *et al.*, 2002); and the West India Coastal Current (WICC) and the East India Coastal Current (EICC) (Shetye and Gouveia, 1998). This highly seasonal circulation north of 10°S is a superposition of tropical and coastal locally and remotely forced waves with frequencies that range from intraseasonal to interannual (Shankar *et al.*, 2002).

Local forcing refers to direct driving by alongshore components of coastal winds and remote forcing refers to any other process and includes offshore wind fields that excite Rossby waves (Schott *et al.*, 2001). The seasonal circulation in the tropical Indian Ocean is driven by a combination of equatorial Kelvin waves, equatorial Rossby waves and coastal Kelvin waves with Ekman drift; all of which depend on the monsoonal winds. The Wyrtki jets which occur during the spring and autumn raise sea-level and deepen the thermocline in the east and reverse in the west (Wyrtki, 1973). Hurlbert *et al.* (1976) demonstrated that Ekman transport enters the equatorial region along the western boundary whereas along the eastern boundary the current flows north and south from the equator in a narrow coastal jet. Wyrtki (1973) suggested that the eastward jets are forced directly by the equatorial westerlies between the two monsoons. O'Brien and Hurlburt (1974) demonstrated this behaviour in a 2-layer model.

They also noted that Rossby waves reflected from the eastern boundary of their model basin were an important part of the equatorial response that tended to cancel the directly forced eastward jet two months after the wind onset. Since the monsoon has variability ranging from intraseasonal to interannual, it follows that the surface ocean circulation manifests the same pattern. Further south, the winds and currents are found to be less variable than in the North Indian Ocean, owing to the absence of reversing monsoon winds (McCreary *et al.*, 1993).

Under the relatively steady southeasterly trades, the westwards South Equatorial Current at approximately 10^0S is dominantly geostrophic, with an additional Ekman contribution in the boreal summer. The eastward South Equatorial Counter Current at 5^0S is mainly geostrophic, but virtually eliminated by the westward directed Ekman component in boreal summer (Hastenrath and Greischer, 1991; Tomczak and Godfrey, 1994).

These currents result in a basin scale region of cyclonic circulation, which has also been identified by ocean model studies of McCreary *et al.* (1993) and referred to as the *Tropical Gyre.* Woodberry *et al.* (1989) have suggested that the tropical gyre is driven by wind stress curl over the ocean interior and associated with the Southern Hemisphere trades. The presence of this cyclonic current shear in the western half of the Indian Ocean basin was later confirmed by Hastenrath and Greischer (1991) and found to persist in varying shapes throughout the year.

Ocean model studies by McCreary *et al.* (1993) have further shown the variable nature of the ECC, which was influenced by the near-equatorial ocean and zonal wind field. Tomczak and Godfrey (1994) suggested that the ECC peaks between December and April in response to the prevailing NE monsoon and the absence of a westward Ekman drift. Consequently, a region of shallow thermocline was observed from the ocean model of McCreary *et al.* (1993) from 2.5^0S to 10^0S. The model results display Ekman suction by raising the thermocline in this region to a minimum depth of 35m through the year.

2.4 The Somali current and Upwelling at the Somali coast

The Somali Current which is driven by the Somali Jet is the only one that reverses its direction of flow under the influence of the monsoon. It flows in a south-westwards direction at about 0.8-1.0 ms^{-1} with the Northeast Monsoon (November to March). During the Southwest Monsoon (April to October), the current reverses its flow and increases its velocity to around 1.0-1.3ms^{-1}. This seasonal development of the Somali Current system was described by Schott *et al.* (1990). Before the onset of the monsoon, the southern Somali Current is an extension of the East African Coastal Current (EACC) that flows northward across the equator to about 3–4°N. There, it turns offshore, and a cold wedge develops along its shoreward shoulder. Farther north, alongshore winds cause an upwelling regime to develop with a shallow northward coastal flow overlying a southward undercurrent. Its width scale is of the order of 50–100 km.

With the monsoon onset in June, the 'Great Whirl' (GW) develops from 4–10°N, and a second cold wedge appears at the latitude where it turns offshore (10–12°N) (Fig. 1.3). Schott and Quadfasel (1982) discussed observations from moorings in the northern Somali-Current regime. During their observational year there was a sudden onset of the monsoon, and they reported that there were distinct westward-propagating signals after the onset. They interpreted them as first-mode Rossby waves, and concluded that the onset of the Great Whirl was a response to the very strong anticyclonic wind-stress curl offshore from the Somali coast by these long Rossby waves which reflected into short Rossby waves at the boundary, accumulating energy there.

The cross-equatorial flow continues during this time, now transporting about 20 Sv in the upper 500 m. It leaves the coast south of 4°N, where part turns eastward and part flows back across the equator in a circulation pattern referred to as the 'Southern Gyre' (SG). After crossing the equator, western boundary currents typically turn offshore to join near-equatorial eastward flows in the interior ocean. The eastward deflections generally occur after the boundary current first overshoots the latitude band of the eastward flow and then retroflects equatorward.

The Southern Gyre appears to develop from a retroflection of this sort. When the Southwest Monsoon dies down, in about October-November, the cross-equatorial Somali Current turns offshore again at 3°N, while the Great Whirl continues to spin in its original position (Schott *et al.*, 2001)(**Fig. 1.3**). During the North East Monsoon, the winds blow away from the Indian Subcontinent and the surface Somali current reverses to flow southwards.

After crossing the equator, the Somali Current encounters the northward flowing East African Coastal Current, resulting in a confluence and eastward turn off at 2-4^{0}S that supplies the South Equatorial Current, (Swallow *et al.*, 1991).

The seasonal variations of the monsoons therefore control the Somalia current. During the strong boreal summer monsoon, the current is intensified in a northeastwards direction while in the austral summer; it reverses its direction and reduces its strength in sympathy with the weakened Northeast monsoon winds. Substantial cooling occurs in the vicinity of Somalia commencing in June at the equator and during July in the Arabian Sea. The cooling is associated with both upwelling and evaporation accompanying the freshening winds of the southwest monsoon (Knox *et al.*, 1987). Figure 2.9 shows mean velocity sections across Somali Current on the equator (northward is positive) during the summer monsoon (left), during the winter monsoon (middle) and annual mean.

The Somali current has been described as a time-dependent, baroclinic inertial boundary current with non-linear effects on time scales longer than two weeks (Hurburt *et al.*, 1976) and has a stable flow as established by Cox (1979) and Sekine (2000) experiments with a slanted western boundary at the same angle as the actual Somali coastline (40^0 east of north). Using a numerical model and assuming a barotropic ocean of 1000m depth, Sekine (2000) demonstrated that a large meander path is found in the case of a current with a northern boundary inclination (NBI) of less than 20^0. However when he increased the NBI to 30^0, the western boundary current became stable with a non-large meander flow.

2.6 Summary

The Somali current is of great interest because unlike the Gulf Stream in the Atlantic and Kuroshio in the Pacific, it is present during only part of the year since the driving wind stress reverses with the monsoons; and it flows across the equator.

The Somali Current Ecosystem is a biotic region, with a wide variety of subsystems. These include coral reefs, mangroves, seagrass beds, beaches, and estuaries (Okemwa, 1998). The rich diversity of many endemic plants and animals are both aesthetically and economically important with tourism and marine wildlife utilization (Okemwa, 1998).
The associated upwelling manifests itself with a southern tongue at about 4-8^{0}N in the early period of the southwesterly monsoon and a northern tongue appearing as the winds intensify in June/July. The southern upwelling region is of interest to the communities living around it, including Kenya, because of its nutrient rich characteristics and major fishing activities.

Although the large scale features of the atmosphere and ocean circulation of the region are fairly well understood, less is known about the mesoscale wind variability in the region and its impacts on the upwelling. Thus, this thesis is aimed at improving the understanding of mesoscale characteristics of wind fields and air-sea interaction on the southern upwelling region.

In order to assess the significance of wind stress to strong upwelling in the region, a significant upwelling event in the past nine years (1999-2007) that QuikSCAT data are available is identified and the temporal and spatial variability of the winds are investigated. Wind and SST co-variability over the region are investigated and wind stress curl is analysed to assess the strength of the upwelling.

A range of data sets from global centres and analytical techniques, described in the following chapter, are employed to address these research objectives.

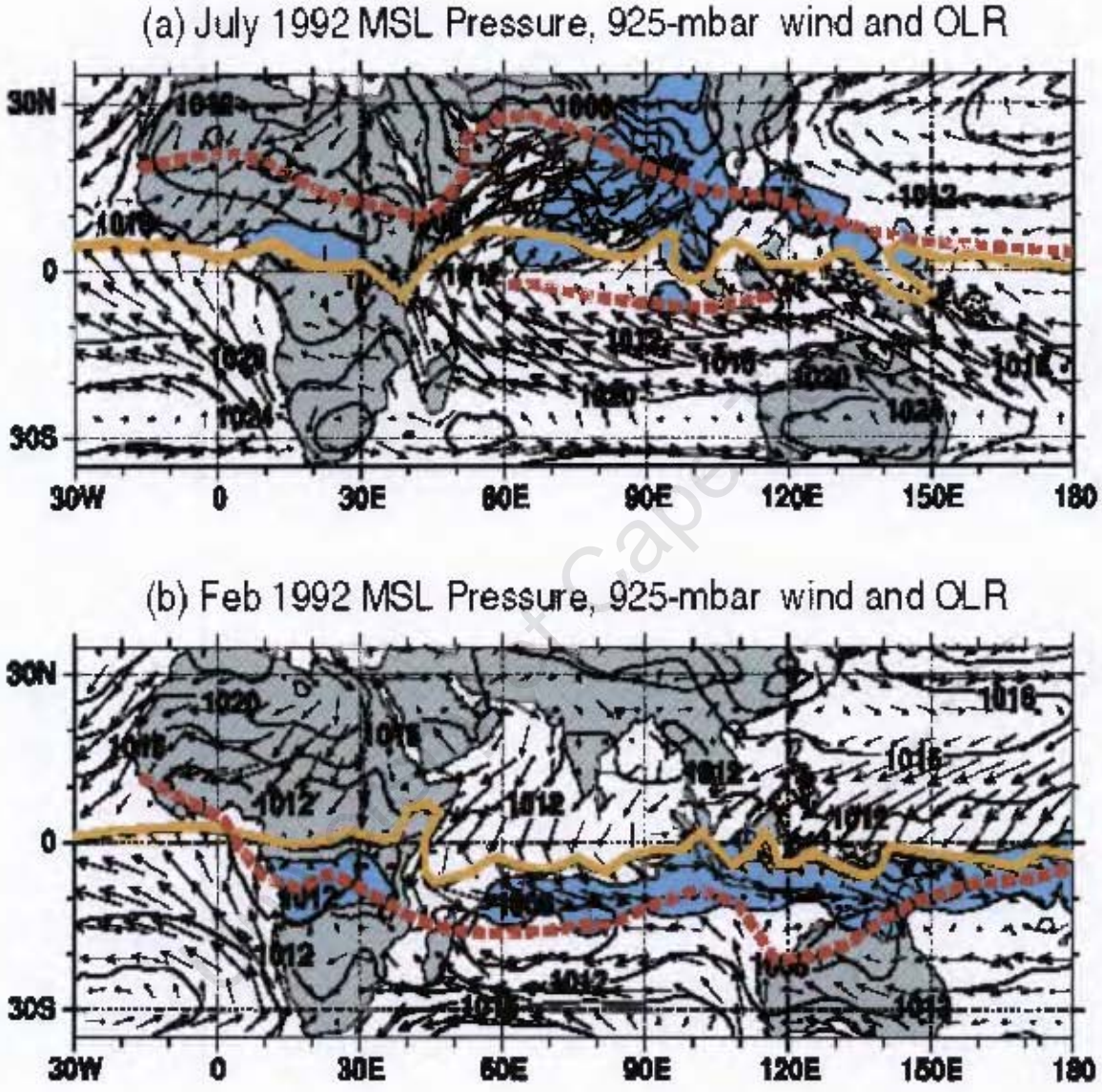

Fig. 2.1Showing movement of the ITCZ (red line)and the zero absolute vorticity contour (yellow line). Surface pressure (black solid contours) and 925--mbar horizontal wind (vectors) for (a) July and (b) February 1992 over the eastern hemisphere are also depicted. Adapted from P. J. Webster et al (1998)

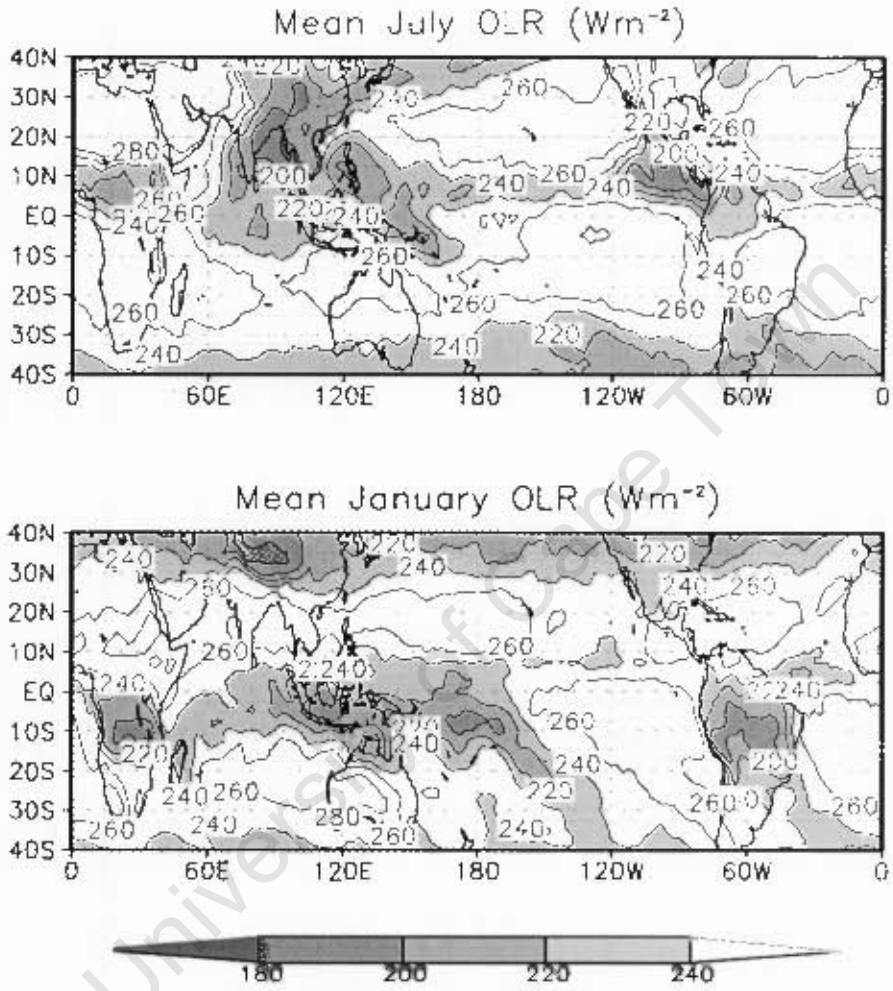

Fig.2.2 Mean OLR (wm^{-2}) for January and July from Gadgil (2003)

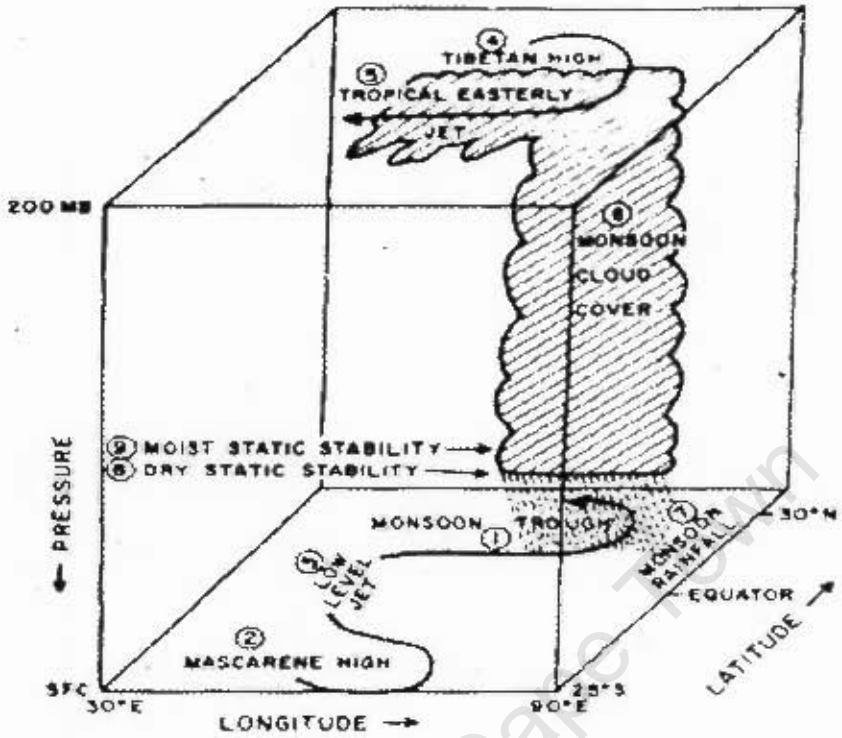

Fig 2.3 Schematic diagram of the nine elements of the monsoon system following Krishnamurti et al. (1976).

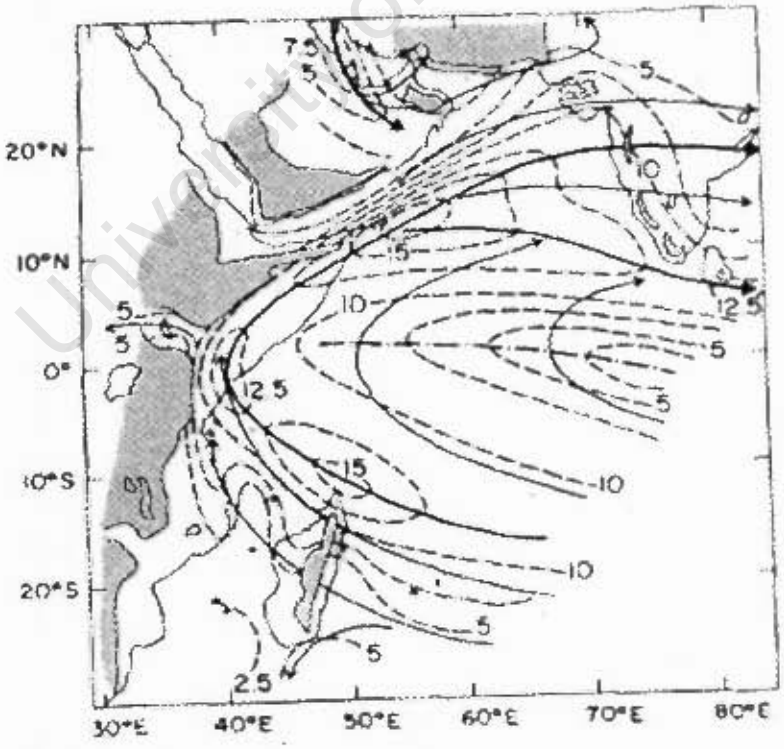

Fig. 2.4. Mean flow pattern at 1 Km level for July. Solid lines denote streamlines. Heavy line is the axis of maximum flow. Dashed lines are isotachs. Dot-dashed line is axis of minimum wind speed. Shaded areas correspond to orography greater than 1km. Following Findlater (1971).

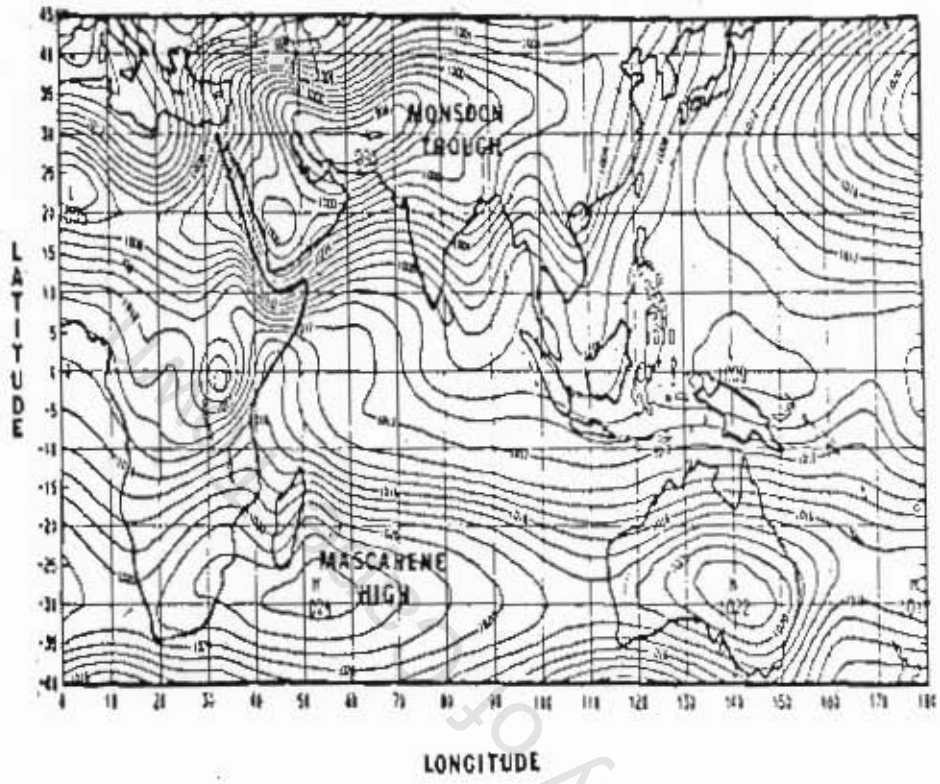

Fig. 2.5 Mean sea level pressure for July (after van de Boogaard, 1977). Contour interval 1 mb

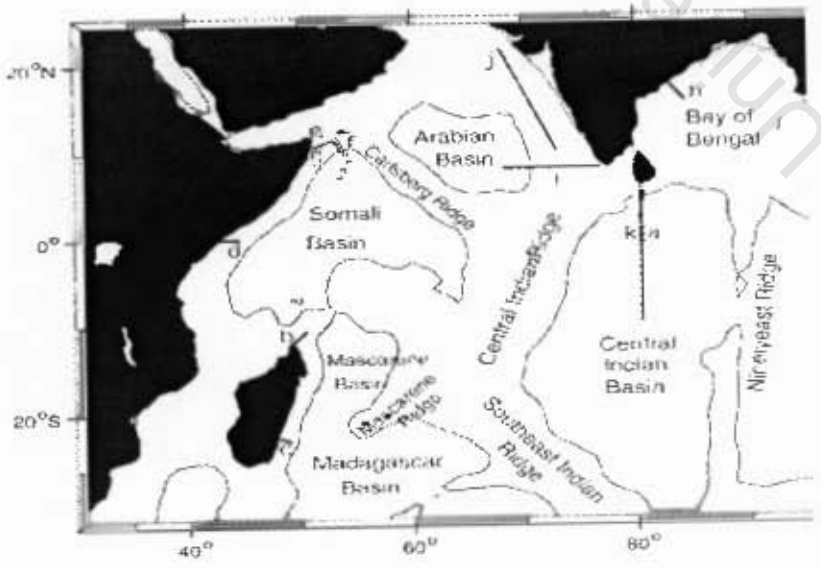

Fig. 2.6 Map western Indian Ocean showing the topography of Somali region with the smoothed 4000 m depth contour.

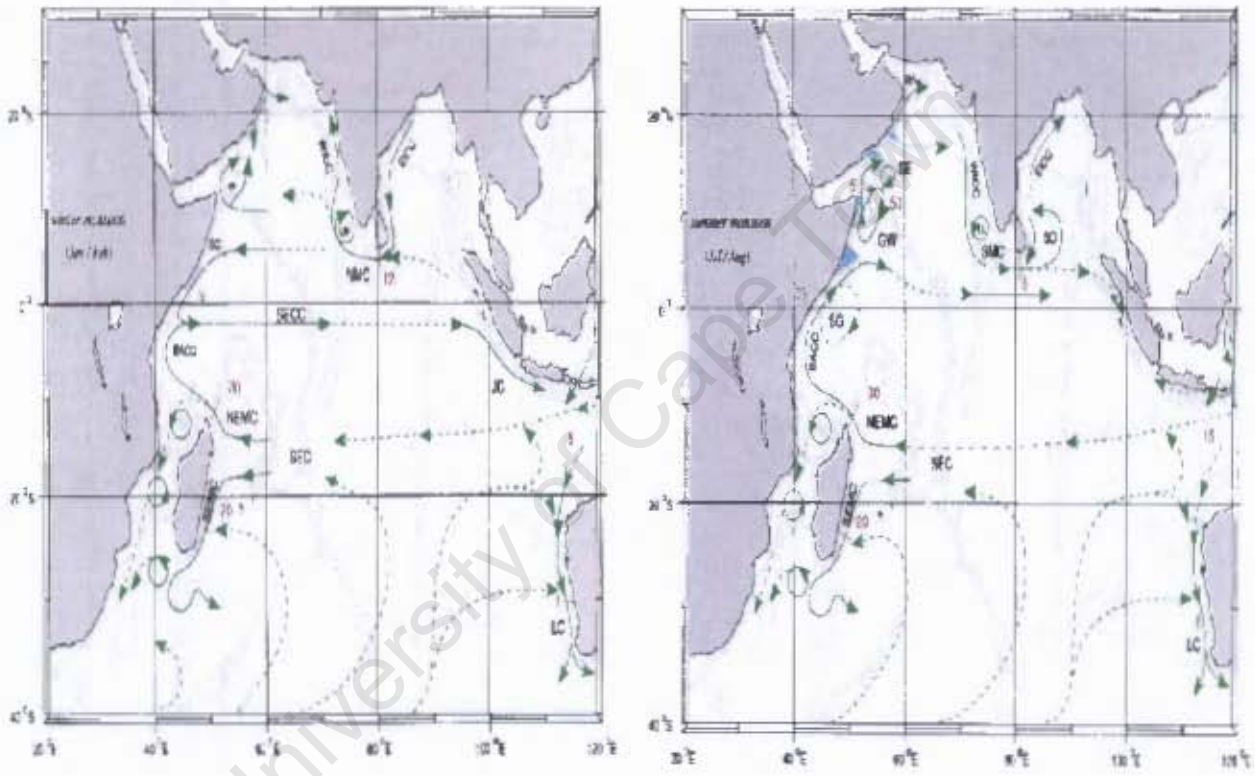

Fig. 2.7 (a) left and (b) right: a schematic representation of currents observed during January–February (Northern winter) and July-August (Northern summer) respectively (Adapted from Schott et al. 2001.

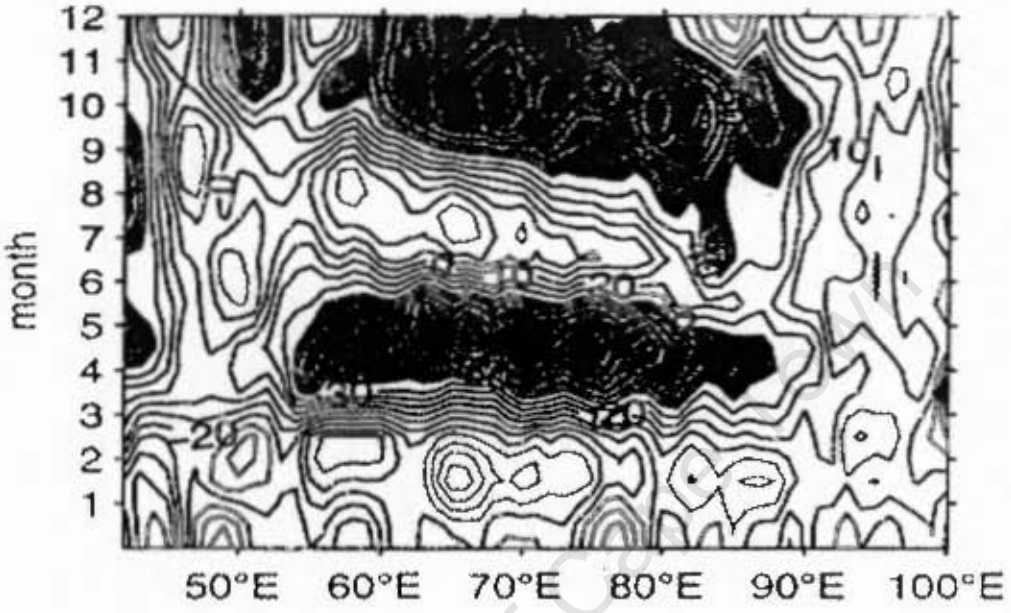

Fig. 2.8: Strong eastwards flowing jets during Northern spring

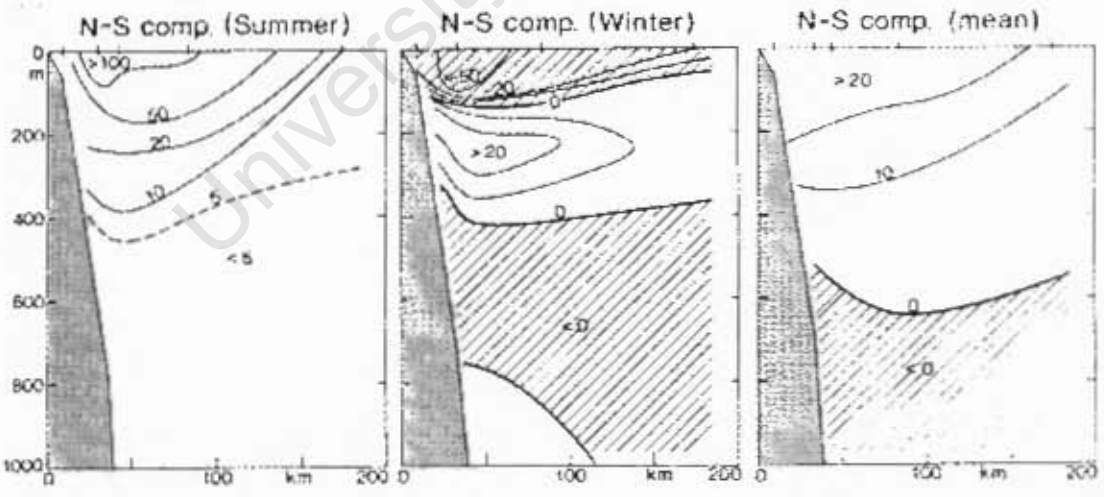

Fig. 2.9 Mean velocity sections across Somali Current on the equator (northward is positive) during the summer monsoon (left), during the winter monsoon (middle) and annual mean (right); (from Schott et al., 1990);

Chapter 3

Data and Methodology

In this chapter, the datasets used in this thesis and the methodology employed to analyse them are discussed. These data include the high resolution TMI weekly (seven day average) Sea Surface Temperatures (SSTs) from the Tropical Rainfall Measuring Mission (TRMM) satellite available from December 1997 to the present. The data are used to investigate a significant upwelling event during the period 1999-2007 and the spatial structure of SSTs over the region 10^0S-20^0N and 35-65^0E. QuikSCAT weekly wind stress and wind stress curl data from the Center for Satellite Exploitation and Research (CERSAT) are used to investigate the temporal variability of the alongshore winds at the upwelling region and the spatial structure of the wind stress curl respectively. Both the TMI SSTs and the QuikSCAT winds are used to investigate SST-Wind co-variability over the the upwelling region. Sea level pressure data from NCEP/NCAR Reanalysis are used to create a *time series* to assess variability in a Sea Level Pressure Index (SLPI).

A variety of statistical techniques are employed to investigate the characteristics of wind fields and air-sea interactions over the upwelling region off the Somali coast. These methods include an extensive use of the MATrix LABoratory (MATLAB) programmes. Through MATLAB programming, Continuous Wavelet Analysis (CWA) is employed in the analysis of temporal variability of the Somali Jet and SSTs over the Somali coast.

3.1 Significant southern upwelling event

To identify a significant upwelling event during 1999-2007, high resolution weekly (seven day average) Sea Surface Temperatures (SSTs) data from the Tropical Rainfall Measuring Mission (TRMM) satellite are used. The weekly sea surface temperatures were preferred because of their more accurate representation of SSTs and upwelling processes than monthly data. Though 3-day averaged data is also available for viewing SSTs, there is inherent problem of missing data in these high resolution data sets.

The TMI SSTs are derived from observations made by a radiometer onboard the Tropical Rainfall Measuring Mission (TRMM) satellite. This radiometer, the TRMM Microwave Imager (TMI) is well-calibrated, and contains lower frequency channels required for sea surface temperature retrievals. TRMM is a joint program between National Aeronautics and Space Administration (NASA) and the National Space Development Agency of Japan (NASDA).

TMI data are provided as daily, 3-day means, weekly means and monthly means and are available from December 1997 to the present. They cover a global region extending from 40S to 40N at a resolution of 0.25^0 x 0.25^0 (~25 km x 25 km). The TRMM satellite produces data collected at changing local times for any given earth location between 40S and 40N.

The production of this data set is a collaborative effort with the TRMM Project at Goddard Space Flight Centre (GSFC) and the Passive Microwave Earth Science Information Partnership (ESIP) for Climate Studies. The Passive Microwave ESIP (PM-ESIP) was established to provide climate products derived from satellite microwave radiometers and is a joint effort among NASA's Global Hydrology and Climate Centre, the University of Alabama in Huntsville, and Remote Sensing Systems.

The measurement of sea-surface temperature (SST) through clouds by satellite microwave radiometers has been an elusive goal for many years.

The early radiometers in the 1980s (i.e., SMMR) were poorly calibrated, and the later radiometers (i.e., SSM/I) lacked the low frequency channels needed by the retrieval algorithm. Finally, in November 1997, the TMI radiometer with a 10.7 GHz channel was launched aboard the TRMM satellite.

The important feature of microwave retrievals is that SST can be measured through clouds, which are nearly transparent at 10.7 GHz. This is a distinct advantage over the traditional infrared SST observations that require a cloud-free field of view. Ocean areas with persistent cloud coverage can now be viewed on a daily basis. Furthermore, microwave retrievals are not affected by aerosols and are insensitive to atmospheric water vapour. However, the microwave retrievals are sensitive to sea-surface roughness, while the infrared retrievals are not.

A primary function of the TRMM SST retrieval algorithm is the removal of surface roughness effects. The microwave and infrared SST retrievals are very complementary and can be combined to obtain a reliable global data set.

Evaluation of TMI SST data is ongoing. However, the accuracy of the TMI SST estimate in rain-free conditions is roughly 0.5^0C (Wentz *et al.,* 2000; Kummerow, 2000). Recent comparisons of the TMI SST estimates with moored observations of near-surface ocean temperature have found that on greater than weekly time scales, the TMI SST successfully reproduces the character of the 1-m-depth buoy-observed temperatures in the tropical Pacific (eg Chelton *et al.,* 2001a).

A comparison of the TMI SST estimate over the Bay of Bengal and the Arabian Sea with moored near-surface (2.5-m-depth) temperatures found a strong correspondence in the evolution of the two SST estimates on a greater than weekly time scales (Senan *et al.,* 2001). The spatial structure of the SST features from TMI compares well with that from the Pathfinder Advanced Very High Resolution Radiometer (AVHRR) satellite-based infrared SST dataset [available from NASA's Physical Oceanography Data Access and Analysis Center, http://podaac.nasa.go/].

Further, TMI SSTs are validated by comparing them with *in-situ* measurements made by moored buoys located in both the tropical Pacific and tropical Atlantic oceans. Validation of the satellite-derived SSTs is necessary to check the retrieval algorithm developed for the TMI 10.7 GHz channel. Data from the tropical Pacific moored ocean buoys which consist of mostly TAO array buoys operated by the Pacific Marine Environmental Lab (PMEL), the US National Data Buoy Centre (NDBC) and PIRATA buoys moored in the tropical Atlantic Ocean are used to compare with and validate the TMI SST estimates (Fig. 3.1). Further information on this data is available at
http://www.ssmi.com/tmi/tmi_description.html

A Hovemoller plot has been created for the four hundred and eight weeks spanning the period under investigation and closer investigation carried out on specific weeks of this data to highlight the temporal changes which occur in the upwelling. The weeks selected for the spatial structure were the second to last week of July and the last weeks of June, August and September for each year under investigation. The evolving Somali Jet during the southwesterly monsoon was considered in choosing the weeks. Using this method, a significant upwelling event was identified around 4.25^0N in July 2005 as discussed in the next chapter.

An inter-annual time series of SSTs at the grid point 4.25^0N and 50.25^0E over the upwelling region was created to assess their temporal variability. Continuous Wavelet Analysis is then applied to investigate dominant modes of variability in the SST time series and how these modes vary with time.

3.2 Temporal variability of alongshore winds

An inter-annual time series has been created to investigate the temporal variability in alongshore winds over the upwelling region. This has been achieved by extracting weekly QuikSCAT wind stress values at 4.25^0N, 50.25^0E. from the Center for Satellite Exploitation and Research (CERSAT)'s 0.25^0 x 0.25^0 gridded data product. Continuous Wavelet Analysis is then used to investigate dominant modes of variability in the wind stress time series and how these modes vary in time.

QuikSCAT wind data are 0.25^0 x 0.25^0 gridded data product from the Center for Satellite Exploitation and Research (CERSAT). A microwave scatterometer SeaWinds (QuikScat) instrument was launched on the QuikBird satellite in June 1999 with a primary mission to measure winds near the ocean surface. These data are also useful for some land and sea ice applications. The SeaWinds instruments are the third in a series of NASA scatterometers that operate at Ku-band (i.e., a frequency near 14 GHz). SeaWinds scatterometers are essentially radars that transmit microwave pulses down to the Earth's surface and then measure the power that is scattered back to the instrument. This "backscattered" power is related to surface roughness. For water surfaces, the surface roughness is highly correlated with the near-surface wind speed and direction. Hence, wind speed and direction at a height of 10 meters over the ocean surface are retrieved from measurements of the scatterometer's backscattered power.

The QuikSCAT Scatterometer data processing uses simultaneous microwave radiometer measurements for rain flagging and sea ice detection. It uses 4 satellite microwave radiometers (F13 SSMI, F14 SSMI, F15 SSMI, and TMI) to determine if rain is present at the location of the QuikScat observation. Using the Special Sensor Microwave Imager (SSMI) daily observations of sea ice, the scatterometer observations can be properly flagged so that reliable wind vectors can be obtained. Risien (2002) found the QuikSCAT data to be highly comparable with NCEP/NCAR climatology (1968-1996),

More information on this data can be found at: http://podaac.jpl.nasa.gov/quikscat/.

3.2.1 Continuous Wavelet Analysis (CWA)

Continuous Wavelet Analysis has been used to investigate dominant modes of variability in the QuikSCAT wind stress and TMI SST time series and how those modes vary in time. CWA is a powerful tool as it allows frequency analysis of a time dependant signal locally in time (Daubenchies, 1990). This is particularly appropriate for geophysical time series due to the non-stationary nature and the numerous scales at which geophysical processes take place (Lau and Weng, 1995).

A brief explanation of the advantages of the CWA technique and the Continuous Wavelet Transform (CWT) used will be given here. More detailed explanations of wavelet analysis and the Complex Morlet Wavelet Transform are provided by Torrence and Compo (1998), Daubenchies (1992) and Lau and Weng (1995).

When doing frequency analysis of non-stationary time series over a large range of frequencies, CWT has advantages over the more commonly used Fourier transform (Fig. 3.2a) in spectral analysis. Ideally, one would like to separate the shorter period oscillations from the longer in a non-stationary time series.

Fourier transforms do not contain any time dependency in the signal and therefore cannot provide any local information regarding the time evolution of its spectral characteristics (Lau and Weng, 1995).

A Windowed Fourier Transform (WFT) Fig. 3.2b, may be used to extract local frequency information under a fixed time frequency window, but is problematic when dealing with a wide range of frequencies. At low frequencies, there are so few oscillations within the window that the frequency localization is impaired, while at high frequency there are so many oscillations that the time localization is again impaired (Torrence and Compo, 1998).

The advantage of using wavelet transforms (Fig. 3.2c) is that the transform can be stretched and translated with resolutions in both frequency and time (Lau and Weng, 1995). As a result, the signal can be decomposed in terms of wavelets which are derived form a 'mother wavelet' $\mathbf{\Psi_0(\eta)}$ by dilations and translations (Lau and Weng, 1995).

The scaled wavelet is defined by Torrence and Compo (1998) as:

$$\psi\left[\frac{(n'-n)\delta t}{s}\right] = \left(\frac{\delta t}{s}\right)^{1/2} \psi_0\left[\frac{(n'-n)\delta t}{s}\right] \quad \text{.....(1)}$$

where the wavelet

$$\psi\left[\frac{(n'-n)\delta t}{s}\right] \quad \text{.....(2)}$$

is translated along the time index **n** (translation parameter) and its scale is varied by the dilation parameter **s.** The **o** subscript has been dropped to indicate that Eq. (2) has been normalized. A energy normalization factor of $\mathbf{S^{-1/2}}$ keeps the energy of the 'daughter wavelets' the same of the 'mother wavelet' ensuring that wavelet transforms at each scale are directly comparable to each other (Torrence and Compo, 1998; Lau and Weng, 1995). This also means that if the 'unscaled mother wavelet' $\Psi_0(\eta)$ is normalized to have unit energy then wavelets at each scale will have unit energy.

This continuous wavelet transform of a discrete signal $\mathbf{X_n}$ is defined as the convolution of $\mathbf{X_n}$ with a set of scaled and translated wavelets (Torrence and Comp, 1998; Lau and Weng, 1995).

$$W_n(s) = \sum_{n'=0}^{N-1} x_{n'} \psi^*\left[\frac{(n'-n)\delta t}{s}\right] \quad \text{.....(3)}$$

Ψ^* is the complex conjugate of Ψ. The CWT reveals a local measure of both relative amplitude and phase at a scale of variability proportional to s and time n. Scale s is synonymous with the period of the wavelet and inverse its frequency and so that CWT is a time-frequency analysis.

Although it is possible to solve the wavelet transform in the time domain using equation (1), it is much simpler to perform the wavelet transform calculation in Fourier space using a Fast Fourier Transform (FFT) of the time series and the wavelet function as described by Torrence and Compo (1998).

The Morlet Wavelet was chosen in this thesis as it is the most commonly used wavelet in geophysical signal detection (Lau and Weng, 1999). The Morlet Wavelet consists of a complex exponential modulated by a Gaussian function as in equation (4)

$$\psi_0(\eta) = \pi^{-1/4} e^{i\omega_0 \eta} e^{-\eta^2/2} \quad \text{.....4}$$

where $\Psi_0(\eta)$ is the Morlet Wavelet value at a non-dimensional time η.
A non-dimensional frequency $\omega_0 = 6$ (Torrence and Compo, 1998) is used which satisfies the admissibility condition (Farge, 1992).

The advantage of the Morlet Transform is that it is able to detect both time-dependent amplitude and phase for different frequencies exhibited in the time series (Lau and Weng, 1995). The resultant wavelet transform coefficient $W_n(s)$ contains both real and imaginary parts which can be used to assess the amplitude and phase of the local components of the signal.

Depicted in two-dimensional space with time on the x-axis and period on the y-axis, the wavelet power spectrum provides a local measure of the time series variance at each period (Torrence and Compo, 1998).

A problem with performing the Wavelet Transform calculation in Fourier space is that this assumes the time series is cyclic resulting in a wraparound effect. To reduce these effects, one end of the time series is equaled to zero.

The time averages over all local wavelet power is defined as the Global Wavelet Spectrum (GWS) (Torrence and Compo, 1998).

$$\overline{W}^2(s) = \frac{1}{N}\sum_{n=0}^{N-1}\left|W_n(s)\right|^2 \quad \text{.....(5)}$$

The GWS is equivalent to the Fourier power spectrum smoothed by the Morlet wavelet function in Fourier space (Farge, 1992).

Because of the 'Uncertainty Principle' (Chui, 1992), the width and height of a time-frequency window cannot be arbitrary (**Fig. 3.3**), Lau and Weng (1995). This means that at high frequencies, high precision in time localization is less precise and frequency resolution higher (Lau and Weng, 1995). Reduction in frequency resolution at small scales results in the peaks in the spectrum being smoothed out, while at larger scales the wavelet although wide in time is narrow in frequency and therefore the peaks are sharper and have larger amplitudes. As a result, the GWS is a biased estimator and one should not use the GWS to determine the relative magnitude of peaks.

The wavelet transform is essentially a bandpass filter of uniform shape and varying location and width, extracting the different local components of the signal by providing amplitude and phase values for every frequency and time (Melice et al, 2001).

The results of the continuous wavelet analysis on the temporal variability of the QuikSCAT winds and SSTs over the upwelling region are discussed in detail in the next chapter.

3.3 Temporal variability in Sea level pressure index during the year 2005

A second time series was created to assess variability in Sea Level Pressure Index (SLPI) based on daily averaged NCEP/NCAR reanalysis sea level pressure data, with a grid of 2.5 x 2.5, from 1st January – 31st December 2005 corresponding to the year of the significant upwelling event. A strong off-shore pressure gradient was observed around 19th July 2005.

The Sea level Pressure data used to investigate the Sea Level Pressure Index is from the NCEP/NCAR Reanalysis (Kalnay et al, 1996). In this reanalysis, data assimilation is performed using a state-of-the-art analysis/forecast system on historical data from 1948 to the present.

A large subset of this data is available from CDC in its original 4 times daily format and as daily averages. The daily averages are means of instantaneous values at the 4 reference times of 00, 06, 12 and 18z. The global data has 2.5^0 horizontal resolutions.

More information is available at:
http://www.cdc.noaa.gov/cdc/data.ncep.reanalysis.html

The spatial variability of wind stress over the upwellng region has been investigated using weekly wind vector plots from QuikSACT website. These plots correspond to the weeks ending 2nd, 9th, 16th, 23rd and 30th July 2005.

The spatial structure of wind stress curl have been plotted for the region 10^0S-20^0N and 35-65^0E to identify areas of positive and negative curl using data from QuikSCAT. These plots are used to identify areas of strong positive curl corresponding to strong upwelling.

Both the TMI SSTs and the 10m QuikSCAT winds were used to investigate SST-Wind co-variability over the upwelling region for a period of 13 weeks from 6 June-29 August 2005.

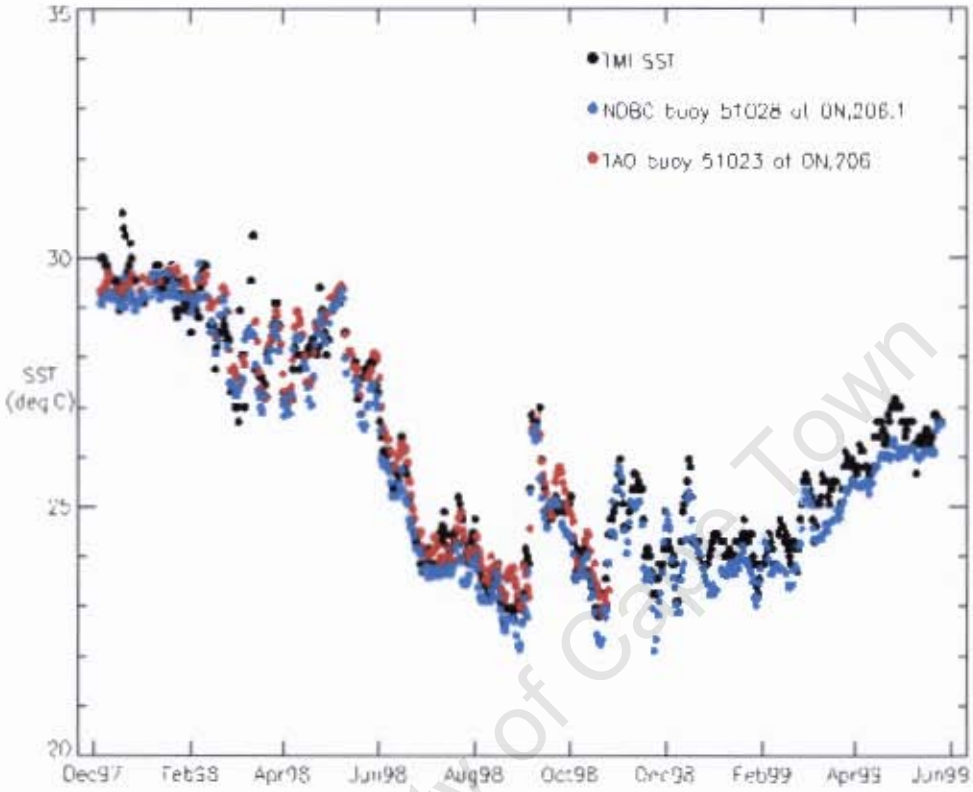

Fig. 3.1 A time series of SSTs showing high correlation between data from two Central Pacific buoys TAO buoy (51023, red), NDBC buoy (51028, blue)and TMI SST data.

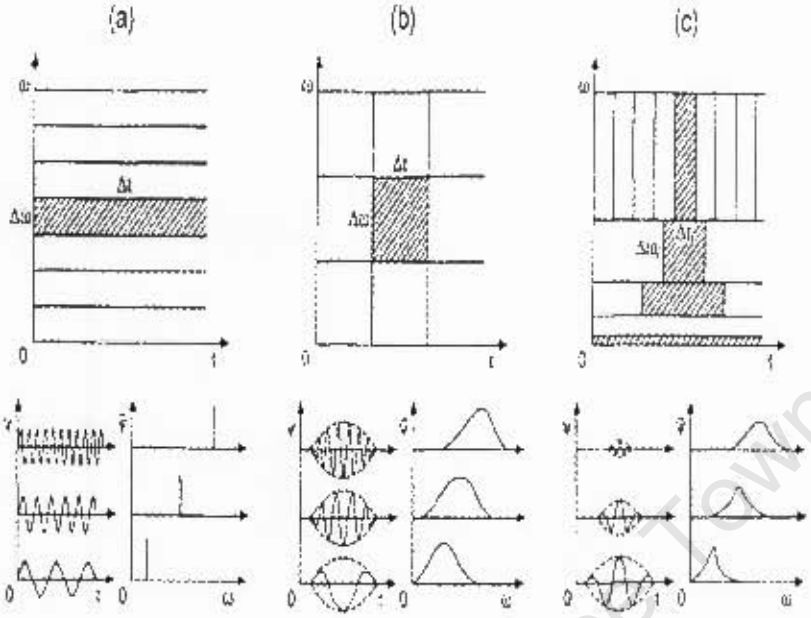

Fig 3.2 Time-frequency windows used in (a) Fourier Transform (FT), (b) a Windowed Fourier Transform (WFT), and (c) Wavelet Transform(WT), and there corresponding time series represented in time space and frequency space, take from Lau and Weng, 1995

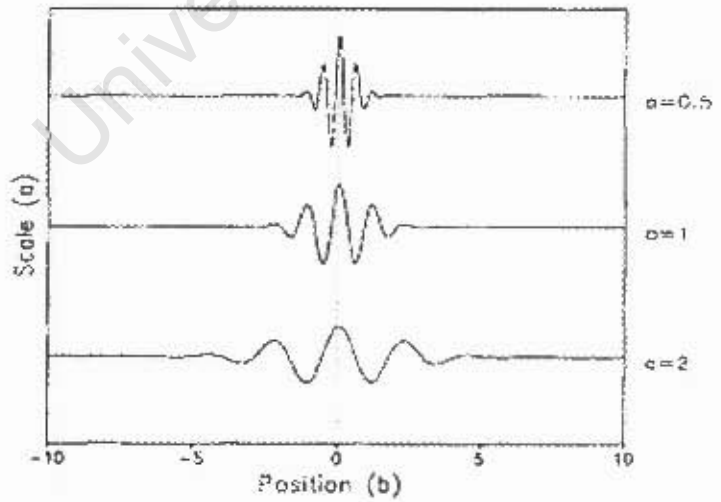

Fig 3.3 Example of morlet Wavelet with different value of scale a, from Lau and Weng (1995)

Chapter 4

Results and Discussion

In this chapter the results of the investigations and findings as outlined in chapter 3 are presented in detail followed by discussion and a summary at the end of each section.

During their study of the Somali current, Schott *et al.* (1990) observed that upwelling occurs where the Somali current turns offshore near 5^0N along the Somali coast and further north near 10-12^0N during the southwest monsoon. The first objective of this thesis is to identify a strong event in the southern upwelling region during the period of nine years from July 1999 to May 2007 when QuikSCAT wind and TRMM SSTs are available. This upwelling event is then analysed as a case study to investigate the mesoscale characteristics of the wind fields over the region during that period. Both temporal and spatial variability of the local winds are then analysed along with the spatial structure of the local SSTs and wind stress curl. The SST-Wind co-variability is also investigated using these data.

4.1 Significant southern upwelling event

A meridional Hovmuller plot of weekly sea surface temperatures (SST) along 50.125^0E between 10^0S and 10^0N was created to identify the significant upwelling event using TMMI sea surface temperatures for the four hundred and eight weeks corresponding to July 1999-May 2007 as shown in Fig. 4.1.

A close investigation of the spatial structure of the SSTs was then undertaken by creating surface plots for the region 10^0S to 20^0N and 35^0E to 65^0E for the weeks corresponding to the second to last week of July and the last weeks of June, August and September each year from 1999- 2006 corresponding to the boreal summer of these years (**Fig 4.2**, panels **i-xxxi**). The evolution of the Somali Jet and the development of upwelling cells was taken into consideration in choosing the weeks.

A critical examination of the Hovmuller plot shows a distinct localized southern upwelling episode characterized by cold sea surface temperatures of below 22^0C at about 4-5^0N during the year 2005. Years 2003 and 2004 show almost similar results but the significant difference between these years and the 2005 event is that the upwelling during 2005 is highly localized with relatively lower temperatures.

Analysis of the northern summer plots show that August and September 2000, June 2002, July 2003, July 2004, July 2005 and June 2006 all had a well marked southern upwelling tongue. However the 2003, 2004 and 2005 upwellings were more intense and exhibited an intensive southern upwelling tongue of cold temperatures.

The 2005 event (panel **xxv** marked with a pink box) exhibits a highly localised nature at around 4.75^0N with rather cold temperatures. It is interesting to note the warmer waters upstream of this upwelling region and a clear southeastward curve orientation of the cold waters. Substantial cooling of surface waters along the entire coast to about 53^0E is visible in all the corresponding plots, mainly in June and July (Panels **vii, xii, xvii, xxi, xxv** and **xxviii**).

The observations by Schott *et al.* (1990) have shown that where the Somali current turns eastward and part flows back across the equator in a circulation pattern referred to as the 'Southern Gyre', a cold wedge develops along its shoreward shoulder. They noted that the fraction of the direct cross-equatorial offshore return in the Southern Gyre appears to vary from year to year. As the monsoon intensifies, the 'Great Whirl' develops further north from about 5-10^{0}N easily identifiable from the plots. The July 2005 significant southern upwelling event is therefore consistent with these observations.

The upwelling region is characterized by extreme cold temperatures with warm waters around it (**Fig. 4.2 panel xxv**). The explanation for this observation will be discussed elsewhere in this thesis.

The substantial cooling of the surface waters along the entire coast up to 53^{0}E visible in all the plots for the northern summer of August 2000, June 2002, July 2003, July 2004, July 2005 and June 2006 (panels **vi, xii, xvii, xxi, xxv,** and **xxviii**) may be explained as cooling due to evaporation, vertical mixing, entrainment and upwelling such that enhanced (reduced) wind speed tends to cool (warm) the oceanic mixed layer.

4.2 Summary

A significant upwelling event characterized by cold sea surface temperatures of below 22^0C with a highly localized nature occurred around 4.75^0N during the southwest monsoon of 2005. This event which occurred in July 2005 was identified by plotting a meridional Hovmuller plot of weekly sea surface temperatures (SST) along 50.125^0E.

Surface SST plots of the region also revealed this upwelling during the week ending 23 July 2005. The cold filament with a clear southeastwards curve orientation is found to be bounded by warm waters around it. Substantial cooling of surface waters along the entire coast to about 53^0E is also visible on the surface plot. This significant and highly localised upwelling event is therefore used as a case study to investigate the characteristics of mesoscale winds over the region in the next sections.

Fig. 4.1 below showing Meridional Hovmuller plot along 50.125E between latitudes 10S and 10N. The localized southern upwelling is clearly discernible somewhere between 05/4 and 06/4 (Colourbar in °C)

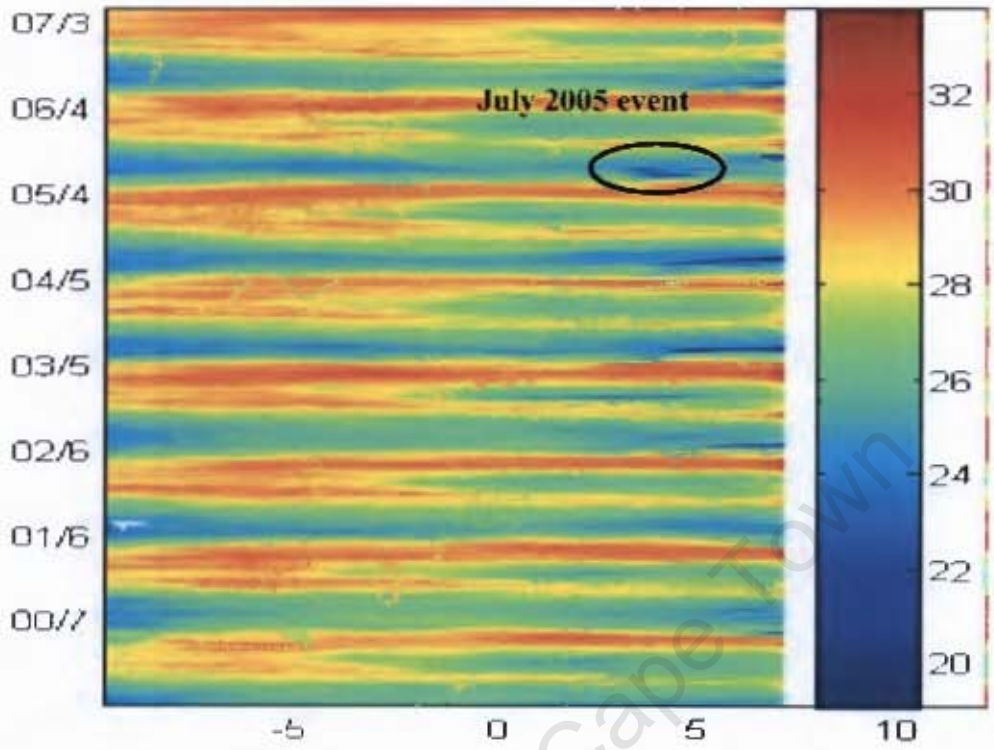

Fig. 4.2 (panels i- xxxi) SST (°C) surface plots for June, July, August and September from 1999 – 2007

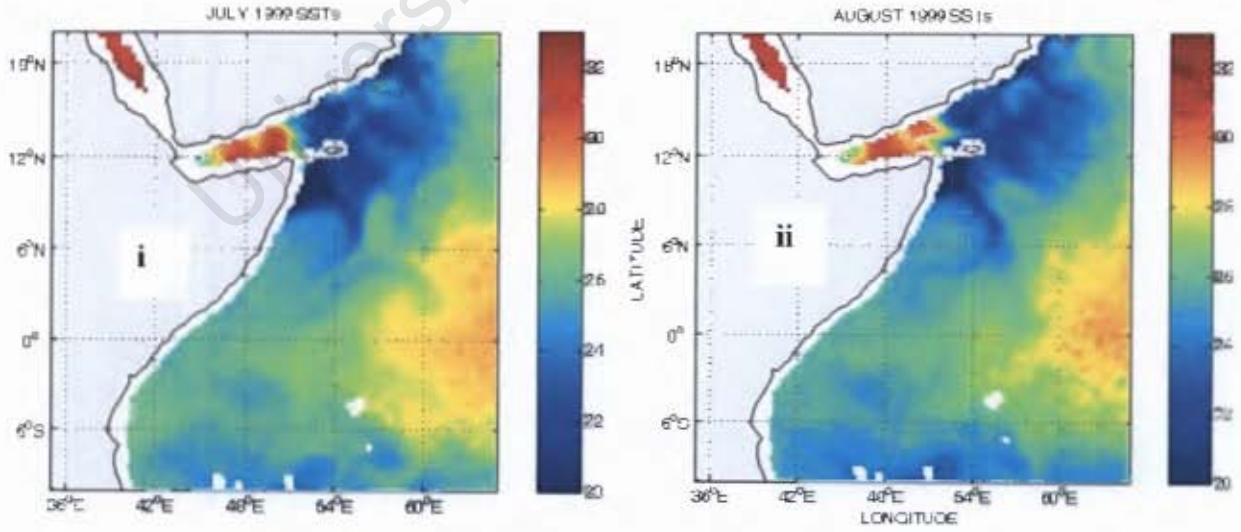

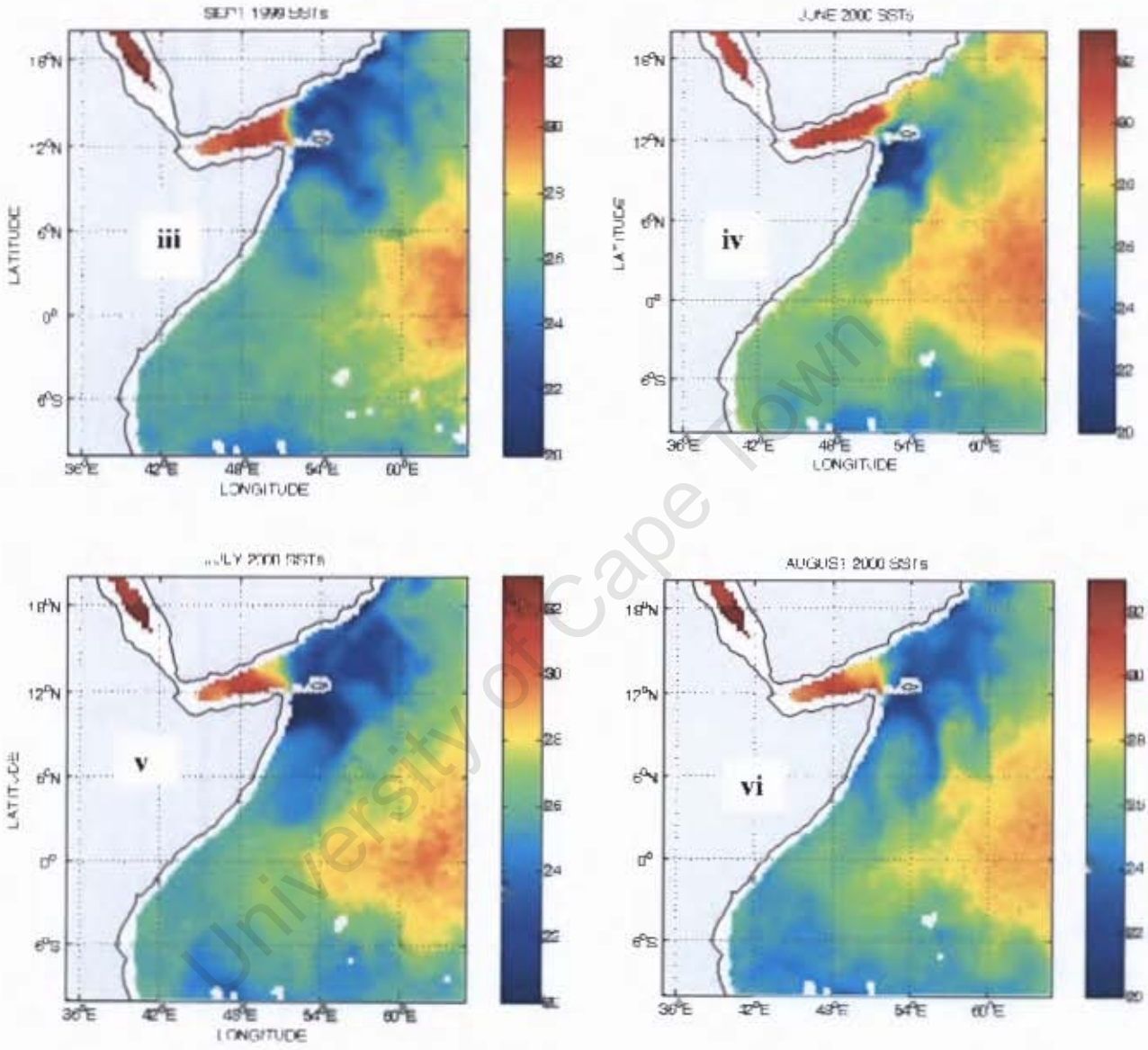

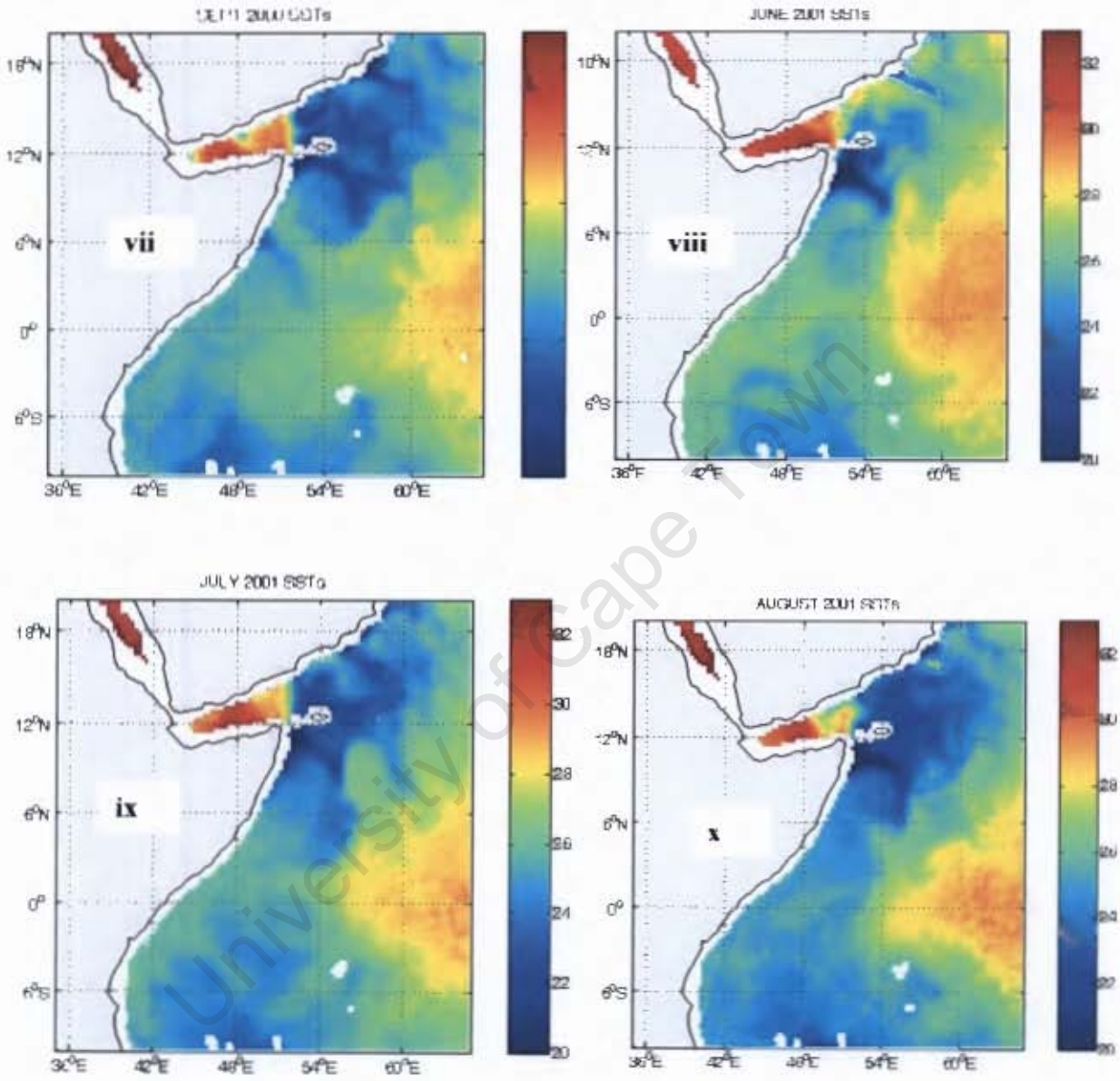

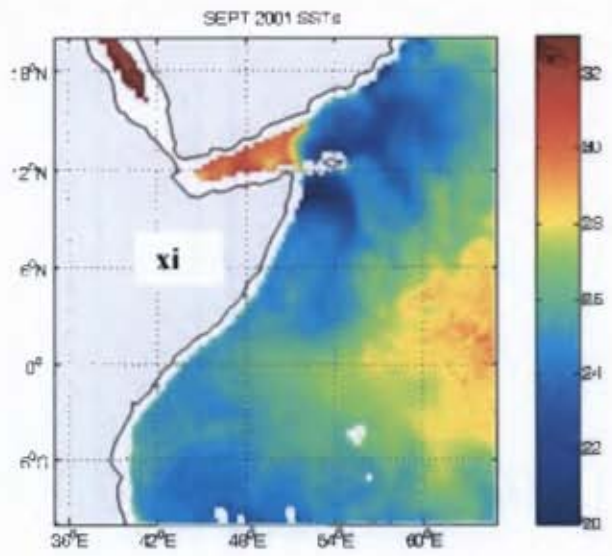

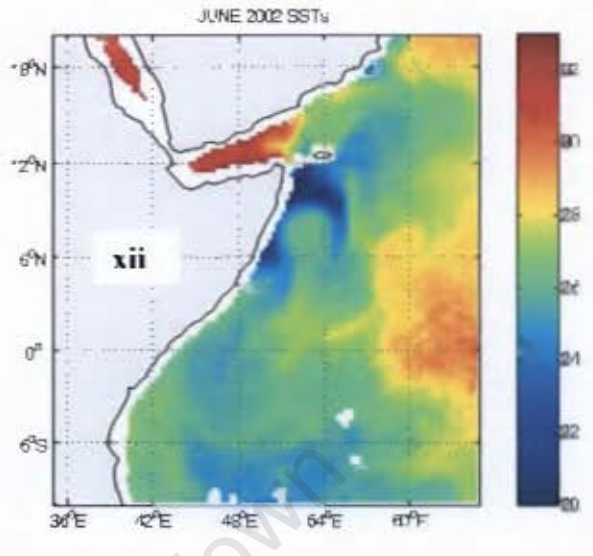

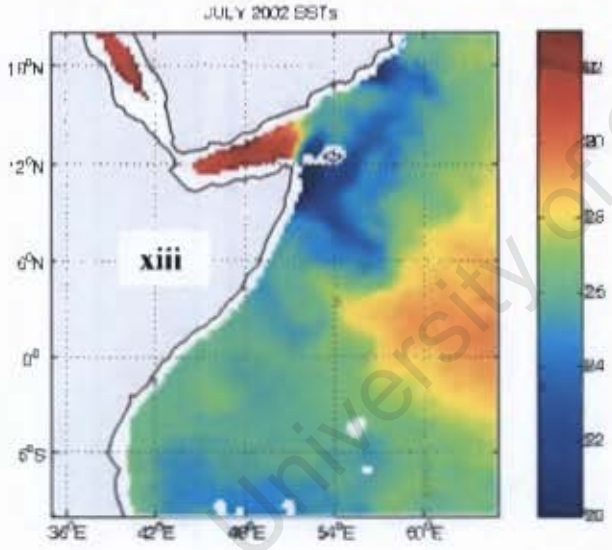

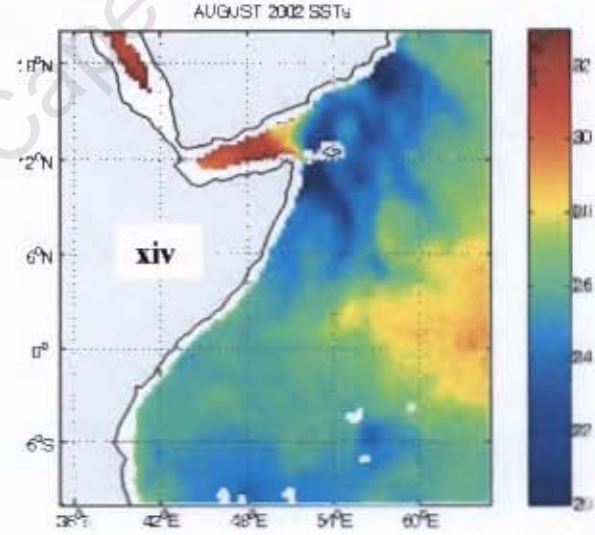

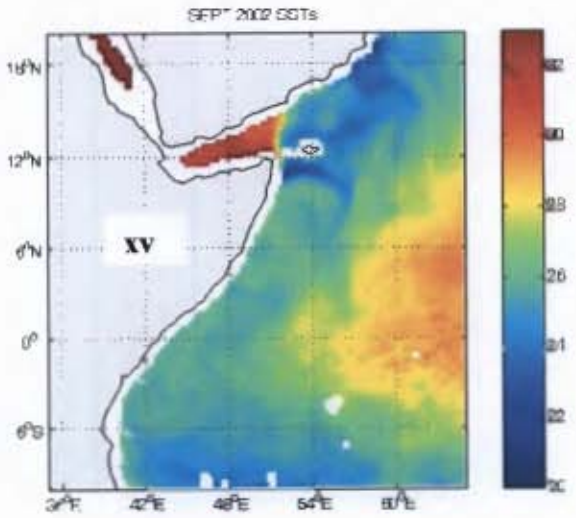

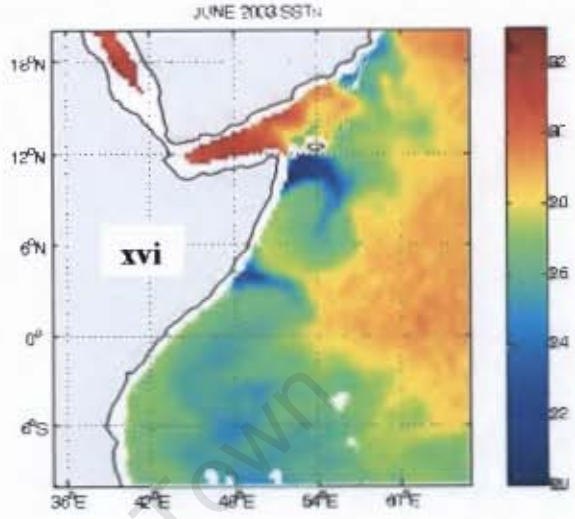

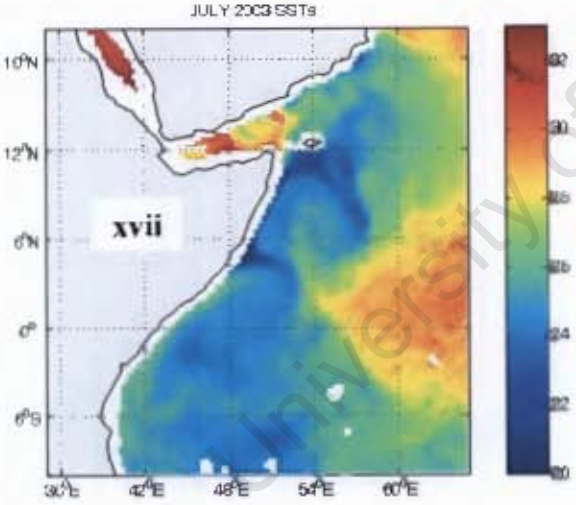

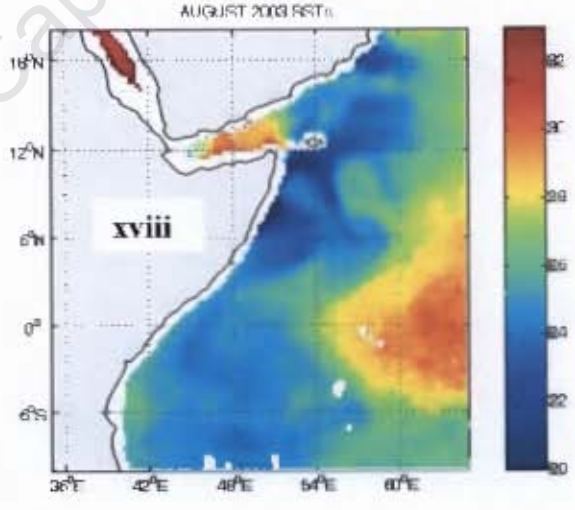

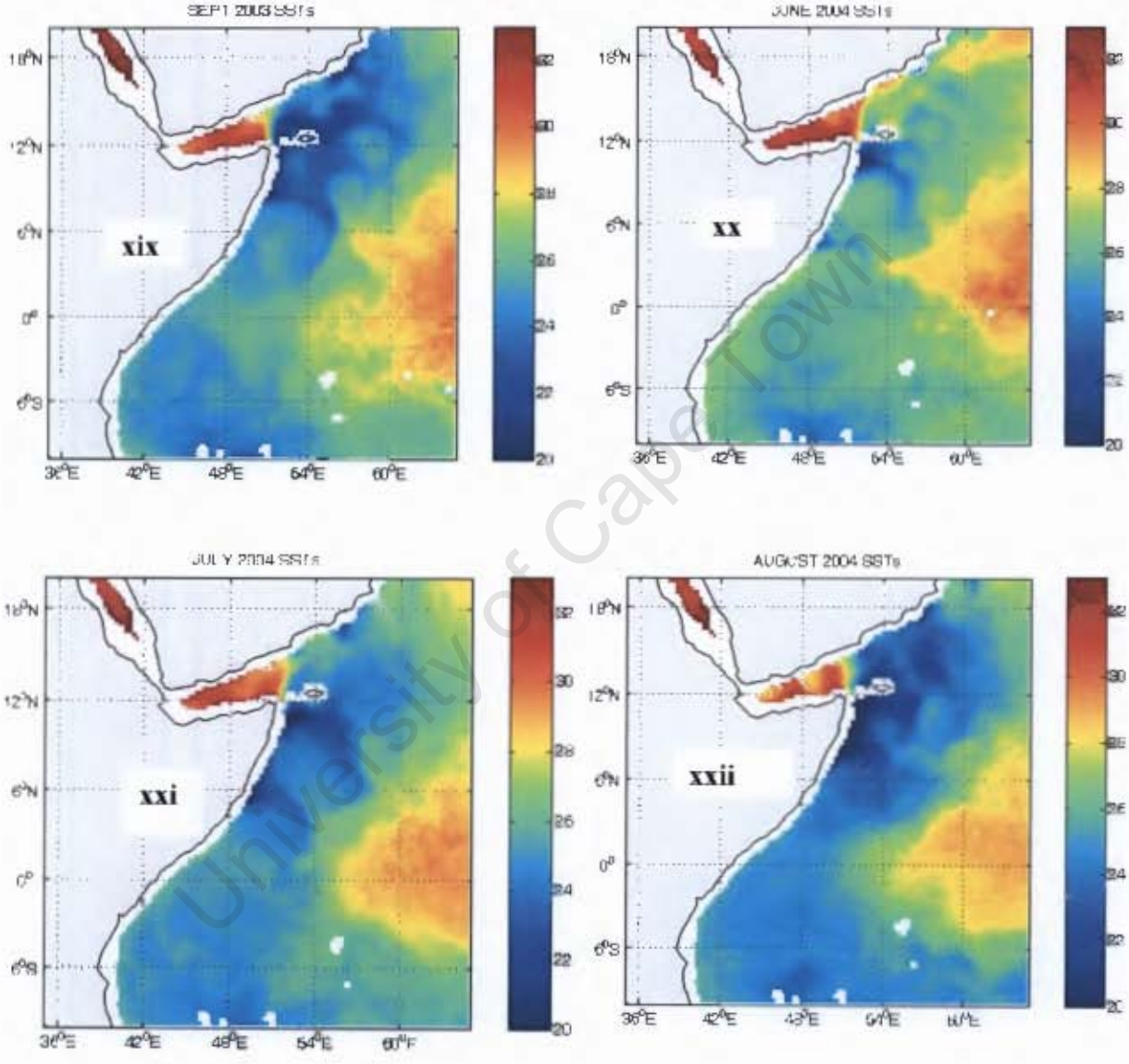

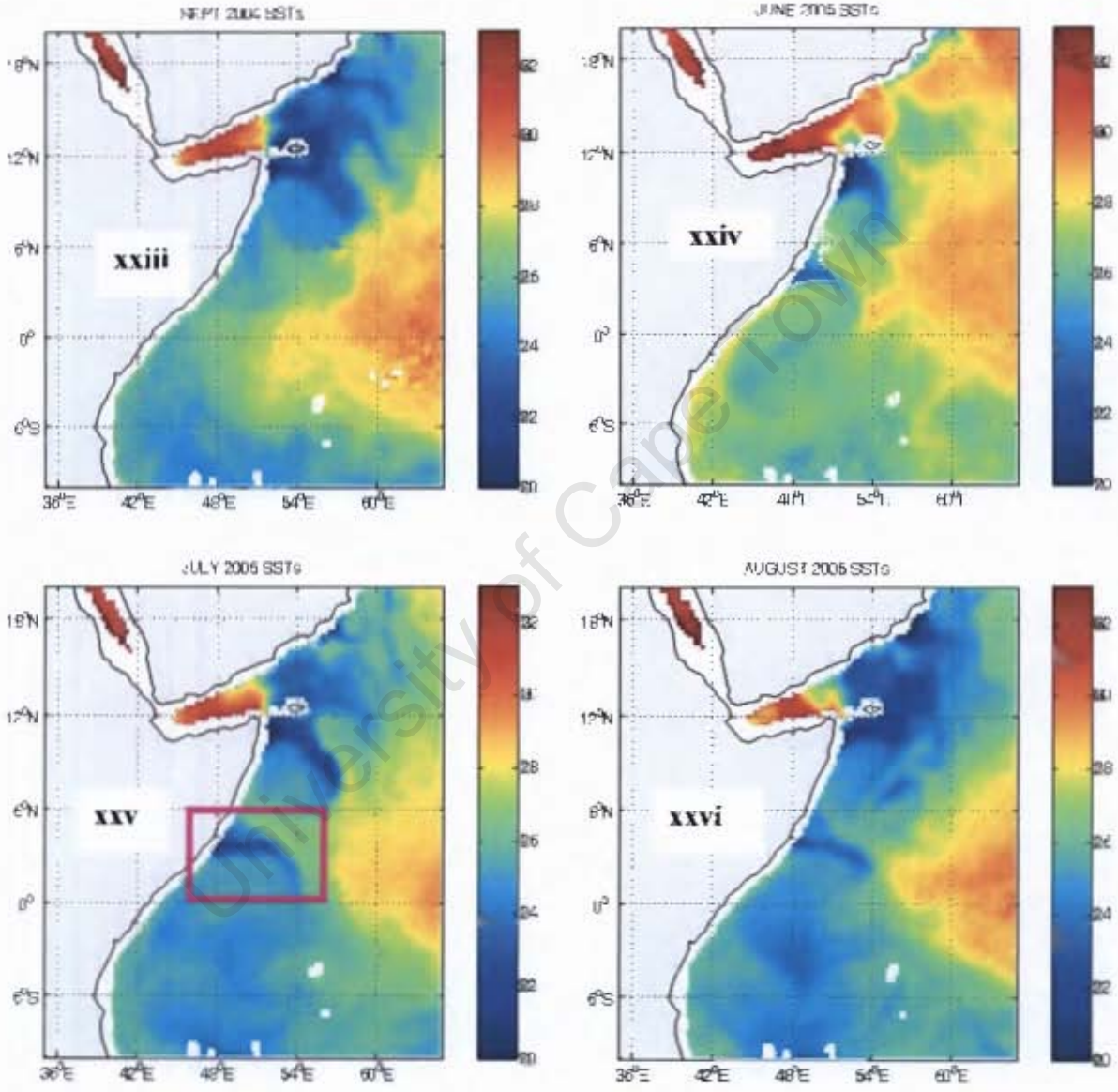

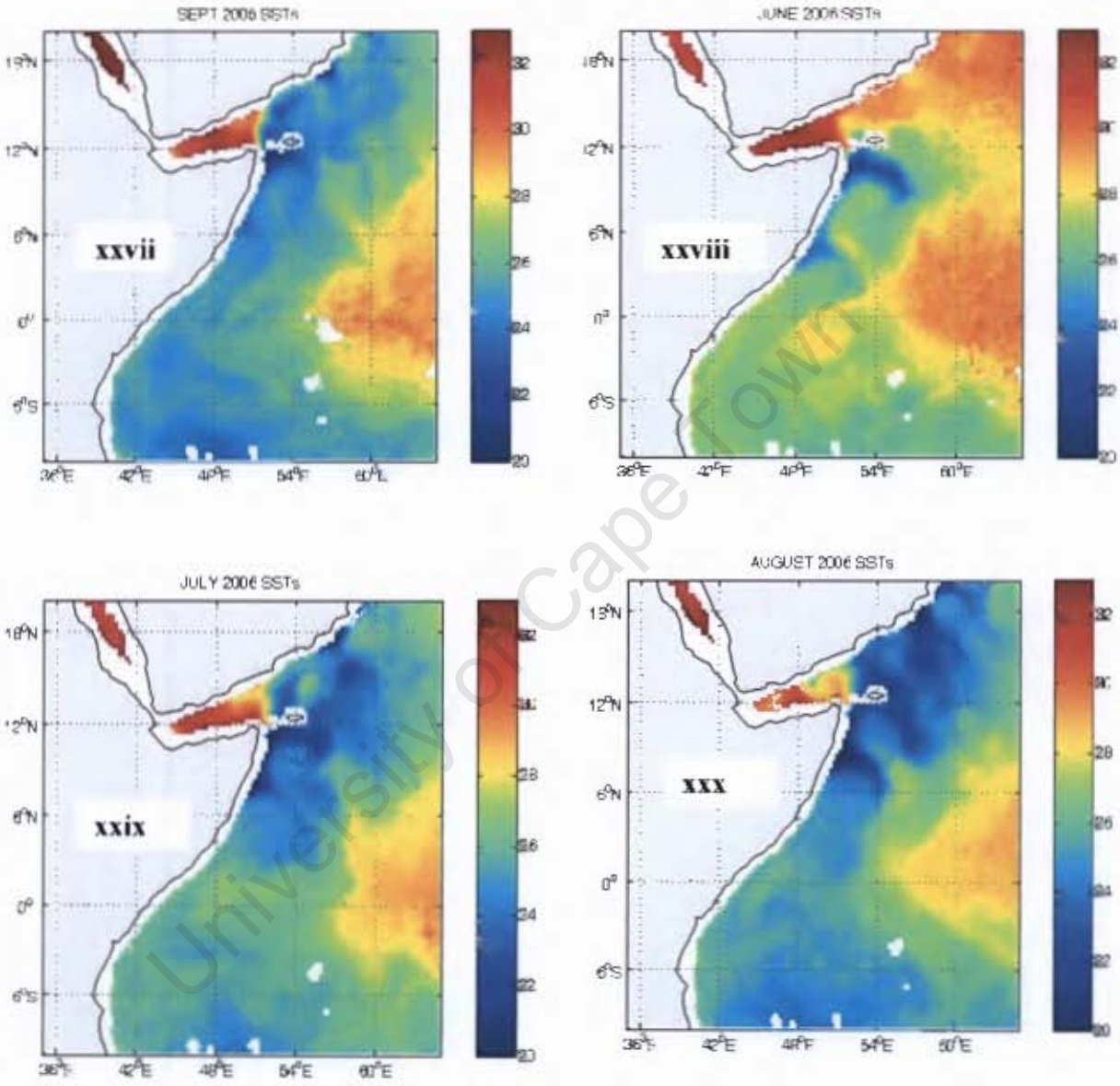

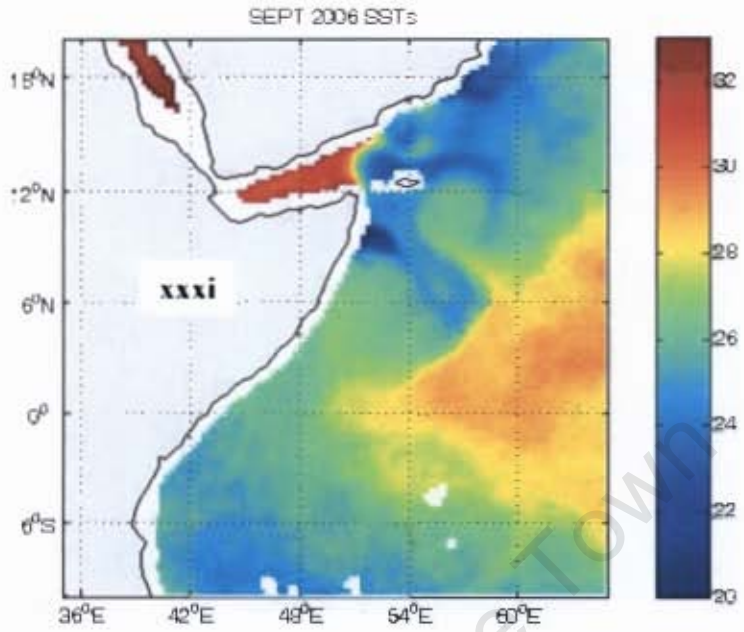

4.3 Temporal variability of Winds over the upwelling region.

A Continuous Wavelet Transform (CWT) has been performed on the wind stress time series to assess the dominant timescales of variability of the Somali Jet over the upwelling region. These winds are usually strong during southwest monsoon. Details about the construction of the time series along with an explanation of the continuous wavelet analysis (CWA) technique used are provided in section 3.2.2 of Chapter 3. To the best of the author's knowledge, no analysis of the jet fluctuations has been pursued using this technique before. In their investigations, Krishnamurti *et al.* (1976) relied heavily on the Fast Fourier Transform.

Weekly QuikSCAT 10m winds were used to create a time series for this investigation at the grid point 4.75^0N and 50.25^0E. The justification for using 10m wind grid point to investigate the low-level jet comes from Murakami (1976) who when analyzing data collected from the Indian Daily Weather Report and upper air observations over the Indian subcontinent during the 1962 summer, found that the zonal and meridional wind anomalies associated with the 10-20-day intraseasonal monsoon mode are in phase over the entire troposphere. Furthermore in investigating the Indian monsoon, Goswami and Mohan (2001) relied on the strength of the 850hPa wind at the single grid point 15^0N and 90^0E.

Prior to the wavelet analysis of the wind stress, a time series correlation of normalised wind stress and SSTs over the upwelling region was constructed for the grid point 4.75^0N, 50.25^0E as in Sciremammano (1979) and wavelet analysis was applied to the SSTs. Fig. 4.3 indicates that strong winds at this point correspond to low SSTs with a correlation coefficient of -0.32 with a confidence level of above 95%. This observation explains the relationship of winds and SSTs as discussed in the previous section. The SST power spectrum (Fig. 4.4b) shows strong power at the semiannual (16-32 week) and annual (52 week) periods and weaker power at other frequencies. Towards the end of 2004 and 2005, the SSTs had higher frequency of variability extending to the intraseasonal periods.

The standardized time series of the wind stress is represented by Figure 4.5a and the results of the Wavelet Transform are presented in Fig. 4.5b which depicts the wavelet power spectrum with time (Year/Month) on the x-axis and period in weeks on the y-axis. The local Wavelet Spectrum provides an indication of dominant timescales of variability of the winds over the entire time series. It is clear from the spectrum that the Somali Jet has three dominant periods of oscillation, one near 2-6 weeks, one near 16-32 weeks, and one at 52 weeks. These periods correspond to intraseasonal, semiannual and annual cycles respectively. In about mid 2001, 2003, 2004 and 2006, strong bifurcations occurred with high power at semiannual periods extending to the intraseasonal scale. An abrupt shift in appearance in the 2004 semiannual oscillations is evident from the amplitude plot (Fig. 4.7) suggesting a strong monsoon shift.

The Morlet Wavelet can be interpreted as a bandpass linear filter. This filter allows the extraction of different local components of the signal like local value, amplitude and frequency by equating all others to zero. Figures 4.6, 4.7 and 4.8, computed using this technique, represent time frequencies of the annual, semiannual and intraseasonal respectively. The blues curves in Figures 4.7 and 4.8 represent the amplitude modulation (the envelopes) of the frequencies.

While the annual amplitude modulation is more uniform (**Fig. 4.6**), the semiannual frequency (red line) and amplitude modulation (blue line) display periodic components of the jet close to biennial **Fig. 4.7**. Though the temporal range of the data used is not enough to arrive at a useful conclusion it would be interesting to investigate the results of a longer time period to see how this pattern evolves.

The results in Fig. 4.5b show a 2-6 week frequency band in the intraseasonal oscillations of the jet with varying strength throughout the time-domain as displayed in the power spectrum. However, a broad and large power spectrum density is noted around July 2005 with a strong power in the 3-7 week frequency range.

The spectra of both the amplitude (blue line) and frequency (red line) modulation, Fig. 4.8, display strong power during July 2005. Significant power is also displayed around July 2000, June 2002, July 2003, July 2004 and June 2006.

These observations are consistent with the results of the surface plots as discussed in section 4.1 and have confirmed the observations of Murakami (1976) that both the zonal and meridional winds associated with intraseasonal fluctuation of the jet are in phase over the entire troposphere, and hence justify the use of 10m QuikSCAT winds to investigate the variation of the jet. The usefulness of using a single grid point (Goswami and Mohan, 2001) to study the jet has also been confirmed.

This analysis of temporal variability in the wind near the Somali coast depicts high intraseasonal oscillations of lower frequencies (3 -7 weeks) in the low-level jet during July of 2005 than the observed 14-day mode.

4.4 Summary

From the power spectrum it is clear that the Somali jet has three significant modes of variations; annual, semiannual and intraseasonal. The main interest in this thesis is to study the high frequency mesoscale spatial variability of the jet. In these results, the jet is identified to have an intraseasonal mode of oscillation ranging from 2-7 weeks throughout the period under investigation from July 1999 to May 2007.

Significant power at intraseasonal frequencies occurred during July 2005 with the frequency of oscillations reaching a high of seven weeks signifying the occurrence of a prolonged active and break oscillations of the jet during this period.

It is hypothesised here that this prolonged active/break oscillation of the jet is associated with the occurrence of the strong localized upwelling event identified in the previous section.

It is also clear from the wind/SST time series that the synoptic winds are highly correlated with the local SSTs with the relationship being that of enhanced (reduced) wind speed coexisting with cool (warm) SSTs.

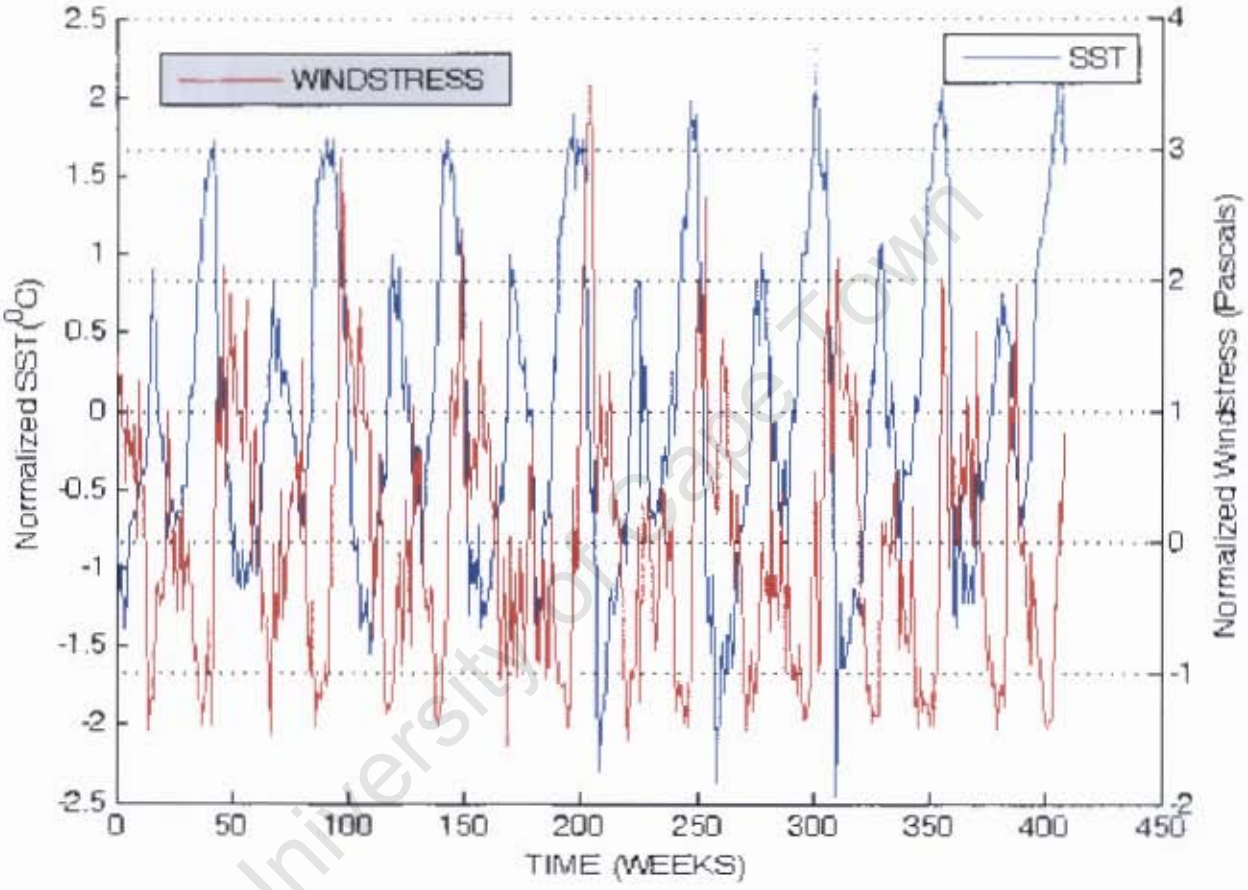

Fig. 4.3 *Time series correlation of normalized SST (^{0}C) and Wind stress (Pascals) at 4.75^{0}N and 50.25^{0}E with a correlation coefficient of -0.32 and 95% significance level.*

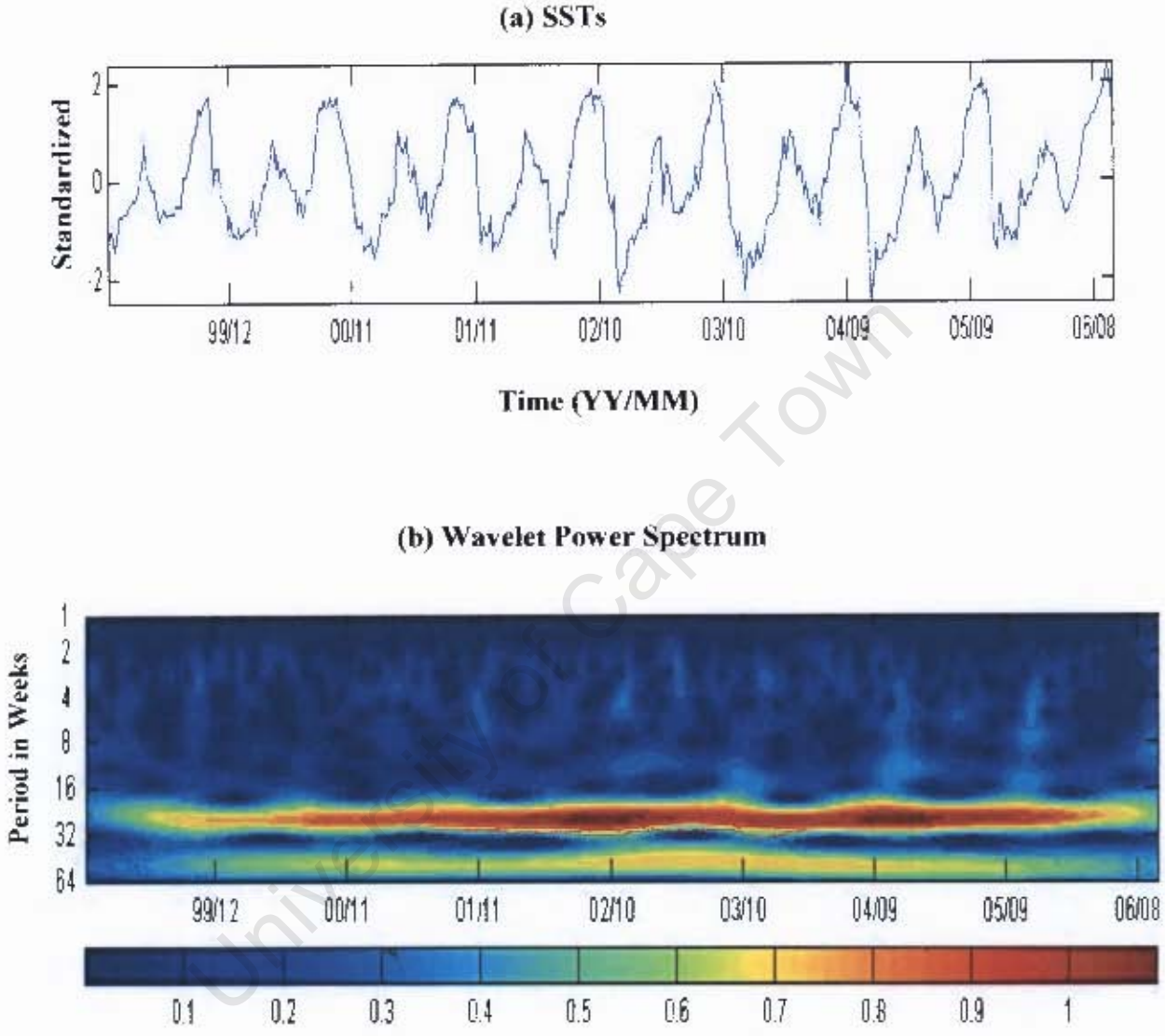

Fig. 4.4 Time series SSTs (^{0}C)at 4.75^{0}N and 50.25^{0}E over the region of the significant upwelling event. (a) Normalized time series SSTs, (b) The wavelet power spectrum using Morlet Wavelet with period in weeks. Red indicates that high activity occurred during that period.

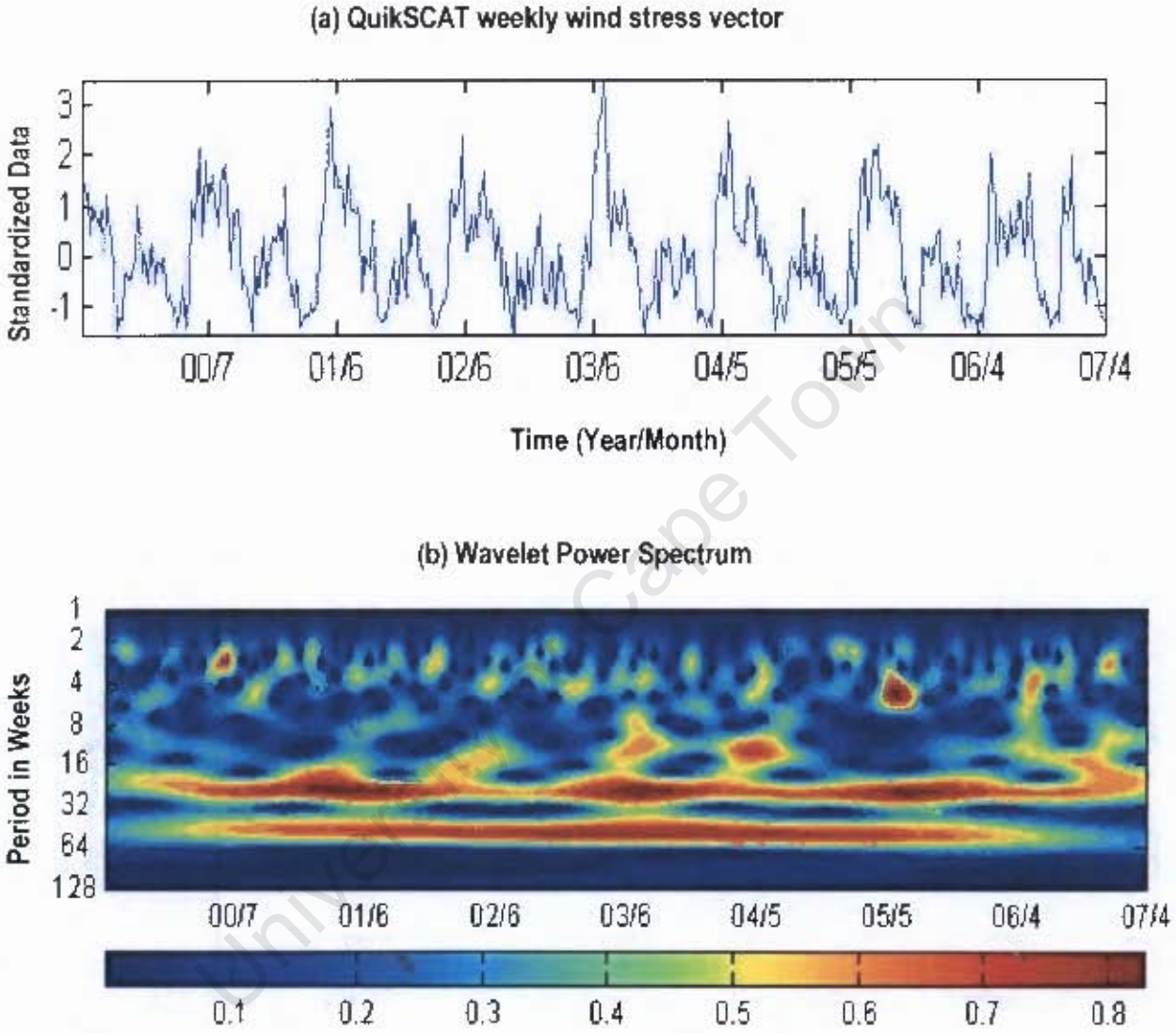

Fig 4.5 *Time series of weeky QuikSCAT winds(ms^{-1}) at $4.75^{0}N$ and $50.25^{0}E$ over the region of the significant upwelling event. (a) Normalized time series of wind stress vector. (b) The wavelet power spectrum using Morlet Wavelet with period in weeks. Red indicates that high activity occurred during that period.*

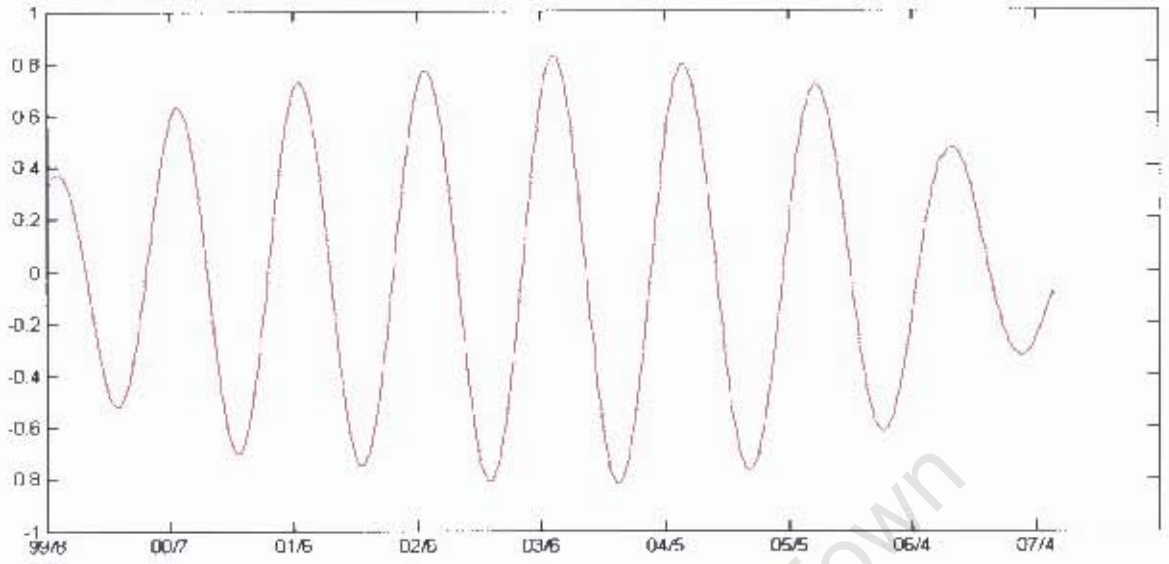

Fig. 4.6 *Standardized frequency plot of the Annual variation of the East African Jet showing a more uniform pattern.*

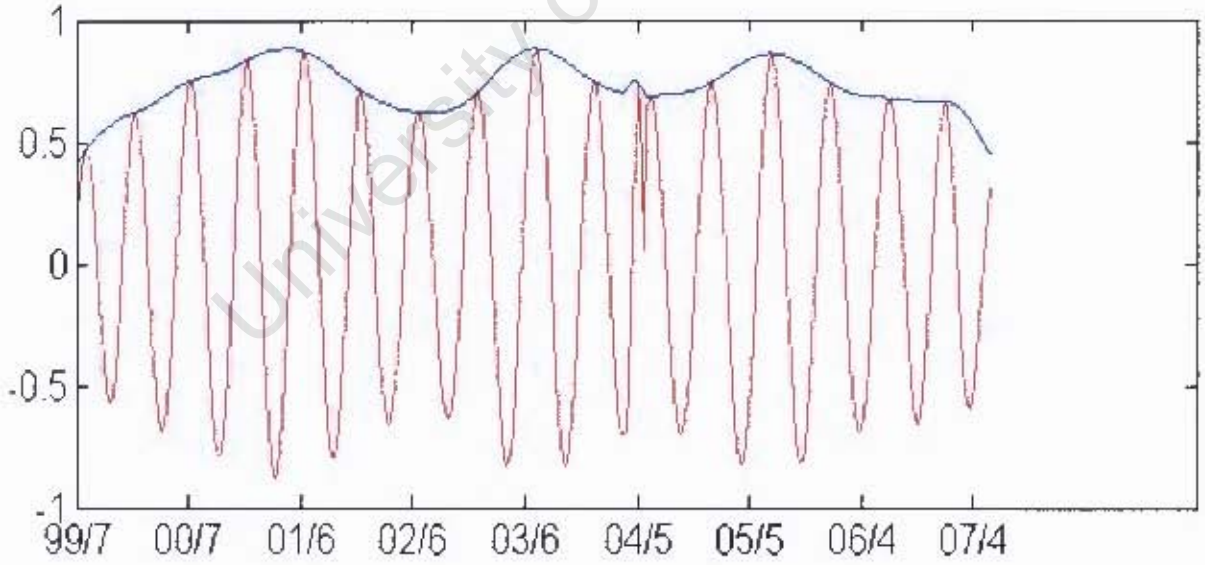

Fig. 4.7 *showing standardized frequency plot of the semiannual variations of the Jet. A pattern seems to develop where years of strong jet are followed by those of a weak one. An abrupt shift in appearance in the 2004 seasonal oscillations is evident*

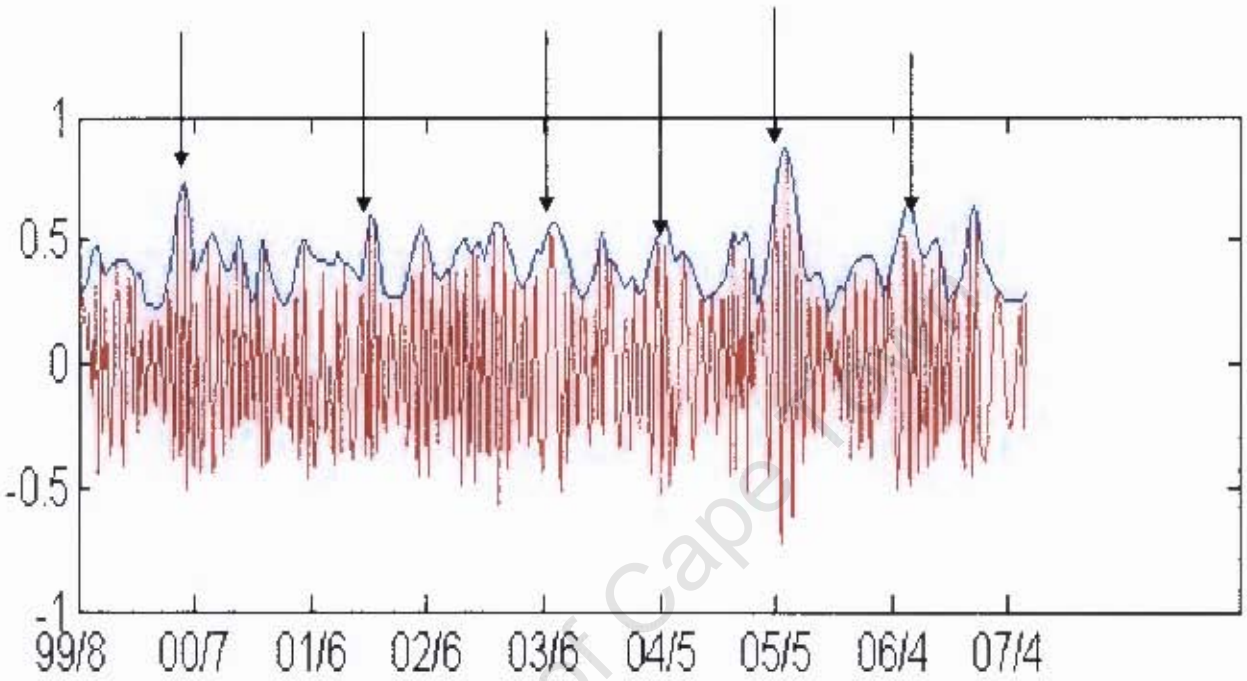

Fig. 4.8 *Standardized series of the 2-7 weeks oscillation of the east African Jet with the instantaneous amplitude (thick blue) and instantaneous frequency (red) showing periods of significant power*

4.5 Spatial variability of winds and SSTs: 26-30 July 2005

To investigate the spatial variability of the winds and SSTs over the region of significant upwelling, wind vector plots were extracted from QuikSCAT weekly data for the weeks ending on 2nd, 9th, 16th, 23rd and 30th July 2005 (**Fig. 4.9** panels **a, b, c, d** and **e**) with corresponding SST structures constructed from TMI weekly data depicted on the left of each panel. Analysis of the spatial variability of the two fields for the period 26 June-30 July 2005 is given below.

Week 1 (26 June-2 July)

The winds during this week (Fig. 4.9 a) have a magnitude of about $10ms^{-1}$ south of the cold filament, weakening to about $5ms^{-1}$ over the offshore extent zone of cold SSTs, and then become stronger downstream to reach a maxima of $15\text{-}20ms^{-1}$. Off the Horn of Africa, a strong monsoonal inflow towards India is evident ($15\text{-}20\ ms^{-1}$). The area offshore of the upwelling region around 75^0E is characterized by a trough of generally weak winds, which extends to the tip of the Indian peninsula.

The SSTs display a somewhat broad region of cold temperatures over the upwelling zone with slightly warm temperatures surrounding it.

Week 2 (3-9 July)

During the second week (Fig. 4.9b), the winds south of the cold filament do not show any significant change from week one. The winds over the cold SST filament continue to be weak. The strength of the wind downstream reduces to 10-15ms^{-1} and remains weaker than the previous week as the flow approaches the Indian subcontinent reaching the western coast as westerlies. The offshore trough of weak winds has slightly shifted southwards and westwards with its centre now located around 68^{0}E, further away from the Indian peninsula.

The cold SST filament becomes narrower but longer and the warm temperatures around it are still visible but slightly cooler than the first week.

Week 3 (10-16 July)

During the third week, (Fig. 4.9c) the winds south of the cold filament are less than 10ms^{-1} and about 5ms^{-1} on the filament itself. Downstream, the zone of strong winds shows an enhancement in intensity and zonal extent compared to week 2 but weaker near the western Indian coast. A southward turning of the flow is evident south and west of the tip of the Indian peninsula. The centre of the offshore trough remained along the same longitude of 68^{0}E as in the previous week but moved farther southwards so that it is completely detached from the Indian peninsula.

The week is characterized by cooler temperatures throughout the region south of the cold SST filament. The filament is slightly shorter and less pronounced than the previous week. A warmer pool of water exists on the northeastern shoulder of this filament and further north the temperatures cool down.

Week 4 (17-23 July)

The wind strength south and up to the cold filament drops significantly during this week (Fig. 4.9d), averaging about $5ms^{-1}$ over a large area. Upstream of the cold filament the winds continue to weaken reaching minimum strength as compared to previous weeks. The winds near the western coast and south of the Indian subcontinent are westerly. The trough offshore and the zone of very weak winds intensifies and increases in the zonal direction extending to as far west as 60^0E. Northward movement of this trough is evident now touching again the tip of the Indian peninsula.

The sea surface temperatures have decreased to the south of the cold filament which now is characterized by colder temperatures with a longer spatial extent offshore than the previous week. Warm temperatures continue to persist north and northeast of the region offshore of the cold temperatures. Further north of the filament, cool temperatures still persist.

Week 5 (24-30 July)

During the fifth week, the winds begin to intensify slightly over a wide area south of the cold filament to average $9ms^{-1}$ with a narrow band of weak winds over the cold SSTs (Fig. 4.9e). Upstream of the filament, the winds increase in intensity and in zonal extent compared to week 4. They also strengthen offshore and the spatial extent of the offshore trough reduces and moves east to about 70^0E. Near the Indian subcontinent, the winds remain westerly as the trough moves farther north towards this landmass.

The week is characterized by cool temperatures south of the cold filament which has now become diffuse. The cold upwelled waters near the Horn of Africa have spread further south cutting off the pool of warmer waters evident near 7^0N in week 4 and pushed them offshore.

The weekly observations reveal that winds south of the cold filament continued to weaken throughout the first four weeks from 26 June to 23 July reaching a minimum of $5ms^{-1}$ before strengthening during the fifth week that ends on 30 July. Upstream of the filament the winds remained persistently strong for the first 3 weeks before weakening in week 4. They started getting stronger again in week 5.

The winds close to the Indian subcontinent were initially strong southwesterlies but became westerlies in the second week. They veered to become northwesterly to northerly in the third and fourth week before becoming westerlies again in the last week.

The offshore equatorial trough of weak winds had its centre at 75^0E but extended up to the tip of the Indian peninsula during the first week. It reduced in intensity with the centre moving further south and west up to 68^0E in the second and third week and then completely detaching from the peninsula. The trough was very strong on the fourth week and moved further to the west with its centre now near 60^0E. A clear northward movement of the trough now covering the southern tip of the Indian peninsula is noticeable during the last week.

The behaviour of the winds over the upwelling region shows that the five week period of 26 June-30 July 2005 was characterized by weakening of winds south of the cold filament and relatively stronger winds upstream of the filament. The weakening of the winds south of the filament started from the week ending 2nd July and reached its weakest point during the week ending 23 July after which they started strengthening again

An analysis of both the meridional and zonal components of the wind stress rotated through 40^0 to compensate for the inclination of the Somali coast (Fig. 4.11) however depicts the meridional component (left panels) remaining strong throughout the period as compared to the zonal component (right panels).

4.6 Summary

During the period 26 June -30 July 2005 the winds over the Somali coast associated with the Somali jet weakened steadily south of the cold filament to reach minimum values of about $5ms^{-1}$ in the week ending 23 July. Upstream of the filament, the winds remained relatively strong throughout the period weakening on the week ending 23 July.

The alongshore meridional component of the wind stress, however, is seen to be stronger than the zonal component throughout the period 26 June-30 July 2005 as depicted in Figure 4.11. It is this component which is crucial in the investigation of upwelling.

Fig. 4.9 panel a,b,c,d,e *showing the evolution of SSTs (^0C) (left) and wind vector(ms^{-1}) (right) during the 5 weeks from 26 June-30 July 2005*

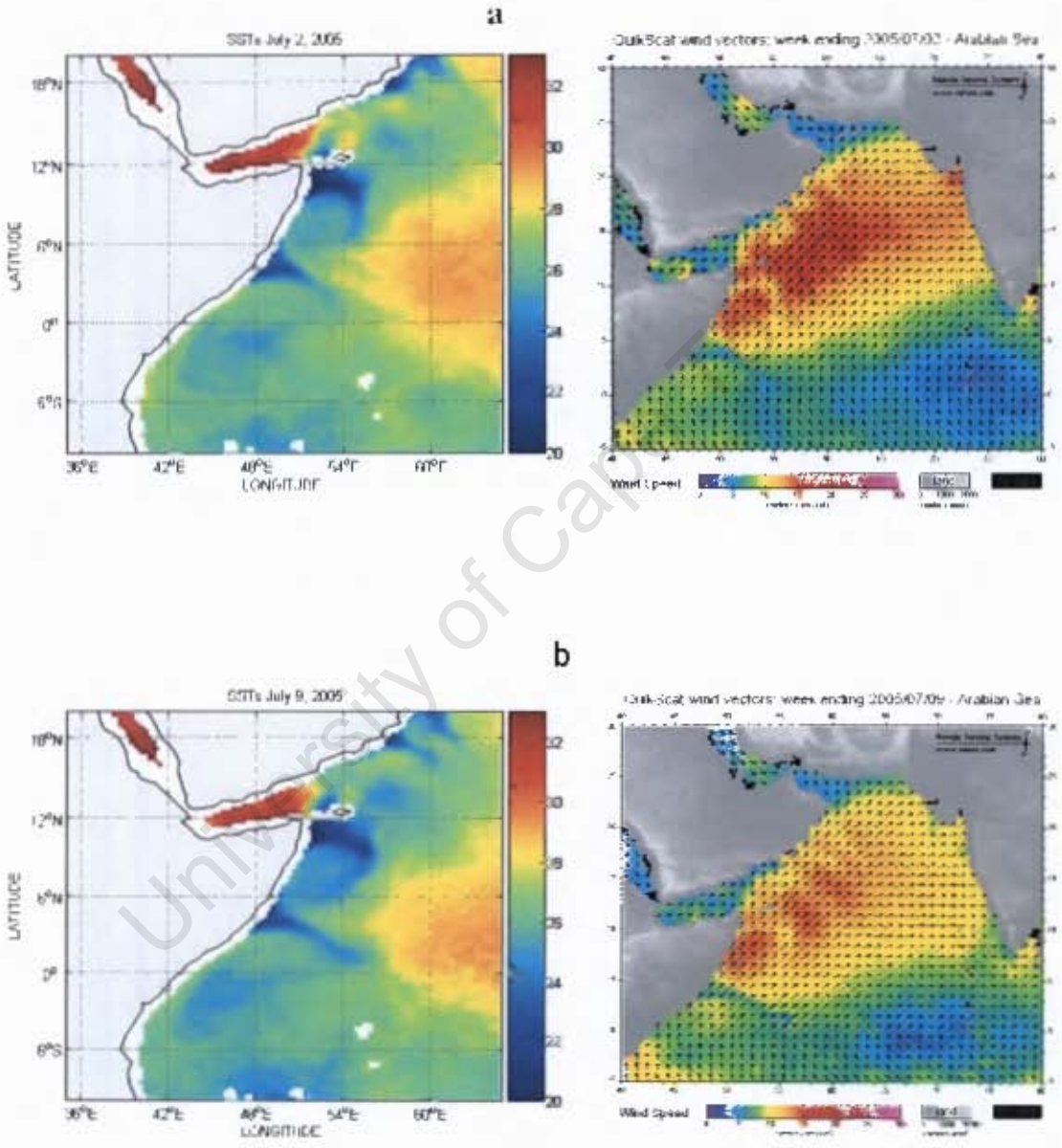

c

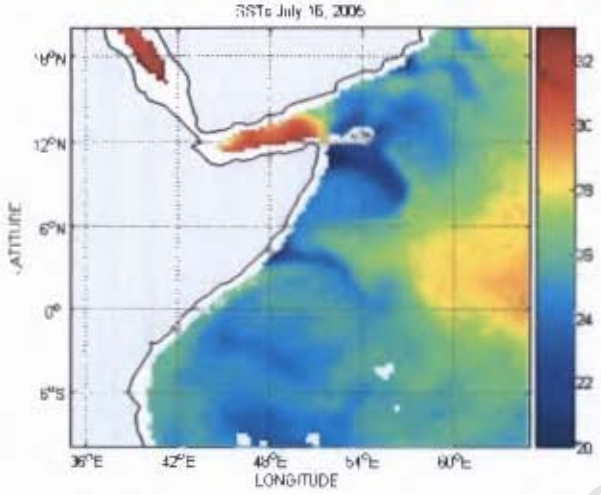

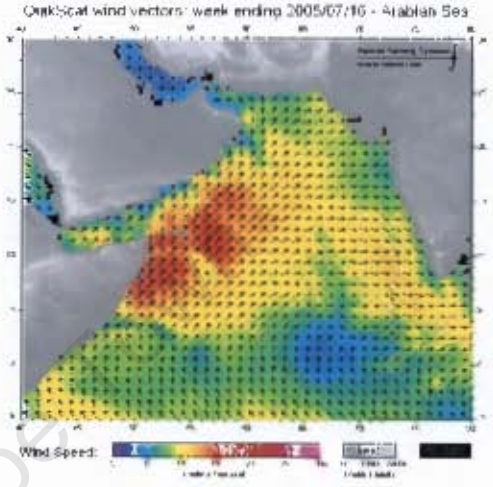

d

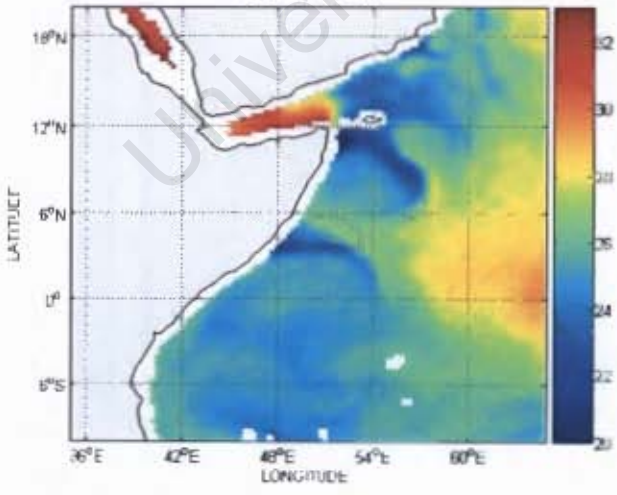

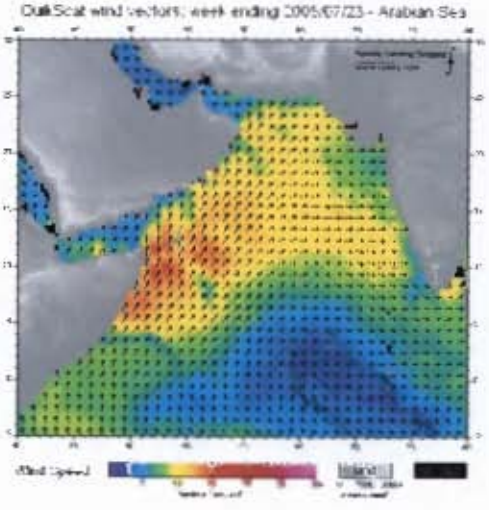

e

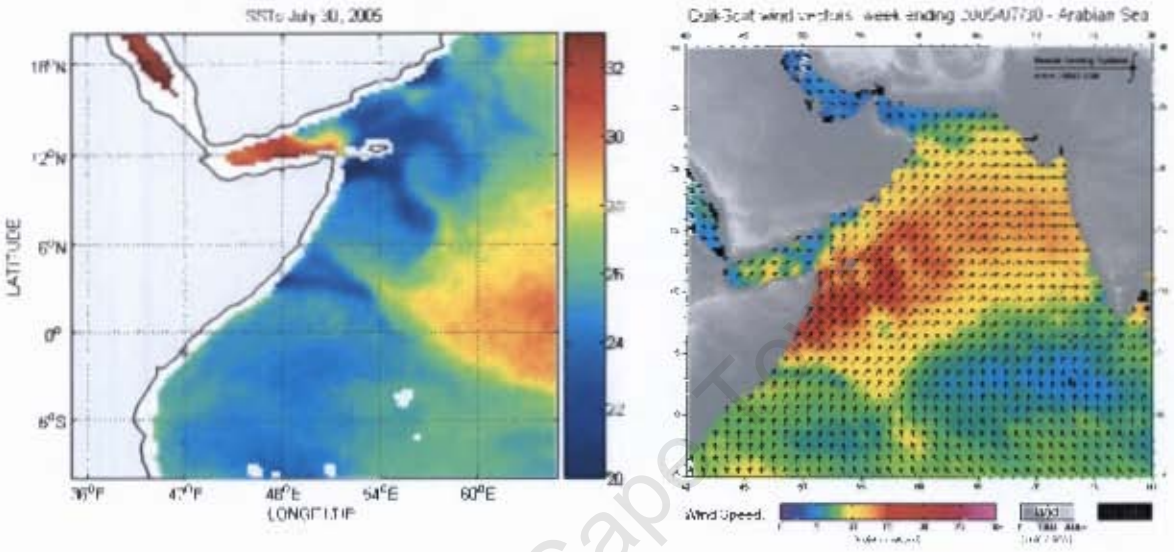

4.7 Mesoscale SST-Wind co-variability over the upwelling region

The cold filament over the upwelling region is associated with marked changes in the surface winds as described in the previous section and depicted in the panels of Fig. 4.9.

It is evident from the observations in that figure that the region exhibited strong spatial variability in SSTs and winds during the period 26 June-30 July 2005. The changes in SSTs and winds exceeded 4^0C and 5ms^{-1} respectively over a wide region that could extend to 200km in width. These changes in wind speeds result in changes to both the wind divergence and curl fields over the region. Recent studies of the Somali jet using surface winds from satellite data has shown the jet to exhibit significant spatial variability (Halpern *et al.*, 1998; Halpern and Woiceshyn, 1999).

A strong co-variability of the two fields with cold (warm) SSTs being coincident with locally weak (strong) winds is evident from Figure 4.9 throughout the period. Fig. 4.10 indicates 13-week time series of wind stress and SSTs averaged over the region 3.25 – 4.25^{0}N and 49.25 – 52.25^{0}E from 6 June – 29 August 2005. Although the two curves do not show a perfect match, there seem to be some relationship between the mesoscale winds and the SSTs. The two time series have a correlation coefficient of +0.5 with a statiscal significance of 80%.

The SST-wind coupling as observed here over the upwelling region of the Somali coast can be assumed to be the sea surface temperature modulation of atmospheric stability and the resultant vertical shear adjustment as described by Wallace *et al.* (1989).

Over the upwelling region, the latent heat loss associated with strong southwest monsoon winds is dramatically reduced over the cold SST due to the reduction in wind speeds, the increase in atmospheric stability and the increase in relative humidity. As the relative humidity increases over the cold SST filament, the net heat flux across the air-sea boundary drops leading to a heat gain of the ocean over the cold waters e.g Vecchi *et al.* (2004). **Table 1** illustrates the strong positive correlation between the difference of air and SST temperatures and the surface heat flux.

The situation described by Vecchi *et al.* (2004) seems to occur in week 3 and 5 (Fig. 4.9 panels (c) and (e)) respectively. The coupled effect over the cold upwelled waters is linked to thermodynamic feedback on the heat flux on the oceanic mesoscale, tending to damp out the surface SST gradient between the upwelled and warmer surface waters as hypothesized by Vecchi *et al.* (2004).

	Q_{LAT}	u	SST
(AT − SST)	0.80	−0.44	−0.76
SST	−0.93	0.64	
u	−0.78		

***Table** 1 Correlation coefficients between variables as found by Vecchi et al. in the Western Arabian Sea showing strong positive correlation between At-SST and heat flux Q*

4.8 Summary

The spatial winds exhibited high co-variability with the sea surface temperatures over the period 26 June-30 July 2005. During the week ending 23 July the jet winds weakened upstream and up to the cold SST filament while the SSTs in this region cooled down significantly over a large area and the temperatures of the cold filament dropped to about 21^0C. The alonshore wind component however continued to be strong depicting stronger winds downstream in line with the warmer temperatures north and northeast of the cold filament.

This co-variability of the SSTs and winds is as result of the sea surface temperature modulation of atmospheric stability and the resultant vertical shear adjustment. Over warmer SSTs, the unstable atmosphere brings down high winds from above the boundary layer leading to an acceleration of the surface winds. Over cold waters on the other hand, a stable atmosphere decelerates the surface winds Chelton *et al.* (2001a).

The changes in wind speeds as the wind stress crosses over the cold filament and the resultant changes in wind divergence and stress curl are important in the study of upwelling as described in the next section.

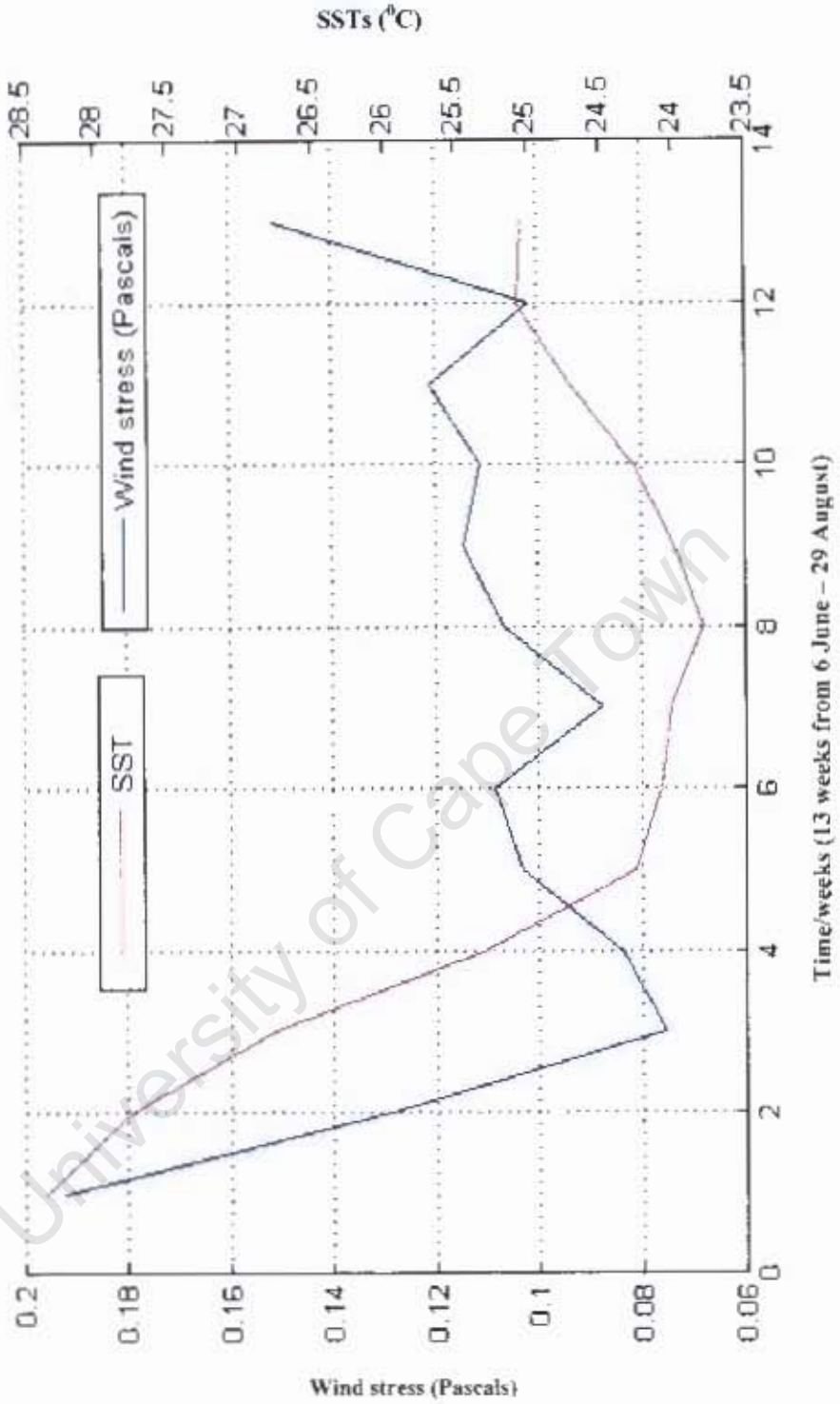

Fig. 4.10 *Time series of alongshore wind stress(Nm^{-2}) (blue) and SSTs (^0C) (red) extracted from the box bounded by 3.25 – 4.25^{0}N and 49.25 – 52.25^{0}E over the upwelling region for the period 6 June 29 August.*

4.9 Alongshore wind stress, Wind Stress Curl and the significant upwelling.

In this section, the variability of the alongshore and across-shore winds and the wind stress curl will be investigated and an attempt will be made to explain the significant and highly localized upwelling event of July 2005 over the Somali coast.

4.9.1 Variability of the alongshore and across-shore winds.

Both the meridional and zonal wind stress at the upwelling region rotated by 40^0 (angle of coastline orientation) to get alongshore and across-shore wind stress were investigated to assess their strengths during the period 26 June – 30 July 2005. Figure 4.11 shows the variability of these wind stresses during that period.

The alongshore plots (left panels) show strong wind stresses over the western Indian ocean up to the Horn of Africa throughout the whole of the period with the weeks ending 9 and 16 July depicting stronger winds south of the upwelling region. The week ending 23 July shows a weakening of these wind stresses.

The across-shore wind stresses (right panels) were highly variable over the region north of the cold filament up to the Horn of Africa during the period. They were strong during the first week and weakened in the next three weeks to reach minimum strength on the fourth week. The region south of the cold filament was characterized by weak across-shore wind stress throughout the period.

Wind stresses over the cold filament were weak throughout the period for both the across-shore and alongshore components.

Fig. 4.12 shows a horizontal feature of a thermal front during July of 2005 constructed from NOAA/NCEP reanalysis. A maximum offshore gradient appears to be concentrated between latitudes $4\text{-}5^0$N with maximum average positive temperature anomalies of about 0.5^0C occurring between $42\text{-}46^0$E.

Differing thermodynamic properties of land and sea induce large offshore temperature gradients over the area of study as shown in Fig.4.12. An interior heat dome on the land is contrasted with cool air which is mixed over the upwelling region during July of 2005. High pressures resulting from the cooler temperatures over the ocean and low pressures due to the warmer temperatures over land induce the strong offshore pressure gradient which was particularly high during the third week of July.

A box average plot of the sea-level pressure index between two boxes, one at 2.5 – 5.0^{0}N, 50.0 – 52.5^{0}E and the other at 2.5 – 5.0^{0}N, 42.5 – 45.0^{0}E (shown as green boxes in Fig.4.12) was constructed to assess the variability of the cross-shore pressure gradient during 2005. The pressure gradient plot (Fig. 4.13) depicts high gradients around mid July. This onshore pressure gradient strengthened the alongshore winds during the period of significant upwelling.

The strong geostrophic flow associated with this pressure gradient and weak Coriolis effect helped to strengthen the alongshore wind stress during the week ending 23 July 2005.

4.9.2 Wind stress curl and upwelling.

The spatial variability of the wind stress curl is displayed in **Fig. 4.14** which shows weekly plots of Wind Stress Curl from 26 June – 30 July 2005.

The results display a slow build up of positive wind stress curl over the upwelling region from week one to the fourth. Close observation of the wind stress curl contours during the week ending 23 July shows a relatively strong and localized positive curl (shown in red circle) with negative values upstream. The low resolution of the satellite data along the coast slightly obscures this.

The deceleration of the winds upstream of the cold filament from $15ms^{-1}$ on the first week ending 2 July and weakening to less than $5ms^{-1}$on the week of the significant upwelling lead to changes in both the wind divergence and curl fields. This explains the relatively strong wind stress curl patterns over the region during the week of 17-23 July 2005.

Consistent with the direct relationship between the mesoscale speed of the jet and SSTs, a wind stress curl dipole forms over the cold filament with positive on the upstream and negative on the downstream of the zonally oriented part of the filament. Positive (negative) wind stress curl is a measure of upwelling (downwelling).

As the winds cross the cold filament, they decelerate upstream and accelerate downstream resulting in convergence and divergence respectively. This convergence (divergence) in the lower atmosphere leads to mesoscale oceanic divergence (convergence) and hence upwelling (downwelling) in the coastal ocean.

Chelton *et al.*,(2001a) found that over a cold filament the wind stress convergence and divergence are locally strongest where the wind blows parallel to the SST gradient (perpendicular to the isotherms). This situation could have also occurred during the week ending 23 July when the cold filament had a horizontal inclination on its shoreward end and the wind stress had a strong alongshore component as compared to the across-shore.

In this study, the region of enhanced positive curl corresponds with the position of the cold filament during the week ending 23 July. High curl values result in uplifted doming of the thermocline due to strong vertical velocities driven by Ekman pumping, with vertical mixing bringing cool thermocline water to the surface.

The strong convergence in the lower atmosphere due to the significant deceleration of the winds upstream of the cold filament is expected to have enhanced the upwelling due to the strengthened oceanic divergence over the region.

4.10 Summary

It has been seen that the alongshore winds strengthened throughout the three weeks leading up to July 23, 2005. Strong alongshore winds during the period can also be deduced from the high pressure gradients depicted on the sea level pressure index plot. From the SST plots, panels a, b and c, Fig 4.9, it can be seen that there was a continuous build up of the cold SST filament throughout these three weeks.

During the period of study, strong winds – SST co-variability was evident with cold (warm) SSTs being coincident with locally weak (strong) winds. As a result, strong convergence and divergence of the near-surface wind occurred upstream and downstream of the cold filament respectively. A wind stress curl dipole formed over the filament with positive curl upstream.

Fig. 4.11 Weekly alongshore (left) and across-shore wind stress (Nm^{-2}) in colour shading and wind stress vectors for the period 26 June- 30 July 2005.

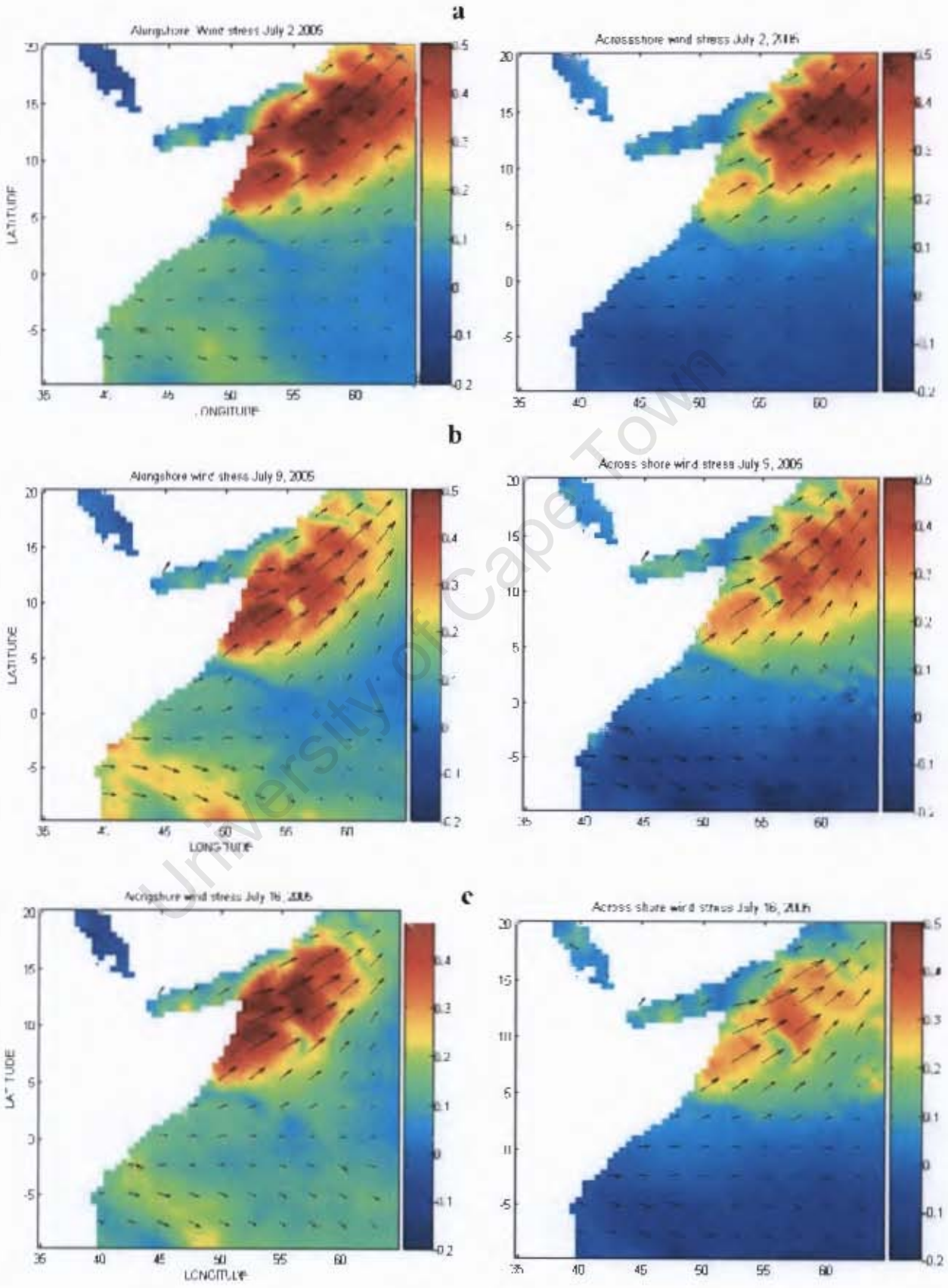

d

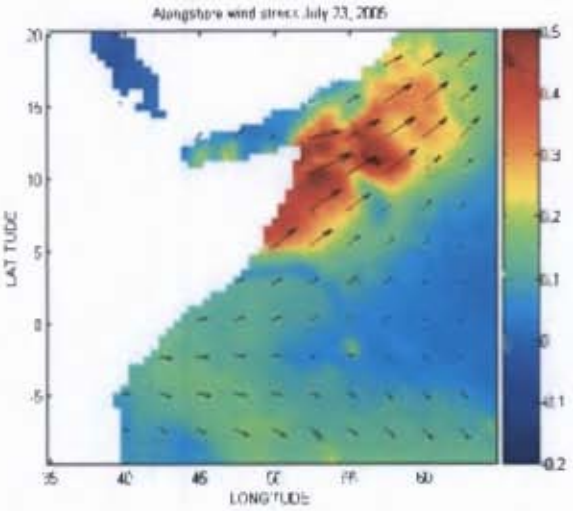

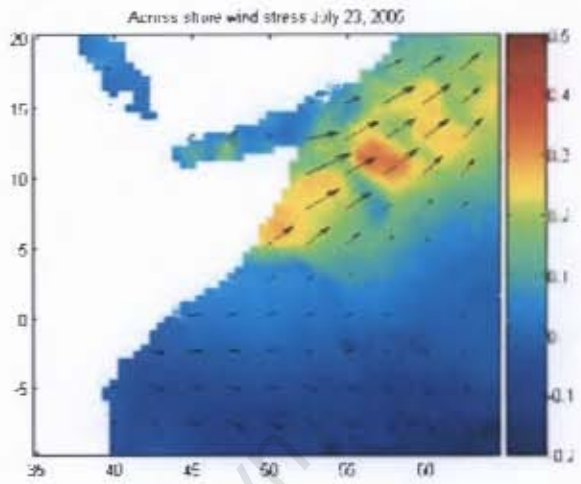

e

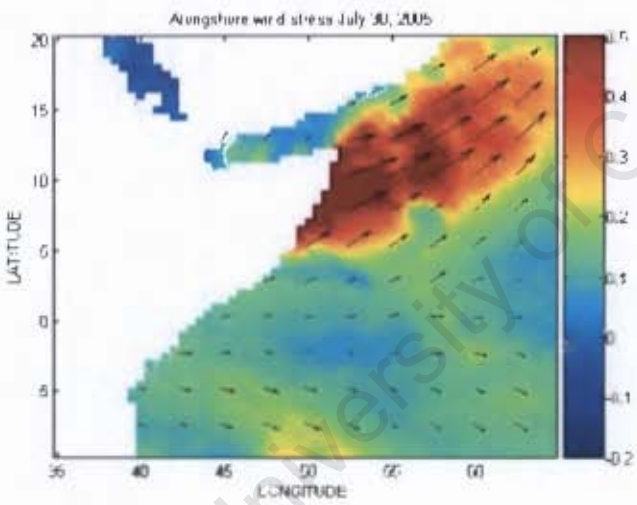

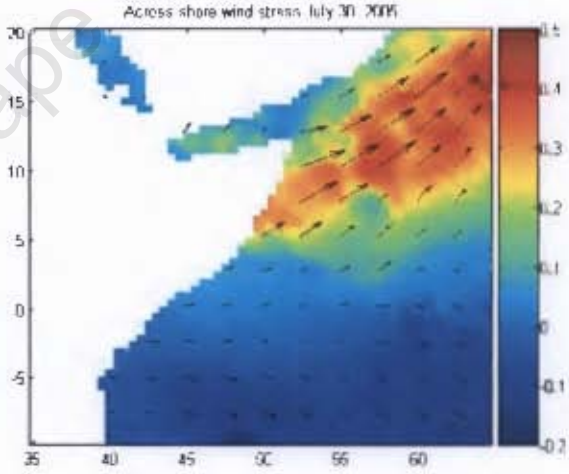

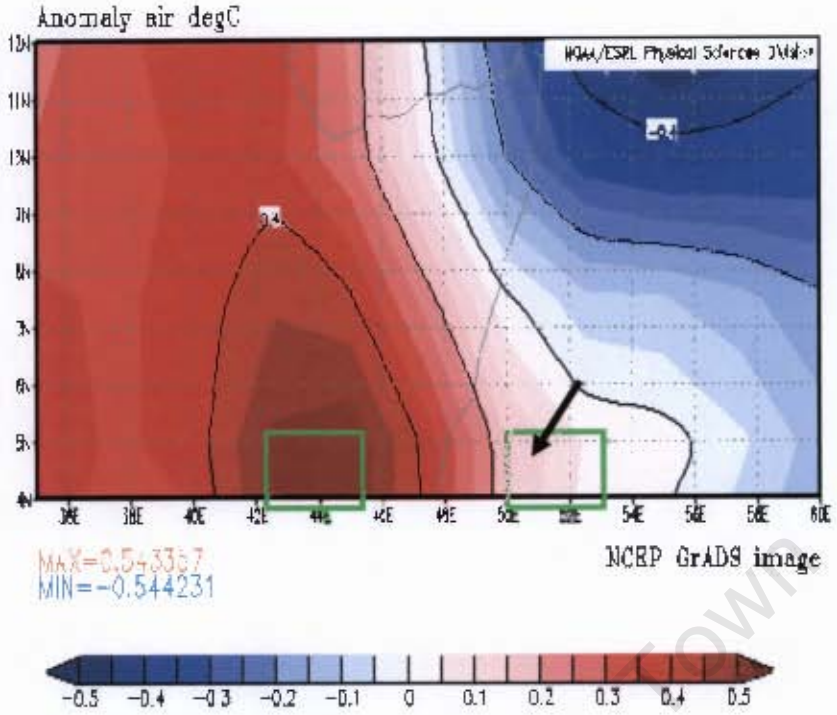

Fig. 4.12 *July 2005 surface temperature anomalies (^{0}C) constructed from NOAA/NCEP Reanalysis showing zonal thermal gradient. The region of upwelling is enclosed in the box to the right and indicated by the black arrow*

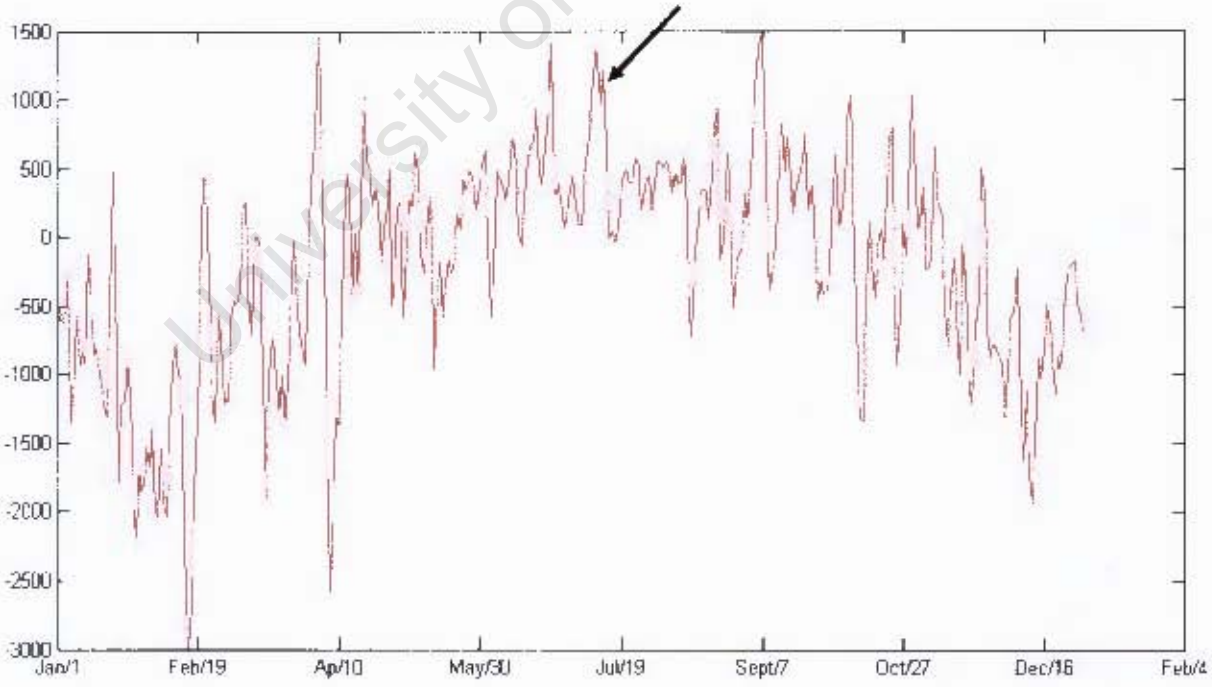

Fig. 4.13 *Box average SLPI (Nm^{-2}) between the boxes 2.5^0 - 5.0^{0}N, 50.0^0 52.5.^{0}E over the ocean and 2.5^0 - 5.0^{0}N, 42.5^0 45.0^{0}E over land for the year 2005 (see green boxes in* ***Fig. 4.11****). The pressure gradient is averagely high between May and September with higher values around 19 July indicated with a black arrow*

Fig. 4.14 Wind stress Curl (pascals m^{-1}) plots for the period 26 June – 30 July 2005

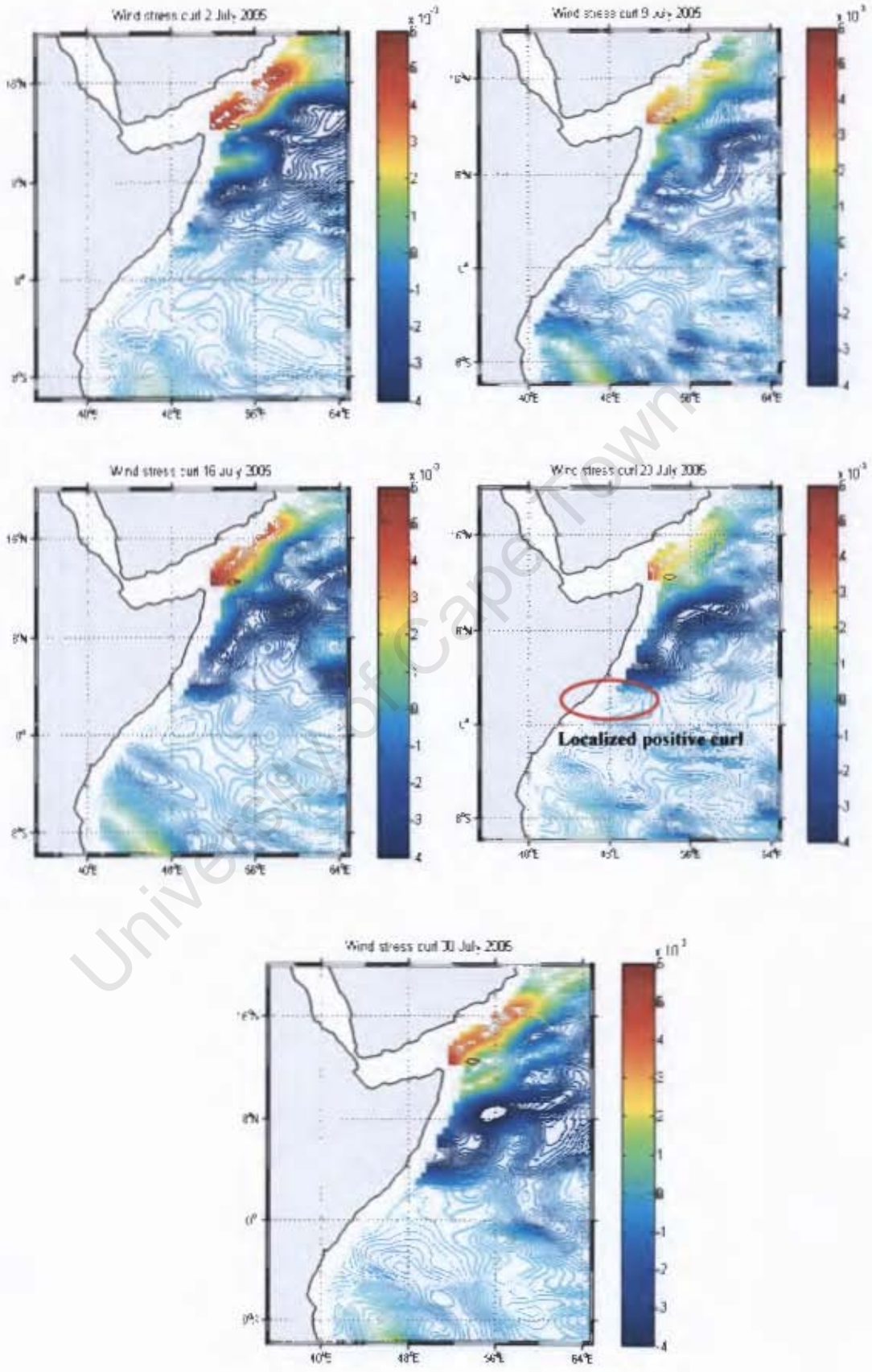

Chapter 5

Summary and Conclusions

During boreal summer, the Somali current forms as a western boundary current in response to the southwest monsoon. It turns east and south-eastwards at around 4-5^{0}N and further north at around 10-12^{0}N to form the 'Southern Gyre' and the 'Great Whirl' eddies respectively. Due to the strong northern summer winds off the Somali coast, referred to as the Somali jet, offshore drifts of surface waters are established east of the coast at both positions of the Gyre and the Whirl. Simultaneously, the SSTs at the shoreward shoulders of these eddies, whe re the offshore drifts occur, drop as the thermocline is lifted by localized Ekman suction and upwelling. This thesis set out to investigate the characteristics of mesoscale wind fields over the southern upwelling region of the Horn of Africa. Although the synoptic wind patterns of the southwesterly monsoons responsible for the upwelling are fairly well understood, the spatial and temporal variability in local winds resulting from the adjustment of the large scale flow to regional thermal gradients is less well understood and it is this aspect that has been examined in this thesis through analysis of an identified significant southern upwelling event.

Previous studies have shown that the cross-equatorial low-level jet (Somali jet) on the East African coast is forced by low-level divergence in the subtropical high-pressure belt over the South Indian Ocean and convergence in the monsoon trough over India (Anderson, 1976; Hart, 1977; Cadet and Desbois, 1981) and has a quasi-biweekly oscillation [Krishnamurti *et al.*, 1976; Joseph and Sijikumar, 2004]. The jet is modulated by the movement of the Intertropical Convergence Zone (ITCZ) and the East African topography (Gatebe *et al.*, 1999). Weakening of the jet is related to a wind discontinuity to the east of Madagascar, due to fluctuations of midlatitude weather systems to the south which pulse the trade winds (Cadet and Desbois, 1981). These fluctuations drastically reduce the flow into the source area of the jet.

The mesoscale winds over the region, on the other hand, are driven by local topographic and thermal contrasts. Large temperature gradients exist between the land and the ocean during July over the region (Hart *et al.,* 1978) indicating that the effect of localized land-sea heating contrast is present in the pressure field and, consequently, the wind field. Over the ocean, strong thermal gradients exist between the cold SST upwelling region and warm waters upstream and downstream.

Based on the Hovmuller and surface plots, a highly localized significant upwelling event characterized by cold sea surface temperatures of below 22^0C was identified around 4.75^0N during the week 17-23 July 2005. The cold filament had a clear southeastwards curve orientation with a longer spatial extent offshore. This event was then selected as a case study and the temporal and spatial variability of the winds over the region during a period of five weeks from 26 June – 30 July 2005 were investigated. Because station observations in the region are very limited, 10m QuikSCAT winds, TMI SSTs and sea level pressure from NCEP/NCAR were used to undertake the investigations.

From the continuous wavelet analysis, it can be concluded that the Somali jet has three significant modes of variations on time scales of weeks to a year; annual, semiannual and intraseasonal. The intraseasonal mode of oscillation ranging from 2-7 weeks was identified throughout the period under investigation from July 1999 to May 2007. Significant power at the intraseasonal frequencies occurred during July 2005 with the frequency of oscillations being three to seven weeks. This indicates that the jet was oscillating at lower frequencies during this period than the bi-weekly mode observed in earlier studies e.g Krishnamurti *et al.* (1976) and others.

The spatial variations of the winds over the upwelling region were investigated from wind vector plots extracted from QuikSCAT weekly data for the weeks ending on 2^{nd}, 9^{th}, 16^{th}, 23^{rd} and 30^{th} July 2005. During the period 26 June -30 July 2005, the QuikSCAT plots indicate that winds over the Somali coast weakened steadily south of the cold filament to reach minimum values of about $5ms^{-1}$ in the week ending 23 July.

Upstream of the filament, the winds remained relatively strong throughout the period weakening on the week ending 23 July. The alongshore wind stress shows stronger values than the across-shore component throughout the period. These winds increased for three weeks from late June to mid July 2005. However the winds weakened significantly during the fourth week (ending 23 July). The corresponding SST plots show that there was a continuous build up of the cold SST filament throughout the first three weeks. The filament had a larger spatial extent in the fourth week, ending 23 July. During the same period, strong alongshore winds were deduced from the high pressure gradients depicted on the sea level pressure index plot

The spatial winds also exhibited high co-variability with the SSTs over the period. This co-variability of the SSTs and winds occurs as a result of the changes forced by SSTs on the atmospheric stability leading to vertical shear adjustment. Over warmer SSTs, the unstable atmosphere brings down high winds from above the boundary layer leading to an acceleration of the surface winds. Over cold waters on the other hand, a stable atmosphere decelerates the surface winds. These observations were hypothesized by Wallace *et al.* (1989) and confirmed by Chelton *et al.* (2001a). The mesoscale changes in speeds as the winds cross over the cold filament result in changes of wind convergence and divergence upstream and downstream of the cold filament respectively. A wind stress curl dipole forms over the filament as observed in the plots with positive curl upstream.

From these observations, it can be concluded that from 26 June – 30 July 2005 the Somali jet oscillated at a lower frequency than the observed bi-weekly mode. It exhibited strong alongshore winds from the week ending 2 July to that ending 16 July and these winds could have been enhanced by the strong offshore pressure gradient. These strong winds are believed to have contributed to the strong upwelling seen in the week ending 23 July through the strengthening of the Ekman pumping. This is confirmed by the SST plots, which showed a continuous build up of the cold SST filament throughout the three weeks.

The Somali current is expected to have strengthened during the first three weeks of the study period due to the strong alongshore winds. The subsequent significant weakening of the winds during the fourth week of 23 July is assumed to have decelerated the current with the result of it turning east and southeastwards over the upwelling region around 4-5^0N to form the Southern Gyre. A cold wedge of upwelled waters then developed along the gyre's shoreward shoulder. This gyre organized the upwelling into a cold filament by advecting the cold coastal upwelled waters offshore, first eastward and then to the south. This mechanism gave the filament its southward curve seen during this week.

The strong wind – SST co-variability observed during the study period with cold (warm) SSTs being coincident with locally weak (strong) winds is expected to have resulted in strong low-level convergence and divergence of the winds upstream and downstream of the cold filament respectively. A wind stress curl dipole formed over the cold filament with positive curl upstream.

It is hypothesised here that the eastward turning of the current, which resulted in strengthened Ekman transports, and the existence of strong local atmospheric convergence and cyclonic (positive) wind stress curl, which corresponds with local oceanic divergence, strengthened the upwelling and generated the observed highly localized pool of cold waters during the week ending 23 July 2005.

The results in this thesis suggest that strong southern upwelling near 4-5^0N on the East African coast occurs when the Somali jet undergoes oscillations with lower frequencies than those of bi-weekly range observed in previous studies. In these circumstances, there is a prolonged period of an active jet followed by significant weakening of the winds in the beginning of a break phase. It has been suggested in this thesis that during the transition period of prolonged active/break period of the jet, coupled with wind-SST co-variability, strong atmospheric convergence is realised over the southern upwelling region leading to oceanic divergence and hence strong upwelling.

The Indian monsoon has been seen to undergo intraseasonal variations (e.g. Krishnamurti *et al.*, 1976 and others). In studies of this monsoon, 5 - 15-day oscillations in the Somali jet were observed (e.g. Murakami, 1976). These near quasi-biweekly oscillations of the jet have been found to be related to similar oscillations in rainfall over India associated with break and active monsoon phases, with cross-equatorial winds being stronger during a strong monsoon than a weak one. A correlation has been found between rainfall over the western coast of India and the intensity of low-level equatorial winds over Kenya. Further studies have shown that a break of the monsoon rain over India occurs when the wind intensity is weak along the East African coast.

These observations suggest a need to look at the relationship between a strong southern Somalian upwelling event, the Indian monsoon and rainfall over the coastal region of Kenya. The hypothesis is that the occurrence of significant southern upwelling may be related to the rainfall over the coastal region of Kenya due to the significant weakening of the jet and atmospheric convergence over the region. Hence this forms the recommendation for further study in this area.

References

Anderson, D. L. T., 1976: The low-level jet as a western boundary current. *Mon. Wea. Rev.*104, 907-21.

Annamalai H., Slingo J. M., 2001: Active/break cycles: Diagnosis of the intraseasonal variability of the Asian summer monsoon. *Clim.Dyn.* 18, 85–102.

Ardanuy, P., 1979: On the Observe Diurnal oscillation of the Somali Jet. *Mon. Wea. Rev.* 107, 1694-1700.

Atkins, G. R., 1970: Winds and Current patterns in False Bay. *Trans. R. Soc. S. Afr.*, 39 Part 2, 139-148.

Atkinson, G. R., 1981: Mesoscale Atmospheric Circulation. *Academic Press. London pp* 495.

Bakun, A., 1973: Coastal Upwelling Indices, West Coast of North America. 1946-1971, *U. S. dept of Commer., NOAA Tech. Rep. NMFS-SSRF* 671 pp 103.

Bakun, A., 1978: Guinea Current Upwelling, *Nature*, 271, 5641, 147-150.

Bang, N. D., 1973: Characteristics of an intense ocean frontal system in the upwelling regime west of Cape Town. *Tellus,* 25, 256–265.

Bannon, P. R., 1979a: On the Dynamic of the East African Jet I: Simulations of Mean conditions for July. *American Met. Soc. J. Atmos. Sci*, 36, 2139-2152

Bannon, P. R., 1979b: On the Dynamic of the East African Jet II: Jet Transients. *American Met. Soc. J. Atmos. Sci,* 36, 2153-2168.

Bannon, P. R., 1982: On the Dynamics of the East African Jet. Arabian sea Branch, *J. Atm. Sci.* 39, 2267 – 2278.

Beal L. M. and Chereskin T. K., 2003: The Volume transport of the Somali Current during the 1995 Southwest Monsoon. *Deep Sea Research Part II: Topical Studies in Oceanography* Vol. 50 pp 2077-2089.

Bond, N. A., 1992: Observations of planetary boundary layer structure in the eastern equatorial Pacific. *J. Climate,* 5, 699–706.

Boyd, A. J., 1981: An intensive study of the currents and general hydrology of an anomalous upwelling area off South West Africa, *Msc. Thesis Dept. of Oceanography UCT.*

Bunker, A. F., 1965: A low-level jet produced by air, sea and land interactions, *Sea-Air Int. Lab, Rep. 1, J. Spar (ed.) Washington* 225-238.

Burls, N., 2006: Simulation of High Resolution winds over the Southern Benguela Upwelling system. *Msc. Thesis, Dept. of Oceanog., UCT.*

Cadet, D. L. and Bradley Diehl, 1984: Interannual Variability of the Surface Fields over the Indian Ocean during Recent Decades, *Mon. Weath. Rev.* 112, 1922-35.

Cadet, D., and M. Desbois, 1981: A case study of a fluctuation of the Somali jet during the Indian summer monsoon. *Mon. Wea. Rev.*109, 182-87.

Chao S. Y., 1985: Coastal Jets in the Lower Atmosphere. *J. Phys. Ocenogr.* 15: 361-371.

Charney, J.G., 1969: The intertropical convergence zone and the Hadley circulation of the atmosphere. *Proc. WMO/IUCG Symp. Numer. Weather Predict. Jpn. Meteorol. Agency* III: 73–79

Chelton, D. B., and co-authors, 2001a: Observations of coupling between surface wind stress and sea surface temperature in the eastern tropical Pacific. *J. Climate,* 14, 1479–1498.

Chui, C. K., 1992: An Introduction to Wavelets. *Academic Press., Inc.Harcourt Brace Jovanovich,* 266 pp.

Clancy, R. M., Thompson, J. D., Hulbert, H. E. and Lee, J. D., 1979: A model of Mesoscale air-sea interaction in a sea-breeze coastal upwelling regime, *Mon. Wea. Rev.* 107, 1476-1505.

CLIVAR–GOOS Indian Ocean Panel and others, 2006: Understanding the Role of the Indian Ocean in the Climate System — Implementation Plan for Sustained Observations *WCRP Informal Report* No. 5/2006.

Cox, M. D., 1979: A numerical study of Somali Current eddies. *Journal of Physical Oceanography*, *9*, 311–326.

Csanady, G. T., 1982: Circulation in the coastal ocean, *D. Reidel Pub. Co., Dordrecht* pp 279.

Daniel, C. and Desbois, M., 1980: A Case Study of the Somali Jet During the Indian Summer Monsoon, *American Met. Soc. Mon. Wea. Re.* 109, 182-187.

Denman, K. L. and Freeland, H. J., 1995: Correlation Scales, Objective mapping and Statistical Test of Geostrophy over the Continental Shelf; *J. of Mar. Res.* 43, 517-539.

Daubechies, I., 1990: The wavelet transform time-frequency localization and signal analysis. *IEEE Trans. Inform. Theory,* 36, 961–1004.

Daubechies, I., 1992: Ten Lectures on Wavelets. *Society for Industrial and Applied Mathematics,* 357 pp.

Ekman, V., 1905: On the Influence of the earth's rotation on Ocean currents, Arkiv Mat. Astronoch Fysik, 2, 11 Stockholm.

Elliot, A. J., and Savidge, G., 1990: Some features of the upwelling off Oman. *Journal of Marine Research, 48,* 319–333.

Elliot, D. and O'brien, J., 1977: Observational studies of the marine boundary over an upwelling region, *Monthly. Wea. Rev.*, 105, 86-98.

Evenson, A. J., and Veronis, G., 1975: Continuous representation of wind tress and wind stress curl over the world ocean, *J. Mar. Res.*, 33, 131-144.

FAO Rome, 1997: Review of the State of World Fishery Resources: *Marine Fisheries. Fisheries Circular* No. 920 FIRM/C920.

Farge, M., 1992: Wavalet transform and their applications to turbulence. *Annu. Rev. Fuid Mech.* 24, 395-457.

Ferranti, L., Slingo, J. M., Palmer, T. N., Hoskins, B. J., 1997: Relations between interannual and intraseasonal monsoon variability as diagnosed from AMIP integrations. *Q. J. R. Meteorol. Soc.* 123, 1323–57.

Findlater, J., 1966: Cross-equatorial jet streams at low levels over Kenya. *Meteor. Mag.,* 95, 353–364.

Findlater, J., 1967: Some further evidence of cross-equatorial jet streams at low levels over Kenya. *Meteor. Mag.,* 96, 216–219.

Findlater, J., 1969a: Inter-hemispheric transport of air in the lower troposphere over the western Indian Ocean. *Quart. J. Roy. Meteor. Soc.*, 95, 400–403.

Findlater, J., 1969b: A major low level current near the Indian Ocean during northern summer. *Quart. J. Roy. Meteor. Soc.*, 95, 362–380.

Findlater, J., 1971: Mean monthly airflow at low levels over the western Indian Ocean. *Geophysical Memoirs*, *115*, 55.

Findlater, J., 1972: Aerial explorations of the low-level cross-equatorial current over east Africa, *Q. J. R. Met. Soc.*, 98, 274-289.

Findlater, J., 1977: Observational aspects of the low-level cross-equatorial jet stream of the western Indian Ocean. *Pure Appl. Geophs.* 115, 1251-62.

Fischer, J., Schott, F., and Stramma, L., 1996: Currents and Transports of the Great Whirl-Socotra Gyre System during the Summer Monsoon August 1993. *Journal of Geophysical Research*, *101*, 3573–3587.

Gadgil, S., 2003: The Indian monsoon and its variability. *Annu. Rev. Earth Planet. Sci.* 31, 429–67

Gatebe, C. K., P. D. Tyson, H. Annegarn, S. Piketh, and G. Helas, 1999: A seasonal air transport climatology for Kenya. *Journal of Geophysical Research*, 104, 14,237–14,244.

Gill, A. and Clak, A. J., 1974: Wind induced upwelling coastal currents and sea-level changes, *Deep Sea Res.*, 21, 325-345.

Godfrey J. S. and co-authors, 1995: The Role of the Indian Ocean in the Global Climate System: Recommendations Regarding the Global Ocean Observing System. *Report of the Ocean Observing System Development Panel, Texas A&M University, College Station, Tex, USA*. 89pp.

Godwin, J. A., 1979: A study of surface winds off the coast of Peru. *CUEA TECH. REP.* 58, Dept. of Met., Florida State Univ., pp. 82.

Goswami, B. N, Sengupta D, Suresh Kumar G., 1998: Intraseasonal oscillations and interannual variability of surface winds over the Indian monsoon region. *Proc. Indian Acad. Sci.Earth Planet. Sci.* 107, 45–64.

Goswami, B.N, Mohan, R. S. A., 2001: Intraseasonal oscillations and interannual variability of the Indian summer monsoon. *J. Clim.* 14, 1180–98.

Halley, E., 1686: An historical account of the trade winds and monsoons observable in the seas between and near the tropics with an attempt to assign a physical cause of the said winds. *Philos. Trans. R. Soc. London,* 16, 153–68.

Halpern, D., 1976: Measurements of near surface wind stress over an upwelling region near the Oregon Coast. *J. Phys. Oceanogr.* 6, 108-112.

Halpern, D., and P. M. Woiceshyn, 1999: Onset of the Somali jet in the Arabian Sea during June 1997. *J. Geophys. Res.,* 104, 18 041–18 046.

Halpern, D., Freilich, M. H., and Weller, R. A., 1998: Arabian sea surface winds and ocean transports determined from ERS-1 scatterometer. *J. Geophs. Res., 103* (C4), 7799–7805.

Hantel, M., 1970: Monthly Charts of Surface Wind Stress Curl over the Indian Ocean. *Mon. Wea. Rev.* 98, 765-773.

Hart, J. E., 1977: On the theory of the East African low-level jet stream. *Pure App. Geophys.*, 115, 1263-1282.

Hart, J. E., G. V. Rao, H. van de Borgaard, J. A. Young and J. Findlater, 1978: Aerial observations of the East African low-level jet stream. *Mon. Wea. Rev.* 106, 1714-1724.

Hashizume, H., S.-P. Xie, W. T. Liu, and K. Takeuchi, 2001: Local and remote atmospheric response to tropical instability waves: A global view from space. *J. Geophys. Res.*, 106, 10 173–10 185.

Hashizume, H., S.-P. Xie, M. Fujiwara, M. Shiotani, T. Watanabe, Y. Tanimoto, W. T. Liu, and K. Takeuchi, 2002: Direct observations of atmospheric boundary layer response to SST variations associated with tropical instability waves over the eastern equatorial Pacific. *J. Climate,* 15, 3379–3393.

Hastenrath, S., and Greischar, L., 1991: The monsoonal current regimes of the tropical Indian Ocean: observed surface flow fields and their geostrophic and wind-driven components. *Journal of Geophysical Research*, *96*, 12619–12633.

Hawkins, J., 1977: A study of the mesoscale wind circulation in a land-sea breeze regime. *CUEA TECH. REP. 32, Dept. of Met., Florida State Univ.*

Hawkins, J., 1979: Atmospheric structural variations that result in upwelling off Oregon. *CUEA TECH. REP. 52, Dept. of Met., Florida State Univ. pp. 72.*

Hawkins, J., and Stuart, D. W., 1980: Low Level Atmospheric changes over Oregon's coastal upwelling region, *Monthly Wea. Rev.*, 108.

Hayes, S. P., M. J. McPhaden, and J. M. Wallace, 1989: The influence of sea surface temperature on surface wind in the eastern equatorial Pacific. *J. Climate,* 2, 1500–1506.

Holladay, C. G. and O'brien, J. J., 1975: Mesoscale variability of Sea Surface Temperatures, *J. Phys. Oceanogr.* 5, 761-772.

Hoskins, B. J., 1994: the role of potential vorticity in symmetric stability and instability. *Quart. J. Roy. Meteor. Soc.,* 100, 480-482.

Hurlburt, H. and Thompson, J. D., 1976: Numerical Model of the Somali Current: *J. Phy. Ocean.* 6, 646-664.

Hulburt, H. E. and James O'brien, 1974: Equatorial Jet in the Indian Ocea. *Theory Science, 184, 1075-77.*

Johnson, A., and O'brien, J. J., 1973: A study of an Oregon seabreeze event, *J. App. Met.,* 12, 1267-1283.

Joseph, P. V and S. Sijikumar, 2004: Intraseasonal Variability of the Low-Level Jet Stream of the Asian Summer Monsoon. *Journ. of Clim.* 17, 1449-57.

Jury, M. R., 1983: Wind Shear and Differential Upwelling along the S. W. tip of Africa. *PhD Thesis Dept. of Oceanography UCT.* pp 1-1 to 2-15.

Kalnay, E., N. and co-authors; 1996: The NCEP/NCAR, 40-Year Reanalysis Project, *Bull. Am. Meteorol.* Soc. 77(3), 437-471.

Karstensen J and D Quadfasel, 2002: Formation of southern hemisphere thermocline waters: water mass conversion and subduction. *J. Phys. Oceanogr.* **32**(11), 3020–3038.

Koteswaram P., 1950: Upper air lows in low latitudes in the Indian area during southwest monsoon season and "Breaks" in the monsoon. *Ind. J. Met. Geophys.* 1, 162–64.

Knox, R., 1976: On a long series of measurements of Indian Ocean equatorial currents near Addu Atoll. *Deep-Sea Research*, *23*, 211–221.

Knox, R. A., and Anderson, D. L. T., 1987: Recent advances in the study of the low-latitude ocean circulation. *Progress in Oceanography*, *14*, 259–317.

Krishnamurti, T.N., and E. D. Rodgers, 1970: 200mb wind field June, July, August 1967. *Tech. Rep*. No. 70-2, Meteor. Dept., Florida State University, 161 pp.

Krishnamurti , T.N., 1971: Observational study of tropical upper tropospheric motion field during Northern Hemisphere summer. *J. App. Meteorol*., 10, 1066-96.

Krishnamurti, T.N., and M. Kanamitsu, 1973: A study of a coasting easterly wave. *Tellus,* 25, 568-586.

Krishnamurti, T.N., S. M. Daggupaty, J. Fein, M. Kanamitsu and J. D. Lee, 1973: Tibetian High and upper tropospheric tropical circulation during northern summer. *Bull. Amer. Meteor. Soc*., 54, 1234-1239.

Krishnamurti T. N, Bhalme H. N., 1976: Oscillations of a monsoon system. Part 1. Observational aspects. *J. Atmos. Sci.* 33, 1937–54.

Krishnamurti, T. N, Subrahmanyan D., 1982: The 30–50 day mode at 850mb during MONEX. *J. Atmos. Sci.* 39, 2088–95.

Krishnan R, Zhang C, Sugi M., 2000: Dynamics of breaks in the Indian summer monsoon. *J. Atmos. Sci., 57*, 1354–72.

Kummerow, C., and Coauthors, 2000: The status of the Tropical Rainfall Measuring Mission (TRMM) after two years in orbit. *J. Appl. Meteor.*, 39, 1965–1982.

Lawrence, A. M, 1977: Long-period Equatorial Topographic Waves; *J. Phy. Ocean.* 8, 302-314.

Leetma, A., 1970: The response of the Somalia Current to the Southwest monsoon of 1970. *Deep Sea Res.* 19, 319-325.

Lighthill, M. J., 1969: Dynamic Response of the Indian Ocean to Onset of the Southwest Monsoon. Ph. *Trans. Roy. Soc. L.* 265, 45-92.

Liping Wang, Koblinsky, C. J. and Howden, S., 2000: Annual Rossby Wave in the Southern Indian Ocean: Why Does It "Appear" to Break Down in the Middle Ocean? *J. Phy. Ocean.* 31, 54-74.

Lau, K. M. and Weng H., 1999: Interrannual, Decadal-Interdecadal and Global Warning Signals in Sea Surface Temperatures during 1955-1997. *J. Clim.* 12, 1257-1267.

Lau, K. M. and Weng H., 1995: Climate Signal Detection Using Wavelet Transform: How to make a Time series Sing. *Bull. of Ame. Meteor. Soc.* 76, 2391-2402.

Lawrence, D. M, Webster P. J., 2001: Interannual variations of the intraseasonal oscillation in the South Asian summer monsoon region. *J.Clim.* 14, 2910–22.

Luther, M. E., James O'Brien: Modelling the Variability of the Somali Current: Florida State Univ. *Mesoscale Air-Sea Interactions Group Tallahassee,* FL 32306-3041.

Luyten, J. R. Roemmich,D. H, 1982: Equaqtorial Currents at Semi-Annual Period in the Indian Ocean. *J. Phys. Oceanog.* 12, 406-412.

Madden, R.A, Julian P.R., 1972: Description of global-scale circulation cells in the tropics with a 40–50 day period. *J. Atmos. Sci.* 29, 1109–23.

Magana, V., Webster P. J., 1996: Atmospheric circulations during active and break periods of the Asian monsoon. Preprints Conf. Global Ocean-Atmos.-Land Syst. (GOALS), 8th. *Am. Meteorol. Soc.,* Atlanta, GA

McCreary, J. P. Jr., Kundu, P. K., and Molinari, R. L., 1993: A numerical investigation of dynamics, thermodynamics and mixed layer processes in the Indian Ocean. *Progress in Oceanography*, *31*, 181–244.

McPhaden, M., 1982: Variability in the central Indian Ocean. Part I: Ocean dynamics. *Journal of Marine Research*, *40*, 157–176.

Melice, J. L., Coron, A., Berger, A, 2001: Amplitude and Frequency Modulations of the Earth's Obliquity for the last Million Years. *Jour. of Clim*, 14, 1044-54.

Moody, G., 1979: Aircraft derived low level winds and upwelling off the Peruvian coast during March, April, and May, 1977. *CUEA TECH. REP.* 56, Dept. of Met., Florida State Univ.

Munk, H. N, 1950: Wind Driven Ocean Circulation, *Journ. of Met.* 7, 79-92.

Murakami, T., R. Godbole and R. R. Kelkar, 1970: Numerical Simulations of the monsoons along 80^0E, *Proc. Conf. on Summer monsoon of the Southeast Asia, Navy Weath. Res. Facility, Norfolk, Va.*, 39-51.

Murakami, T., 1976: Cloudiness fluctuations during the summer monsoon. *Journ. Meteorol. Soc. Japan.,* 54, 175–81.

Murakami, M., 1987: Satellite cloudiness in the monsoon area. In *Monsoon Meteorology*, eds. CP Chang, TN Krishnamurti, pp. 354–402. New York: Oxford Univ. Press.

Mysak, L. A., 1978: Long Period Equatorial Topographic Waves. *Journ. of Phys. Oceanog.* 8, 302-14.

Nelson, C. S., 1977: Wind stress and wind stress curl over the California Current, NOAA Tech. Re. NMFS-SSRF-714 pp 87.

Nelson, G., and L. Hutchings, 1983: The Benguela upwelling area. *Progress in Oceanography,* Vol. 12, Pergamon, 333–356.

New, A. L. and Stansfield, K., 2005: Physical and Biochemical aspects of the flow across the Mascarene Plateau in the Indian Ocean. *Phil. Trans. R. Society,* 363, 151-168.

O'Brien, J. J., and Hurlburt, H. E., 1974: An equatorial jet in the Indian Ocean theory. *Science*, 184, 1075–1077.

Okemwa, E. N., 1998: Large marine ecosystems of the Indian Ocean: Assessment, sustainability, and management. pp. 73-99.

Parrish, R. H., Nelson, C.S. and Bakun, A., 1981: Transport mechanism and reproductive success of fisheries in the California current, *Biol. Oceanogr.* 1(2), 175-203.

Parthasarathy B, A.A Munot, D.R Kothawale., 1992: Indian summer monsoon rainfall indices: 1871–1990. *Meteorol. Mag.,* 121, 174–86.

Parthasarathy B, A.A Munot, D. R. Kothawale., 1995: Monthly and seasonal rainfall series for all-India homogeneous regions and meteorological subdivisions: Indian Institute of Tropical Meteorology, Pune, India 1871–1994, *IITM Research Report-065*,

Pedlosky, J., 1974: Longshore currents, upwelling and bottom topography *J. Phys. Oceanogr.* 4, 214-226.

Philander, S.G.H., 1978: Upwelling in the Gulf of Guinea, *J. Mar. Res.*, 37, 23-33.

Philander, S.G.H., Fedorov. A. V., Pacanowski R. C. and Boccaletti, G.; 2004: The effect of Salinity on the Wind-Driven circulation and the Thermal Structure of the Upper Ocean. *Journ. of Phy. Oceanog.* 34, 1949 - 1965.

Raghavan, K., 1973: Break monsoon over India. *Mon. Weather Rev,* 101, 33–43.

Raghavan, K. and co-authors, 1978: Interaction between the West Arabian Sea and the Indian monsoon, *Mon. Wea. Rev.,* 106, 719-724.

Ramamurthy K., 1969: Monsoon of India: some aspects of the 'break' in the Indian southwest monsoon during July and August. *Forecast. Man.* 18.3(No. IV):1–57. India Meteorol. Dept., Poona, India

Rao, G. V. and J. L. Haney, 1982: Kinematic and thermal structures of two surges of flow in the northern Mozambique Channel area. *Quart. J. Roy.Meteor. Soc.* 108, 957–974.

Reid Joseph L., 2003: On the total geostrophic circulation of the Indian Ocean flow patterns, tracers, and transports. *Progress in Oceanography,* 56, 137–186.

Riehl H., 1954: *Tropical Meteorology*. New York: McGraw Hill.pp.392.

Riehl H., 1979: *Climate andWeather in the Tropics*. San Diego/New York: Academic. pp. 611.

Risien, C. M., 2002. Wind Stress Variability over the Benguela upwelling System. Masters thesis, University of Cape Town.

Risien C. M., C. J. C. Reason, F. A. Shillington, and D. B. Chelton, 2004. "Variability in satellite winds over the Benguela Upwelling System during 1999-2000" *J. of Geophy. Res.* 109(C3):C0301010.1029/2003JC001880.

Rodwell, M. J., and B. J. Hoskins, 1995: A model of the Asian summer monsoon. Part II: Cross-equatorial flow and PV behavior. *J. Atmos. Sci.*, 52, 1341–1356.

Rodwell, M. J., 1997: Breaks in the Asian Monsoon: The Influence of Southern Hemisphere Weather Systems *J. of Atm. Sc.*, 54, 2597 – 2610.

Schott, F.A., and D. R. Quadfasel, 1982: Variability of the Somali Current system during the onset of the southwest monsoon, 1979. *J. Phys.Oceanogr.*, 12, 1343–1357.

Schott, F, 1983. Monsoon response of the Somali Current and associated upwelling. *Prog. Oceanogr.*, 12, 357-382.

Schott, F., Swallow, J. C., and Fieux, M., 1990: The Somali Current at the equator: annual cycle of currents and transports in the upper 1000 m and connection to neighboring latitudes. *Deep-Sea Research, 37*, 1825–1848.

Schott, F, J. Fischer, U. Garternicht, and D. Quadfasel, 1997: Summer monsoon response of the northern Somali current, 1995. *Geophys. Res. Lett.*, 24, 2565–2568.

Schott, F.A., Julian P. McCreary Jr, 2001: The monsoon circulation of the Indian Ocean. *Progress in Oceanography,* 51, 1–123.

Sciremammano, F., 1979: A suggestion for the presentation of Correlations and Their Significance Levels, *J. Phys.Oceanogr.*, 9, 1273 – 1276.

Sekine Yoshihiko, 2000: Numerical study on the Coastal topography effect of a peninsula on the western boundary currents. *J. Phys.Oceanogr.*, 30, 369-383.

Senan, R., D. S. Anith, and D. Sengupta, 2001: Validation of SST and windspeed from TRMM using North Indian Ocean moored buoy observations. *Indian Institute of Science Tech. Memo.* CAOS Rep. 2001AS1, Bangalore, India, 29 pp.

Senan, R., Debasis, S., Goswami, B. N., 2003: Intraseasonal "monsoon jets" in the Equatorial Indian Ocean. *Geoph. Res. Lett.* 30 pp 4 (1-4).

Shankar, D. A, P.N. Vinayachandran b, A.S. Unnikrishnan, 2002: The monsoon currents in the north Indian Ocean. *Progress in Oceanography,* 52, 63–120.

Shetye, S. R., & Gouveia, A. D., 1998: Coastal circulation in the north Indian Ocean. Coastal segment (14,S-W). In *The Sea, Vol. 11* (pp. 523–556).

Sikka, D.R, Gadgil S., 1980: On the maximum cloud zone and the ITCZ over India longitude during the Southwest monsoon. *Mon.Weather Rev.*, 108, 1840–53.

Simpson G., 1921: The south-west monsoon. *Q.J. R. Meteorol. Soc., 199*, 150–73.

Slingo, J. Hilary Spencer, Brian Hoskins, Paul Berrisford and Emily Black, 2005: The meteorology of the Western Indian Ocean, and the influence of the East African Highlands, *Phil. Trans. R. Soc. A* 363, 25–42.

Smith R. B., 1982: Synoptic Observations and theory of orographically distributed wind and pressure, *J. Atm. Sc.*, 39, 60-70.

Smith, R. L., 1968: Upwelling, Oceanogr. *Mar. Biol. Annual Rev.*, 6, 11-46.

Spencer, H., Rowan, T. S. and Julia Silango, 2004: Indian Ocean Climate Variability in Hadley Center Coupled GCM.

Sperber, K. R., J. M. Slingo, and H. Annamalai, 2000: Predictability and the relationship between subseasonal and interannual variability during the Asian summer monsoon. *Quart. J. Roy. Meteor. Soc.*, 126, 2545–2574.

Stommel, H and Frassetto, R. 1968: The Time of Appearance of Cold Water off Somalia. *Proc. Nat. Ac. of Scs. U.S.A*, 60, 750-751.

Stommel, H and Wooster W.S., 1965: Reconnaissance of the Somali Current during the Southwest Monsoon. *Proc. Nat. Ac. of Scs. U.S.A.*, 54, 18-13.

Stuart, D. W., 1979: The mesoscale Meteorology of selected upwelling regions. *Proc. Nat. Oceanogr. Symp. UCT.*

Stuart, D. W., Godwin, R. J., Duval, W. P., 1981: A comparison of surface winds and winds measured at 152m during JOINT I 1974 and JOINT II 1977, Coastal Upwelling, *Amer. Geophys. Union*, 39-43.

Swallow, J. C., and J. G. Bruce, 1966: Current measurements off the Somali coast during the southwest monsoon of 1964. *Deep-Sea Res.*, 13, 861–888.

Swallow, J. C., R. L. Molinari, J. G. Bruce, O. B. Brown and R. H. Evans, 1983: Development of near surface flow patterns and water mass distribution in the Somali Basin in response to the Southwest Monsoon of 1979. *J. Phys. Oceanogr*, 13, 1398-1415.

Swallow, J.C., F. Schott and M. Fieux, 1991: Structure and transport of the East African Coastal Current. *J. Geophys. Res*. 96. C12, 22 254-22 257.

Tomczak, M. and Godfrey, S. J., 1994: Regional Oceanography: an Introduction. Pergamon, New York, 1994. 422 pp.

Torrence C. and Compo, G. P., 1998: A practical Guide to Wavelet Analysis, *Bull. of Am. Met. Soc.*, 79, 61-77.

Tychsen, J., 2006: KenSea. Environmental Sensitivity Atlas for Coastal Area of Kenya, 76 pp. Copenhagen; Geological Survey of Denmark and Greenland (GEUS); ISBN 87-7871-191-6.

Uhart, M., 1976: A case study of land-sea breeze phenomena over the Western African coast, *CUEA TECH. REP.* 28, Dept. of Met., Florida State Univ., pp. 125.

Van ieperen, M. P., 1971: Hydrology of Table Bay, Dept. of Oceanogr., Univ. of Cape Town, pp. 48.

Vecchi, G. A., Xie, S., Fischer, A. S., 2004: Ocean Atmosphere Covariability in the Western Arabian Sea, *Journ. Climate,* 17, 1213-1224.

Wallace, J. M., T. P. Mitchell, and C. Deser, 1989: The influence of sea surface temperature on surface wind in the eastern equatorial Pacific: Seasonal and interannual variability. *J. Climate,* 2, 1492–1499.

Wang, L. Chester J. K., Stephan H., 2000: Annual Rossby Wave in the Southern Indian Ocean: Why Does It "Appear" to Break Down in the Middle Ocean? *Journ. of Phys. Oceanog*, 31, 54-73.

Watson, A. I., 1978: A study of low level mesoscale winds observed off the Peruvian coast during March and April 1976, *CUEA. TECH. REP.*41 Dept. of Met., Florida State Univ., pp. 121.

Webster, P. J., 1987. The elementary monsoon. In *Monsoons, ed. JS Fein, PL Stephens*, pp. 3–32. New York.

Webster PJ, Magana VO, Palmer TN, Shukla J, Tomas RA, 1998: Monsoons: processes, predictability, and the prospects for prediction. *J. Geophys. Res.*103(No. C7):14451–510

Wentz, F. J., 1992: Measurement of oceanic wind vector using satellite microwave radiometers. *IEEE Trans. Geosci. Remote Sens.,* 30, 960–972.

Wentz, F. J., 1997: A well-calibrated ocean algorithm for special sensor microwave/imager. *J. Geophys. Res.,* 102, 8703–8718.

Woodberry, K. E., Luther, M. E., & O'Brien, J. J., 1989: The wind-driven seasonal circulation in the southern tropical Indian Ocean. *Journal of Geophysical Research*, 94, 17985–18002.

Wyrtki, K., 1973: An Equatorial Jet in the Indian Ocean. *Science New Series,* 4096, 262-64

Xie, S.-P., M. Ishiwatari, H. Hashizume, and K. Takeuchi, 1998: Coupled ocean–atmospheric waves on the equatorial front. *Geophys. Res. Lett.,* 25, 3863–3866.

Zhang, G. J., and M. J. McPhaden, 1995: The relationship between sea surface temperature and latent heat flux in the equatorial Pacific. *J. Climate,* 8, 589–605.

Zhengyu, L., Lixin WU and Bayler E., 1998: Rossby Wave-Coastal Kelvin Wave Interaction in the Extratropics. Part I: Low-Frequency Adjustment in a closed Basin; *J. Phy. Ocean.* 29, 2382-2404.